1978

Synthesis and structural characterization of some compounds involving metal-metal bonding of tellurium, bismuth, and zirconium

Alan Cisar
Iowa State University

INFORMATION TO USERS

This material was produced from a microfilm copy of the original document. While the most advanced technological means to photograph and reproduce this document have been used, the quality is heavily dependent upon the quality of the original submitted.

The following explanation of techniques is provided to help you understand markings or patterns which may appear on this reproduction.

1. The sign or "target" for pages apparently lacking from the document photographed is "Missing Page(s)". If it was possible to obtain the missing page(s) or section, they are spliced into the film along with adjacent pages. This may have necessitated cutting thru an image and duplicating adjacent pages to insure you complete continuity.

2. When an image on the film is obliterated with a large round black mark, it is an indication that the photographer suspected that the copy may have moved during exposure and thus cause a blurred image. You will find a good image of the page in the adjacent frame.

3. When a map, drawing or chart, etc., was part of the material being photographed the photographer followed a definite method in "sectioning" the material. It is customary to begin photoing at the upper left hand corner of a large sheet and to continue photoing from left to right in equal sections with a small overlap. If necessary, sectioning is continued again — beginning below the first row and continuing on until complete.

4. The majority of users indicate that the textual content is of greatest value, however, a somewhat higher quality reproduction could be made from "photographs" if essential to the understanding of the dissertation. Silver prints of "photographs" may be ordered at additional charge by writing the Order Department, giving the catalog number, title, author and specific pages you wish reproduced.

5. PLEASE NOTE: Some pages may have indistinct print. Filmed as received.

University Microfilms International
300 North Zeeb Road
Ann Arbor, Michigan 48106 USA
St. John's Road, Tyler's Green
High Wycombe, Bucks, England HP10 8HR

Synthesis and structural characterization of some compounds involving metal-metal bonding of tellurium, bismuth, and zirconium

by

Alan Cisar

A Dissertation Submitted to the

Graduate Faculty in Partial Fulfillment of

The Requirements for the Degree of

DOCTOR OF PHILOSOPHY

Department: Chemistry
Major: Inorganic Chemistry

Approved:

Signature was redacted for privacy.

In Charge of Major Work

Signature was redacted for privacy.

For the Major Department

Signature was redacted for privacy.

For the Graduate College

Iowa State University
Ames, Iowa

1978

TABLE OF CONTENTS

	Page
INTRODUCTION	1
EXPERIMENTAL PROCEDURE	14
SALTS OF THE CLUSTER ANIONS Te_3^{2-} AND Bi_4^{2-}	53
THE ZIRCONIUM DICHLORIDES	85
FUTURE WORK	136
BIBLIOGRAPHY	138
ACKNOWLEDGMENTS	144

INTRODUCTION

One of the fastest growing areas of inorganic chemistry is the investigation of compounds involving metal-metal bonds. This dissertation covers investigations into two widely differing types of compounds, salts containing post-transition metal polyatomic or cluster anions and early transition metal subhalides, both of which exhibit metal-metal bonding.

At present there is no review of the homopolyatomic anion species available, however Corbett has recently reviewed the homopolyatomic cations of the post-transition elements,[1] many of which are isostructural and isoelectronic with known anion species. Schäfer, Eisenmann, and Müller have reviewed the structure and bonding of the "Zintl Phases",[2] a name which they apply to all compounds of the alkali and alkaline earth elements. In many of these compounds the more electronegative atom, the post-transition element, forms a homoatomic cluster or chain although few of these clusters can be considered discrete anions due to the extreme charge transfer this would require.

The earliest report of a post-transition metal polyanion species came from Joannis who produced an intensely green solution by the reaction of lead and sodium in liquid ammonia.[3] By the time the correct stoichiometry of this compound, $NaPb_{2.25}$ (Na_4Pb_9), was established electrochemically by Smyth 60 years ago, similar solvated species were already known for antimony, bismuth, mercury, and tin.[4]

Although there are several reports in the early literature of the formation of uncharacterized red or purple polytelluride species by oxidation of the telluride(2-) ion in aqueous base[5] or by solution of the element in hydrogen telluride,[6] the first systematic investigation was carried out by Kraus and Chiu.[7] Their experiments involved the dissolution of a weighed stick of tellurium in a liquid ammonia solution containing a known quantity of sodium. The stoichiometry of the solution was determined by weighing the remaining portion of the tellurium stick. Their results indicated three tellurides; Te^{2-}, which was only slightly soluble, producing a yellow solution, Te_2^{2-}, which forms a clear blue solution, and Te_4^{2-}, the ion in equilibrium with excess tellurium, which forms a clear red solution. The dinegative nature of the anions was determined by vapor pressure measurements.[8]

Zintl, Goubeau, and Dullenkopf found these three ions, and the deep red Te_3^{2-} also, through potentiometric titrations as part of an extensive investigation of the electrochemistry of polyanions of the post-transition elements in liquid ammonia.[9] While the three most reduced species were found reproducibly in both of the published titrations, the tetratelluride, Te_4^{2-}, was only observed once.

Neither group of investigators succeeded in obtaining any solid polytellurides, both reporting only the recovery of one of the known sodium tellurium intermetallic phases, a mixture of known compounds, or a mixture including tellurium.

All of these early experiments have two things in common, the intricacy of apparatus used and the ingenuity of manipulations which were

required to work with these very air sensitive compounds before the advent of modern dryboxes and ground glass joints.

Before the present work was begun, the only polytelluride ion structurally characterized was the ditelluride ion, Te_2^{2-}, such as found in $MgTe_2$, which has the pyrite structure,[10] while for both sulfur and selenium the trichalcide ions, S_3^{2-} and Se_3^{2-} are known in the solid state.[11,12]

Although the tritelluride ion was not known in the solid state, the isoelectronic species, I_3^+, has been deduced in the compound I_3AlCl_4 by Merryman and coworkers and characterized by NQR spectrometry.[13] It will be shown that, as in the case of Pb_5^{2-} and Bi_5^{3+}[14], the isoelectronic species Te_3^{2-} and I_3^+ are also isostructural.

While this study was in progress, the structure of In_2Te_5 was reported.[15] This compound contains Te_3^{2-} groups, but they are not isolated polyanions, having Te-In distances shorter than the Te-Te distances.

The earliest systematic investigation of polybismuth anions came from Zintl et al., who found evidence for the existence of two anions, violet colored Bi_3^{3-} and brown Bi_5^{3-}, by potentiometric titration of liquid ammonia solutions of sodium with BiI_3[9] and a third, yellow-brown Bi_7^{3-}, by exhaustive extraction of bismuth-rich (Bi:Na::3:1) alloys for a period of months.[16]

As has already been noted[17] the identification of the last species as Bi_7^{3-} appears questionable. The conclusion was based on the analytical result $Na_3Bi_{5.85}$ (or approximately Na_3Bi_6) which was presumed to indicate a mixture of Na_3Bi_5 and Na_3Bi_7 in solution on the grounds that

no other group V anion had been observed with an even number of atoms and that all appeared to be trinegative. However, if the analysis is taken to be correct, the resulting formulation could represent 1.5 Na_2Bi_4 and indicate that the solution species was Bi_4^{2-}, isoelectronic with the known Te_4^{2+}.[18] The polybismuthide anion characterized in this work indicates that this postulate does indeed appear likely and that the Bi_4^{2-} anion has the predicted[17] square planar structure.

There are two recent reports of uncharacterized polybismuthide species. In one, green and rose colored microcrystals are reported to form on evaporation of solvent from the dichroic green-red solution formed by the equilibration of either NaBi or NaBi + Bi and crypt (see below for the meaning of this name) in ethylenediamine.[19] In the other, a brown solution is reported after equilibrating a mixture (composition $NaBi_3$) with ethylenediamine for several months.[20]

Recently there have been several reports of the isolation and characterization of "Zintl ions" in the solid state. In all except one of these reports,[21] the key to the formation of a stable and tractable product has been the use of 2,2,2-crypt[22] to complex the alkali metal counter ion. This compound (see Figure 1), the correct systematic name of which is 4,7,13,16,21,24-hexaoxa-1,10-diazabicyclo[8.8.8]hexacosane ($N(C_2H_4OC_2H_4OC_2H_4)_3N$), is one of a group of cage-like polycyclic amine ethers.[23] Many of these compounds complex alkali and alkaline earth ions extremely well, with a very strong size effect, each compound complexing one alkali metal ion an order of magnitude better than any of the others. Because 2,2,2-crypt is commercially available at a price

Figure 1. A potassium ion complexed by a molecule of 4,7,13,16,21,24-hexaoxa-1,10,-diazabicyclo[8.8.8]-hexacosane (2,2,2,-crypt). The shaded atoms are the six ether oxygens (along the chains) and two tertiary amine nitrogens (at the bridgeheads) which coordinate to the potassium (at the center). When the volume occupied by the 36 hydrogen atoms (not shown) is included this spherical complex cation has an approximate radius of 5.5Å.

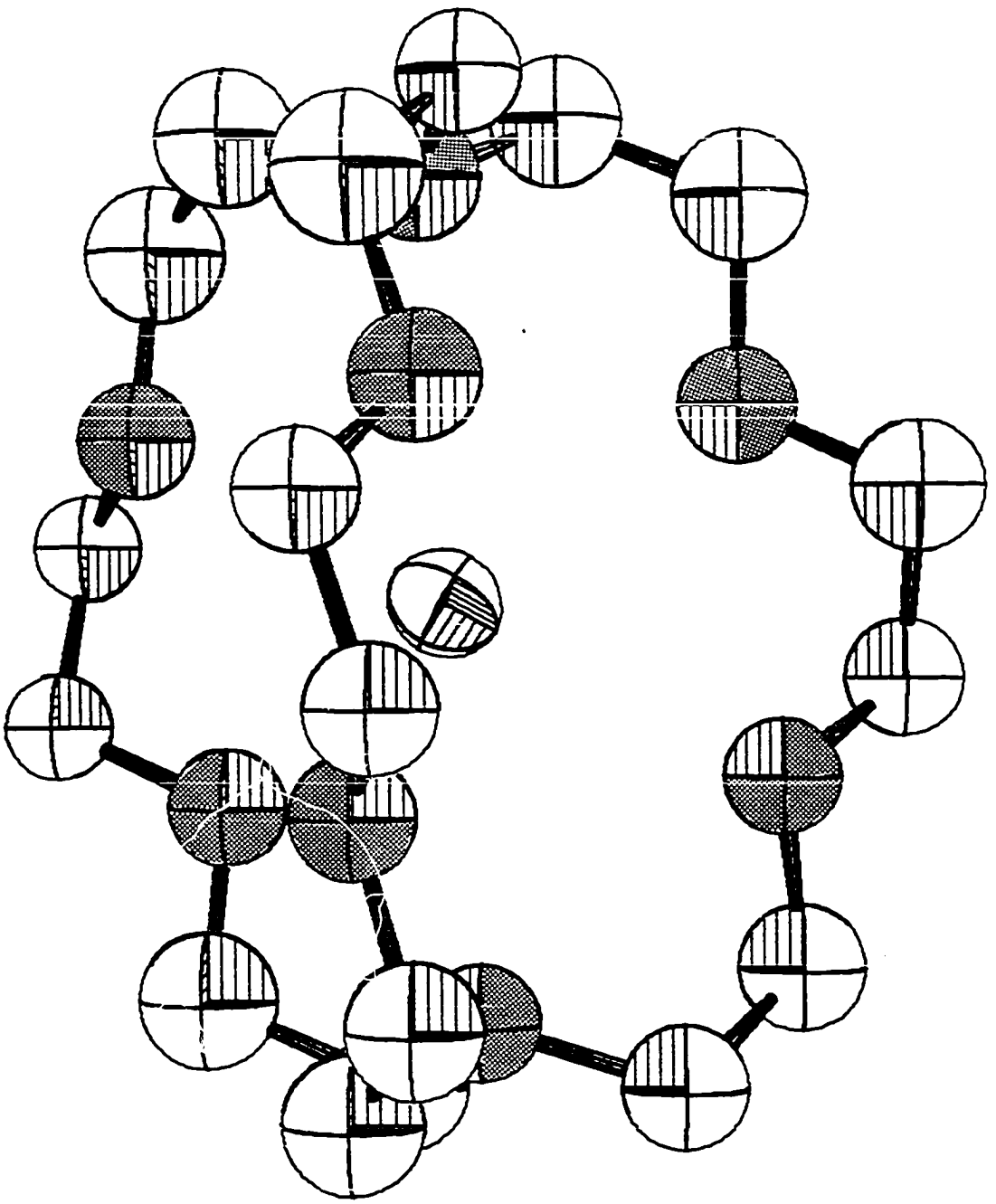

significantly below any of the other ligands, it was the compound of choice, and because its most stable complex (for a monovalent ion) is formed with potassium,[24] this element was chosen as the cation.

The use of crypt to complex the cation promotes the formation of crystalline polyanion salts in two ways. First is an increase in solubility. Intermetallic compounds which dissolve in pure ethylenediamine dissolve faster with crypt present, and many compounds which are insoluble in pure solvent, such as KBi_2, readily form solutions when crypt is present. The second effect is to furnish an energetically favorable alternative to the intermetallic compound in the solid state. Clearly the intermetallic compound with relatively small charge separations, few if any like-charged nearest neighbors, and some degree of electron delocalization has more binding energy than a compound containing a larger complex discrete polyanion which would yield a low Madelung energy and would require either cation-cation contacts or a very open structure. With the use of crypt to complex the cation the complexation energy replaces the binding energy lost with the increase in metal atom separations and the increased cationic radius (5.5Å instead of 1.3Å in the case of potassium[25]) easily keeps the polyanions separated.

To date, six "Zintl ions", Pb_5^{2-}, Sb_7^{3-},[17] Sn_5^{2-},[14] Sn_9^{4-},[26] Ge_9^{2-} and Ge_9^{4-},[27] have been isolated as the salts of cryptate cations and characterized crystallographically. The work described in this dissertation includes the synthesis and crystal structures of two more such species, Te_3^{2-} and Bi_4^{2-}. Much of this material has already been published.[28,29]

One of the above ions, Sn_9^{4-} has also been isolated as the salt of sodium complexed by ethylenediamine.[20] This last complex is far less stable than any of the cryptate salts, all of which are very air sensitive and many of which decompose under x-ray exposure.

There are five zirconium chlorides known, with oxidation states ranging from four down to one.[30] Of these, the white insulating $ZrCl_4$, which consists of chains of octahedra sharing two non-opposing edges, is the only one not exhibiting some form of metal-metal bonding.

The trichloride is the most studied of the reduced chlorides, accounting for virtually all of the early reports in this area. This olive-green compound, like the tribromide and triiodide, consists of chains of octahedrally coordinated zirconium atoms joined together by sharing opposite faces of the octahedra.[31,32] With a metal-metal distance of 3.067Å along the chain, this diamagnetic semiconductor definitely has metal-metal bonding along the chain. This compound is nonstoichiometric, with a range from $ZrCl_{2.94}$ to $ZrCl_{3.03}$.[33] A shear mechanism has been advanced by Copley and Shelton to explain the substoichiometry.[34] Although this may explain the non-stoichiometry near $ZrCl_{3.00}$, their suggestion that this mechanism applies for the reduction all the way to a composition of $ZrCl_{1.6}$ is definitely incorrect. Daake has shown that this reduction leads to $ZrCl_2$, with a two phase region between $ZrCl_{2.94}$ and $ZrCl_2$.[30]

The compound Zr_6Cl_{15} has only been found as isolated crystals grown along with other compounds in transport reactions. It is isostructural with Ta_6Cl_{15}, having isolated M_6 octahedra, with chlorine

atoms bridging all of the edges and the clusters linked by chlorine bridging from a vertex on one cluster to a vertex on an adjacent cluster.[30]

Zirconium monochloride was first prepared by the electrochemical reduction of zirconium in a $SrCl_2$-NaCl-$ZrCl_4$ melt (63:34:3).[35] Struss and Corbett report the production of this compound by the reduction of $ZrCl_4$ with an excess of zirconium foil.[36] A modification of this procedure has made it possible to produce this stoichiometric compound in quantity for use as a reductant, a role in which it has proven far more facile than metallic zirconium.[30]

The monochloride, which is a metallic conductor with very anisotropic electrical properties, has a slab-type structure with four close-packed layers (Cl-Zr-Zr-Cl) in each slab and three slabs in each repeating sequence.[37] Although this was the first compound found possessing this double metal layer structure, several other monohalides (ZrBr, ScCl, HfCl, GdCl, and TbCl) have recently been found to also have this type of structure.[38]

Zirconium dichloride was first reported by Ruff and Wallstein in 1923 as a product of either the disproportionation of the trichloride or the reduction by aluminum of the tetrachloride. They described it as an amorphous, air sensitive black compound with a density of 3.6 g/cm^3.[39] Until recently most references treated the compound as the stoichiometric result of the disproportionation of $ZrCl_3$.[40-46] Two reports[30,34] describe the dichloride as non-stoichiometric with the limiting reduced composition about $ZrCl_{1.6}$, and Daake has suggested that the oxidized

limit for the "dichloride" with the same powder pattern as observed in this work may be as low as $ZrCl_{1.75}$.[30]

Swaroop and Flengas have reported the synthesis af anhydrous $ZrCl_2$ by the reduction of the trichloride with an excess of finely divided metal at 675° in a quartz tube lined with 10 mil Pt foil. After two reactions their platinum linings were so badly attacked as to be unusable. Although their analytical data appear to indicate a composition of $ZrCl_2$ and they describe their product as an air sensitive black powder,[47] the material produced definitely was not $ZrCl_2$. As can be seen in Table I, the powder pattern they report for their product is virtually identical to that of Baddeleyite, the low temperature form of ZrO_2. At first it might seem that this is simply a result of poor sample handling, with the oxide being the result of the decomposition of the chloride in air. This is clearly not the case, as the pattern obtained was too sharp for the material to have been formed at low temperature, indicating that the oxide was formed during the initial synthesis.

Struss and Corbett were the first to report a powder pattern for $ZrCl_2$ which agrees with the results in this work.[36] This pattern was confirmed by Troyanov and Tsirel'nikov, who reported $ZrCl_2$ to be isostructural with the isoelectronic 3R-MoS_2.[48] They deduced this structure using film data from a non-single crystal produced by a controlled disproportionation of $ZrCl_3$. They did not fully refine the structure (the reported R factor was 28%) or offer any explanation for the deviation of their material (which analyzed as $ZrCl_{1.87}$) from the 2:1

Table I. Comparison of the powder patterns of Swaroop and Flengas's "$ZrCl_2$" with that of ZrO_2

"$ZrCl_2$"[a]		ZrO_2[b]	
I/I_o	d(Å)	d(Å)	I/I_o
20	5.067	5.036	6
40	3.686	3.690	18
		3.630	14
100	3.164	3.157	100
80	2.844	2.834	65
60	2.630	2.617	20
		2.598	12
20	2.535	2.538	14
		2.488	4
10	2.332	2.328	6
		2.285	2
40	2.206	2.213	14
		2.182	6
10	2.015	2.015	8
40	2.008	1.989	8
40	1.855	1.845	18
40	1.817	1.818	12
		1.801	12
10	1.750	1.780	6
20	1.701	1.691	14
40	1.660	1.656	14

[a] From reference 47.

[b] From reference 49.

Table I (Continued)

"$ZrCl_2$"[a]		ZrO_2[b]	
I/I_o	d(Å)	d(Å)	I/I_o
		1.640	8
20	1.618	1.608	8
10	1.593	1.591	4
		1.581	4
30	1.551	1.541	10
10	1.516	1.508	6
20	1.482	1.495	10
		1.476	6
10	1.455	1.447	4
30	1.427	1.420	6
10	1.389		
10	1.368	1.358	2
		1.348	2
30	1.331	1.321	6
10	1.310	1.309	2
		1.298	2
30	1.274	1.269	2
20	1.252	1.261	2

stoichiometry of the ideal structure beyond the suggestion of unspecified "crystal defects".

In this work the structures of the two types of zirconium dichloride will be examined, as well as the mechanism for nonstoichiometry in the slab type dichloride. The recent volume by Hulliger[50] is a good source

for an explanation of the peculiar nomenclature of slab type compounds (such as 3R-MoS_2) and a review of the many known structures of the early transition metal dichalcides.

EXPERIMENTAL PROCEDURE

Because of the air-sensitive nature of the compounds used in this research, all manipulations were carried out utilizing either a drybox or high vacuum line. All of the dryboxes used had inert atmospheres of nitrogen and were continuously purged. Dryness was maintained in the range of 6 to 20 ppm water vapor by recirculating the gas through a column of dried Molecular Sieve with a squirrel cage fan and exposing the atmosphere to an open container of phosphorus pentoxide.

Standard vacuum line techniques were used for the manipulations carried out on the vacuum line. For a good description of such techniques the book by Shriver should be consulted.[51]

Preparation of the polyanionic salts

There are three compounds reported in the potassium-tellurium system, the normal telluride, K_2Te, which has the antifluorite structure (a_o = 8.168Å), and two tellurium rich compounds, K_2Te_2 and K_2Te_3, both of which possess more complex but unknown structures.[52] Two of these, K_2Te and K_2Te_3, were synthesized and used in this study.

K_2Te was synthesized from potassium (J. T. Baker, "purified") and tellurium (United Mineral and Chemical, 99.999%) using the method described by Klemm in which the product precipitates from a liquid ammonia solution of potassium when it reacts with tellurium.[53] Although this source describes the compound as pale yellow, in this

study, it was found to be snow white when pure but darkening to pale yellow on handling in a drybox. This difference is probably due to the improvement in the quality of the starting materials available during the intervening 40 years, with the white color being correct.

K_2Te_3 was produced by combining stoichiometric quantities of K_2Te and tellurium in a porcelain crucible sealed inside an evacuated Vycor jacket. This apparatus was heated to 500° for 0.5 h and then to 700° for an additional 0.5 h. The resulting friable, silvery grey solid (which had been molten at 700°) showed no evidence of the starting materials in its powder pattern (Debye-Scherrer).

There are four compounds known in the potassium-bismuth system; K_3Bi, which has the Na_3As structure (hexagonal, a = 6.190Å, c = 10.955Å),[54] K_3Bi_2, K_5Bi_4, and KBi_2, which has the $MgCu_2$ structure (cubic, a_o = 9.501Å).[55] All four were prepared by fusing together stoichiometric amounts of the elements (bismuth, Oak Ridge National Laboratory, 99.999%) in sealed tantalum tubes, a method found satisfactory in a previous study.[56] For K_3Bi and KBi_2, which melt congruently at 671° and 565° respectively, a single heating to 700° followed by slow cooling was sufficient to produce a thoroughly crystalline product. With K_3Bi_2, which melts barely congruently at 442°, annealing for 16 hours just below the melting point was added to the above procedure. The remaining compound, K_5Bi_4, melts incongruently at 381°. It was produced by initially heating the reactants to 700° to give a homogeneous melt, then equilibrating the material at 440° (above the point where the first solid nucleates) for several hours, quenching to near room temper-

ature, and then annealing at 375° for ten days.

The compounds are all friable and range in color from metallic green for K_3Bi, through bluish-silver for K_3Bi_2 and K_5Bi_4, both of which develop a golden surface coating after handling in the drybox, to silver for KBi_2. Purity was established through Debye-Scherrer powder patterns.

Ethylenediamine (en) was dried by stirring over CaH_2 for about two days followed by refluxing at reduced pressure over fresh CaH_2 for 24 h and distillation onto dried Molecular Sieve for storage. For use in a reaction the solvent was distilled directly from the storage flask to the reaction vessel using a room temperature to ice water temperature gradient.

Liquid ammonia was dried by storage for several days as a liquid ammonia solution of sodium. For use in a reaction the ammonia was distilled into the reaction vessel through a trap, a glass wool filter, or both to prevent the entrainment of the fine particles of sodium formed by either boiling the liquid solution or subliming the ammonia from the frozen solution.

The 2,2,2-crypt (Merck) was used as received from E. M. Laboratories and was handled only in the drybox.

A sketch of a typical apparatus used in the synthesis of the polyanionic salts appears in Figure 2. To produce $(\text{crypt } K^+)_2Te_3^{2-}\cdot en$ stoichiometric quantities of K_2Te and crypt (0.03 and 0.10g respectively) were combined with an excess (0.2-0.3g) of tellurium in section A of the apparatus, the entire apparatus evacuated to below discharge, 40

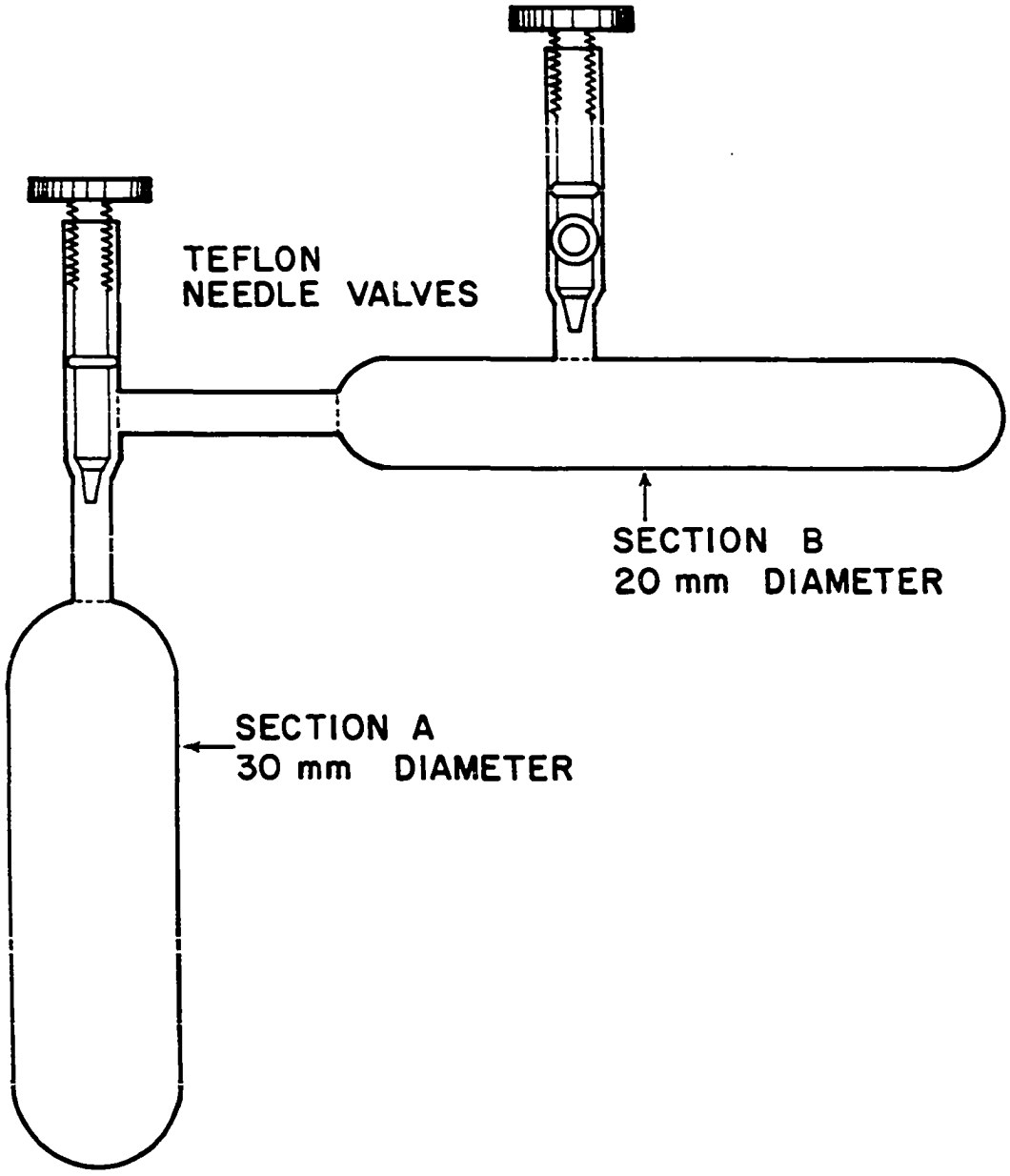

Figure 2. General design for the apparatus used in the synthesis of (crypt K)$_2$Te$_3$·en and (crypt K)$_2$Bi$_4$. All of the Teflon needle valves used had 4 mm bores.

to 50 mL of en distilled in, and the mixture allowed to warm to room temperature. The immediate result was a green solution (from the mixture of yellow Te^{2-} and blue Te_2^{2-}) which over a period of three days became blue (Te_2^{2-}), then purple (a mixture of Te_2^{2-} and red Te_3^{2-}) and finally a deep clear red (Te_3^{2-}) which did not change on further standing. The solution was decanted into section B and away from the excess tellurium, and the deep red hexagonal and triangular crystals grown by evaporation of the solvent. Crystals up to several millimeters on an edge could be obtained by reducing the rate of solvent evaporation.

The same deep clear red solution obtained from the above reaction was obtained in minutes with no hint of either other colors or undissolved solids by condensing en onto a stoichiometric mixture of crypt and K_2Te_3. If crypt is omitted and only K_2Te and tellurium reacted in en the same series of colors is observed, but solvent evaporation yields only a pasty, non-crystalline purplish red sludge.

If sodium is substituted for potassium the same sequence of colors is observed with the same sequence of ions presumably formed. No effort was made to characterize this system however because of the greater stability of the potassium-crypt complex and the superior crystals for the potassium salt.

When liquid ammonia (ℓ NH_3) is used as the solvent, the same series of colors is again observed, however evaporation at low temperature (ℓ NH_3 bath, approximately -40°) produces only a dark red powder. When the evaporation is carried on at room temperature crystals result, but all of those examined have proven to be non-single. The powder

pattern of this material differs drastically from that calculated for $(\text{crypt } K^+)_2Te_3^{2-}\cdot en$.

The tetrabismuthide salt, $(\text{crypt } K^+)_2\ Bi_4^{2-}$, is the unique crystalline product when any of the compounds in the potassium-bismuth system or mixtures of them are reacted with crypt in en at room temperature. In a typical reaction stoichiometric amounts of the intermetallic compound and crypt are loaded into section A of the same type of vessel as used in the telluride reaction, the vessel is evacuated and the solvent distilled in. The exact course the reaction follows after this depends on which starting compound has been used.

The fastest reaction is observed with either of the intermediate compositions in the system. This probably results because these intermetallic compounds are the least stable of the four, as indicated by their lower melting points.

After condensing the solvent, a deep clear green solution rapidly forms and after standing overnight at room temperature the solution is intensely colored and exhibits a dichroic character, green in thin layers and red in thick layers. This solution does not appear to change further for many weeks, although a slight amount of gas evolution, presumably H_2 from solvent reduction, is detectable. After 7-10 days tiny black crystals appear on the walls just above the alloy. These hexagonal appearing crystals exhibit no color under microscopic examination but leave a very dark green streak when ground to a very fine powder in a mullite mortar. After an additional week these crystals were about 0.2 mm in diameter, and the solvent could be decanted and

crystals removed for structural study. If instead the reaction was allowed to continue, the crystals would either grow larger or more would nucleate until all of the starting intermetallic was consumed, at which time the gas evolution ends and the solution fades to a deep clear emerald green. This final color comes from a more reduced solution in equilibrium with the solid salt and is necessary if the salt is to be stable in the presence of en. If fresh en is condensed onto crystals of the tetrabismuthide salt, they disproportionate to form this colored solution and bismuth.

The reaction equation inferred from this, ignoring intermediates only present in solution, is,

$$K_5Bi_4 + 5\ crypt + 3en \rightarrow (crypt\ K^+)_2Bi_4^{2-} + 3(crypt\ K^+)en^- + 3/2\ H_2\ \uparrow$$

where en^- represents the amide formed by removing a proton from an en molecule. The coefficients of this equation can be varied to fit any composition for the starting intermetallic.

If the most reduced compound in the system, K_3Bi, is used as the starting material, the reaction follows the same course, but proceeds much more slowly, with the green solution taking days to form and then becoming dichroic over a period of about two weeks. Crystals take another two weeks to appear, and the entire reaction requires several months to run its course, with more gas evolution than with the less reduced compounds, as expected.

When KBi_2, which already has the correct stoichiometry for the final product, is used, the solution initially formed is brown but it becomes dichroic after about a week. After about a month the same crystals begin

to appear on the surface of the intermetallic compound. The starting material is consumed slowly and even after about a year some of it remains, although the color of the solution reverts to brown after about six months.

When any of the polybismuthide solutions come in contact with the Teflon needle valves they leave a dark deposit. If they remain in contact with it the deposit grows and the solution decolorizes. Much of this deposit can be wiped from the Teflon and most of what does not wipe off dissolves in nitric acid, but in severe cases the plastic is permanently discolored.

Evaporation of any of the intensely colored solutions fails to produce any crystalline material, uniformly yielding a dark brown paste. On several occasions this paste was deposited in a manner superficially quite similar to dendritic crystals, but a closer examination of these promising "crystals" revealed their true paste nature.

Other solvents, such as liquid ammonia and acetonitrile were tried in these reactions, and only the latter showed any activity in a period of days. This was the formation of a coffee-brown solution which did not yield any crystalline material either on standing three weeks or on evaporation of the solvent.

If en is condensed on the intermetallic compound in the absence of crypt no reaction is observed with either K_3Bi or KBi_2, but both K_3Bi_2 and K_5Bi_4 give a purple solution, the color reported by Zintl for Bi_3^{3-}.[9] When this purple solution is poured off the intermetallic compound and onto crypt it immediately reacts to form a green solution.

This reaction is sufficiently exothermic to boil the solvent in the vacuum.

Preparation of zirconium dichlorides

In a recent study it was shown that zirconium monochloride is a far more reactive reductant for the tetrachloride than is metallic zirconium.[30] Therefore ZrCl and $ZrCl_4$, which are the only easily accessible stoichiometric compounds in the Zr-Cl system, were used as starting materials in all efforts to produce zirconium dichlorides. Although the tetrachloride was prepared in glass, all further reactions were carried out in tantalum containers which were arc welded closed with 0.5 atmosphere, or less, of He inside. The use of tantalum for an inert container material avoided the contamination of the product with oxides, silicides, or oxychlorides which form by reaction of the reduced chlorides with glass and allowed the containment of pressures to 30 atmospheres, far higher than ordinary glass containers could withstand.

Zirconium tetrachloride was prepared by passing a stream of chlorine (Matheson Gas Products) over strips of reactor grade zirconium foil (~ 0.05% Hf) heated to 400°. Initially the product was pale yellow due to iron apparently entrained with the chlorine, but this was removed by subliming the tetrachloride from strips of fresh zirconium foil at 235°.

Zirconium monochloride was prepared quantitatively from the tetrachloride and Zr turnings using the method developed by Daake.[30] Stoichiometric quantities of the two materials were sealed in a tantalum tube, and heated gradually, over a period of 2 weeks to 850°, and held there for a week before cooling.

Powdered dichloride samples were prepared by combining weighed quantities of ZrCl and $ZrCl_4$ in a 6 mm tantalum tube and heating it isothermally between 600° and 700°. Because there is a substantial pressure of $ZrCl_4$ formed by the disproportionation reaction;

$$ZrCl_{2(s)} \leftrightarrow ZrCl_{2-x(s)} + ZrCl_{4(g)}$$

a slight excess of $ZrCl_4$ was always required. An unfortunate result of this gas phase was the contamination of all powdered samples with traces of $ZrCl_3$ which is formed by the back reaction of the tetrachloride gas with the dichloride on cooling. This contamination was limited to the surface however, as reactions in this system are generally so slow (6-8 weeks for a typical equilibration) that nothing more than a small amount of back reaction occurs during the few hours necessary for cooling and the bulk of the material is unaffected. Isothermal equilibrations produced the bulk of the dichloride material made, including all of the cluster compound.

Single crystals of the slab-type dichloride were produced by gas transport using this autogenous pressure to furnish a transport medium. In a typical reaction 2.50g of a mixture of ZrCl and $ZrCl_4$ having a net composition of about $ZrCl_{1.3}$ was loaded into an 8.7 mm (i.d.) Ta tube about 14 cm long. For a transport reaction the tube was welded shut at the lowest pressure at which an arc could be maintained, generally about 1/6 atmosphere. After sealing the Ta tube into an evacuated Vycor jacket, thermocouples were attached to the outside of the jacket. To compensate for a reduction in gradient inside the Ta tube because of the

heat conduction of the metal, the thermocouples were placed about 5-7 mm inward from the actual ends of the inner metal tube.

Initially the container was heated isothermally to 350° to affect the reduction of the bulk of the tetrachloride. It was then brought gradually up to the desired gradient temperature, with care being taken to insure that the temperature at the cool end never exceeded the desired final temperature. The gradients used were 750° to 650°, 700° to 650°, 750° to 700°, and 700° to 750°, with the temperature of the starting material listed first in each case.

In each case the double container with attached thermocouples was placed in an Inconel pipe at least 6 cm longer than the Vycor jacket to insure an even gradient. Two methods were used to create gradients. The first of these involved gradually pulling the Inconel pipe out of a tube furnace while increasing the temperature of the furnace until the desired gradient was achieved. When a multiple zone furnace with separate controls for each zone became available it proved advantageous to vary the temperatures of two adjacent zones until the desired gradient was obtained. Reaction times ranged from 3 to 8 weeks after the gradient was established.

In all cases the cooler end of the tube was elevated relative to the hotter to promote convection within. Schäfer states that when the total pressure exceeds three atmospheres in a closed tube transport reaction with a tube about 20 mm in diameter convection becomes the predominant factor in the movement of the material being transported.[57] Although the tubes used here were of significantly smaller diameter than

he described, the pressures were significantly above three atmospheres (actually between 5 and 10 atmospheres when the starting material was at 750° judging from the degree of end cap bulging). Convection was probably contributing to the transport which was significantly faster at this temperature (about twice as much material moved each week) than at 700°.

The only available estimate of the $ZrCl_4$ pressure over $ZrCl_2$ comes from Uchimura and Funaki[44] whose data only extend to 670°. If the equation they derive is used, the result is 1.0 atmosphere at 700°, 1.8 at 750°, and 3.05 at 800°, below the amount needed to account for the cap bulging at 750° and far below the degree of dissociation observed for an isothermal equilibration quenched from 800°.

In all of the transport reactions where the transport was from high to low temperature, crystals were found growing in the coolest 3 to 5 cm of the tube. These crystals of the slab-type dichloride, silvery with a metallic luster, occurred either as platelets with trigonal or hexagonal morphology and at least a 10 or 20 to 1 ratio of width to thickness or as very thin fern-like fronds clearly exhibiting a dendritic growth pattern but still having hexagonal angles. Some good quality crystals could also be found intermixed with the untransported material. This is somewhat surprising for it implies growth in an isothermal region, but in all of the isothermal equilibrations no crystals were ever observed which were large enough to discern individually, even after longer reaction times.

X-Ray diffraction: powder patterns

Powder patterns used for identification of the intermetallic compounds were taken with an 11.46 cm diameter Debye-Scherrer camera and Ni-filtered CuK_α radiation (λ = 1.5418Å) for a dispersion of 1° in 2θ for each 1 mm of film.

For the zirconium dichloride work, where precision lattice constants were needed, an evacuable Model XDC-700 Guinier camera (IRDAB, Stockholm) equipped with a quartz bent-crystal monochromator and adjusted to produce a CuK_{α_1} (λ = 1.54056Å) incident beam was employed. This unit produces a dispersion of 1° in 2θ for each 1.75 mm of film which, coupled with a measurement reproducibility of 0.01 to 0.02 mm for line positions, yields a precision of ±0.005° to 0.010°. To insure accuracy a precision scale was printed on the film before the pattern was taken using an IRDAB SDC Scaling Device. Use of this scale automatically compensates for non-linear film shrinkage as well as for variations in film size due to temperature changes during reading. Line sharpness was further enhanced by developing only the front side of the film. Line positions were referenced to Si powder (NBS Standard Reference Material 640, a_o = 5.43088Å) which was mixed with the sample.

All of the powder samples were mounted in the drybox by placing the material and the internal standard on a strip of tape previously attached to a washer of proper size to fit into the camera. This was covered with a disk of tape previously cut with a cork borer. Very few specimens showed any reactivity towards the tape, and these only reacted slowly.

Lattice parameters were obtained from indexed patterns using a local lattice refinement program which has provision for assigning poorly measured (weak or broad) lines a lesser weight in the refinement.[58] Calculated powder patterns were produced by the program produced by Clark, Smith, and Johnson[59] modified to match local conventions and machine configuration and to add the appropriate Lorentz-polarization factor for the Guinier-Hägg geometry as an option. This program includes intensity corrections for absorption for either Debye-Scherer or flat-plate geometrics.

Two types of intensity measurements were used. For most work visually estimated values, coupled with direct pattern to pattern comparisons, were sufficient. When more accurate values were needed the film was scanned with a Jarrel-Ash microdensitometer and the density profile converted to integrated intensities by either cutting out each peak and weighing it or tracing each peak with a planimeter.

X-Ray diffraction: single crystals

For single crystal studies the reaction vessel was opened in a drybox specially designed for crystal mounting and described in detail elsewhere.[37] Individual crystals with well-developed faces and maximum dimensions in the range of 0.2 to 0.3 mm were selected, picked up with a glass fiber dipped in Vaseline, and inserted into 0.2 or 0.3 mm diameter Lindemann glass capillaries. These capillaries were sealed inside the drybox with a hot wire, outside the drybox again with a gas torch and the ends capped with black wax (Apiezon W). Vaseline was used almost exclusively for mounting crystals as it proved inert towards all

of the compounds. When silicone grease was used to mount a batch of (crypt K^+)$_2$ Bi_4^{2-} crystals, they rapidly decomposed.

All of the crystals successfully mounted were examined with oscillation photographs taken with a standard Weissenberg camera and Ni-filtered CuK_α radiation. With the cluster anion crystals all of the specimens examined were either good quality, or so poor that this was apparent after a simple oscillation photograph.

With zirconium dichloride the crystals were so thin that many bent during mounting such that a crystal which gave good sharp spots in an oscillation photo would give streaks parallel to the direction of translation in a Weissenberg photograph,[60] (or oscillation photograph taken with the film translating). This effect is observed when the crystal is bent to follow the wall of the capillary and the capillary is coincident with the axis of rotation. In this arrangement the same planes of the crystal come into diffracting position at different times for different parts of the crystal. If the film has not moved relative to the crystal, as in a normal oscillation photograph, both parts of the crystal will diffract to the same point, but if the film has moved, as in a Weissenberg photograph, they will diffract to different points on the film. If the crystal makes a continuous curve the diffraction onto moving film will be a streak.

Many of the dichloride crystals were fully aligned and Weissenberg photographs taken. Besides revealing difficulties such as the above these photographs revealed much information which would not have been forthcoming if only diffractometer techniques had been employed.

The data used for the structure refinements were collected using an automated four-circle diffractometer designed and built in the Ames Laboratory and described in detail elsewhere.[61] The indexing scheme used by this unit involves taking additional oscillation photographs on the diffractometer with Polaroid film and then locating these points with the diffractometer by starting with the location indicated by the film. The locations of 8 to 10 reflections determined in this manner are then used to determine the unit cell by an algorithm described in detail elsewhere.[62]

Data collection for $(crypt\ K^+)_2\ Te_3^{2-}\cdot en$

The crystal selected had the form of a triangular pyramid with truncated corners (C_{3v} symmetry) 0.2 mm in height, 0.3 mm on basal edges. Trigonal symmetry with a = 12.26Å and c = 31.33Å was indicated by the initial orientation and integrated intensity data were collected on this basis at a temperature of $\sim$ 25° for $2\theta \leq 50°$ using Mo K_α radiation monochromatized with pyrolytic graphite (λ = 0.70954Å) at a take-off angle of 4.5°. During data collection the intensities of three different standard reflections were monitored every 75 reflections to check for instrument and crystal stability. A total of 5591 reflections were examined over the HKL and $HK\bar{L}$ octants with standard reflection decay of only about 1%. Final unit cell parameters of a = 12.229(1)Å and c = 31.242(4)Å were obtained from the same crystal by a least squares fit[63] to twice the Ω values of 14 reflections each of which was tuned on both Friedel-related peaks to eliminate instrument and centering errors.

These dimensions give a volume of 4046$\mathring{A}^3$ and a density of 1.57 g/cm^3 for Z = 3 and a formula weight of 1274.10.

The observed intensities were corrected for Lorentz and polarization effects, but no absorption correction was made as the linear absorption coefficient was calculated to be only 18.8 cm^{-1}.[64] A total of 2385 reflections were "observed" by the criterion $I>3\sigma(I)$, and 2033 unique reflections remained after averaging of equivalent reflections. The condition $\ell = 3n$ for observation of 00ℓ reflections indicates a three-fold screw axis parallel to c and requires that the compound be in one of ten space groups which make up five enantiomeric pairs, $P3_1$ (C_3^2, No. 144) and $P3_2$ (C_3^3, No. 145), $P3_112$ (D_3^3, No. 151) and $P3_212$ (D_3^5, No. 153), $P3_121$ (D_3^4, No. 152) and $P3_221$ (D_3^6, No. 154), $P6_2$ (C_6^4, No. 171) and $P6_4$ (C_6^5, No. 172), and $P6_222$ (D_6^4, No. 180) and $P6_422$ (D_6^5, No. 181). These choices were reduced to one pair, $P3_1$ and $P3_2$, by the lack of any symmetry higher than $\bar{3}$ in the diffraction data, that is, averaging the data[58] in the higher Laue classes $\bar{3}2/m$ and 6/m gave poor agreement between supposedly equivalent reflections, while in $\bar{3}$ the equivalent pairs matched quite well.

Structure determination and refinement for $(crypt\ K^+)_2\ Te_3^{2-}\cdot en$

The trial structure was obtained by conventional heavy atom techniques, the shape of the anion being readily apparent from the Patterson map.[60] Full matrix least squares refinement of the tellurium and potassium atom positions with isotropic thermal parameters using a locally modified version of Busing et al. ORFLS[65] resulted in an

unweighted factor $R = \Sigma||F_o| - |F_c||/\Sigma|F_o|$ of 0.22. Location of the 52 independent non-hydrogen atoms of the two crypt molecules by Fourier synthesis and refinement of their positions and isotropic temperature factors resulted in R = 0.13.

Examination of an electron difference map calculated with ALFF[66] at this point revealed the presence of four peaks near the tritelluride ion arranged roughly in the manner expected for the non-hydrogen atoms of an ethylenediamine molecule. On introducing these and conversion of the tellurium and potassium atoms to anisotropic temperature factors (of the form $\exp-(h^2\beta_{11} + k^2\beta_{22} + \ell^2\beta_{33} + 2hk\beta_{12} + 2h\ell\beta_{13} + 2k\ell\beta_{23})$) refinement of all 269 independent parameters gave R = 0.095 and $R_w = [(\Sigma w(|F_o| - |F_c|)^2/\Sigma w|F_o|^2]^{1/2} = 0.123$, where w was set equal to σ_F^{-2}. Because of a strong systematic dependence of $||F_o| - |F_c||$ on $\sin\Theta/\lambda$ and F_o the data were reweighted in 20 groups to minimize these dependences, giving final values R = 0.094 and $R_w = 0.103$. The largest shift in any variable during the last cycle of refinement was 0.12σ in en atoms, 0.05σ in crypt atoms, and 0.03σ in heavy atoms. A difference Fourier map indicated residuals only $< \pm 0.5\ e^-/A^{\circ 3}$ except near the tellurium atoms where there were up to $\pm 0.75\ e^-/A^{\circ 3}$. The 80 unlocated hydrogen atoms in this compound account for 12.5% of the total electron density and furnish a plausible explanation for R being above 0.09.

The correct resolution between the enantiomeric space groups $P3_1$ and $P3_2$ was accomplished by refinement of all final parameters to convergence in both of the possible space groups, relying on the anomalous dispersion of tellurium and potassium[67] to indicate the correct choice.

Data collection and structure determination for $(crypt\ K^+)_2\ Bi_4^{2-}$

Monoclinic symmetry and approximate lattice parameters of a = 20.13Å, b = 11.95Å, c = 11.10Å and β = 99.5° with C-centering was indicated by the initial orientation. This turned out to be only an approximation to the true triclinic cell because of an accidental near-equality of a and b in the crude reduced cell combined with the actual near-equality of α and β. Four octants of intensity data were collected for the monoclinic cell at ~25°C for $2\theta \leq 50°$ using MoK_α radiation. During data collection the intensities of three standard reflections were monitored every 75 reflections to check for instrument and crystal stability. Whenever a significant drop in the intensity of one or more reflections was observed all three of the reflections were relocated and their integrated intensities redetermined. A 40% decay in standard intensities was found by the end of the second octant, and 75% by the end of the fourth. A total of 5345 reflections were examined, including 521 not allowed for C-centering which were all unobserved. All intensities were corrected for isotropic decay through a least squares fitting of a third order polynomial to the measured standard intensity sum as a function of reflection count.[68] After decay correction 2978 reflections with $I > 3\sigma_I$ were considered observed.

The observed intensities were corrected for Lorentz, polarization, and absorption effects (μ = 128.8 cm^{-1}),[64] and the data averaged for monoclinic symmetry to yield two different data sets, one with reflections using only the first two octants (sufficient for monoclinic) and the other for all four octants averaged to the unique two. Patterson

maps calculated from both data sets could not be interpreted in any chemically reasonable way given the limitation of four cryptated cations per unit cell imposed by the volume. A careful examination of the data averaging indicated that the data indeed possess only triclinic symmetry. Although many reflections were observed only once, only a statistical number of those observed twice matched well and almost all of the reflections observed four times showed a two-and-two pairing, all typical of averaging for too high a Laue group.

At this point, all of the reflections were reindexed using the primitive triclinic reduced cell which has half the volume of the monoclinic cell and for which all reflections correspond to those allowed with C-centered monoclinic. This cell had only enough volume for two cryptated cations, and the calculated Patterson map clearly revealed the positions of the two bismuth atoms comprising a square planar Bi_4^{2-} anion with C_i point symmetry, indicating $P\bar{1}$ as the correct choice of space group. A Fourier synthesis indicated the position of the potassium atom and a second synthesis with the three heavier atoms revealed all 26 light atom positions. Full matrix least-squares refinement of the structure using anisotropic temperature factors for heavy atoms and isotropic temperature factors for light atoms converged at R = 0.17. A careful examination of the data indicated that the greatest variation between observed and calculated structure factors occurred for the reflections with the largest decay correction, so no further refinement was attempted using these data.

Data were retaken at room temperature using two crystals one of which approximated a hexagonal plate 0.03 mm across and 0.005 mm thick and the other a triangular prism 0.005 mm thick and 0.03 mm long. The initial orientation for both indicated triclinic symmetry and approximate parameters of a = 11.63Å, b = 11.83Å, c = 11.13Å, α = 98.3°, β = 98.0°, and γ = 61.4°, the same as had been obtained before. One hemisphere of integrated intensity data was collected using four standard reflections in an effort to obtain a better measurement of crystal decay. Data collection with the first crystal was terminated at the point when the standard intensities had decayed by 40%, at the end of the first and largest octant, and the remaining reflections were measured on the second crystal with a 36% standard decay during data collection. All corrections were carried out as above, with the transmission coefficients for the first crystal ranging from 0.090 to 0.207 and the second, from 0.135 to 0.328.

Final unit cell parameters of a = 11.604(4)Å, b = 11.796(4)Å, c = 11.096(3)Å, α = 98.12(3)°, β = 98.02(3) and γ = 61.37(3) were obtained from the second of these crystals by a least squares fit[58] to the 2θ values of 29 reflections (24° < 2θ < 32°), each of which was tuned on both Friedel-related peaks to eliminate instrument and centering errors. These dimensions give a volume of 1315.2(7)Å^3 and a density of 2.11 g/cm^3 for Z = 1 and a formula weight of 1667.12. Scattering factors used were those of Hanson et al.[69] and included corrections for the anomalous dispersion of bismuth and potassium.

Of the 4955 reflections examined in four unique octants (HKL, $H\bar{K}L$, $\bar{H}KL$, and $\bar{H}\bar{K}\bar{L}$), 2880 reflections were considered observed with $I>3\sigma_I$. Redundant reflections were averaged when both observations had been made on the same crystal, but when one observation had been made on each crystal that member of the pair was eliminated which required the larger decay correction, leaving 2704 unique reflections. The data from each crystal were scaled separately.

Structure refinement for $(\text{crypt } K^+)_2\ Bi_4^{2-}$

The final atomic parameters deduced with the first data set produced a R value of 0.14 with the new data set with no refinement, and after refinement R = 0.128 and R_w = 0.157. Introduction of anisotropic temperature parameters for the light atoms produced a slight improvement in the unweighted residual, 0.122, and a significant[67] improvement in the weighted R, 0.149. Examination of both the isotropic and anisotropic temperature factors at this point revealed that the carbon atoms at the end of the crypt closer to the anion had much larger and much more anisotropic temperature factors than those at the other end. Drawings of the structure made at this point, Figure 3, indicated that the more anisotropic atoms were elongated in the direction in which the ethylene bridge was least constrained, with rms displacements in the longest dimension about twice those of the atoms at the other end of the ion (Figure 3b).

A difference map calculated with these six atoms (C2, C3, C17, C18, C19 and C20) removed clearly showed doubled peaks for four of the six, C2, C3, C17 and C20, serving to confirm directly the disorder which has

Figure 3. The crypt-potassium cation in (crypt $K^+)_2Bi_4^{2-}$ before the resolution of the disorder among the carbon atoms. The contrast in the anisotropic thermal ellipsoids for the disordered atoms, C2, C3, C17, and C20, which are at the front in (a), and those for the equivalent atoms at the opposite end of the ion, at the front in (b), is apparent.

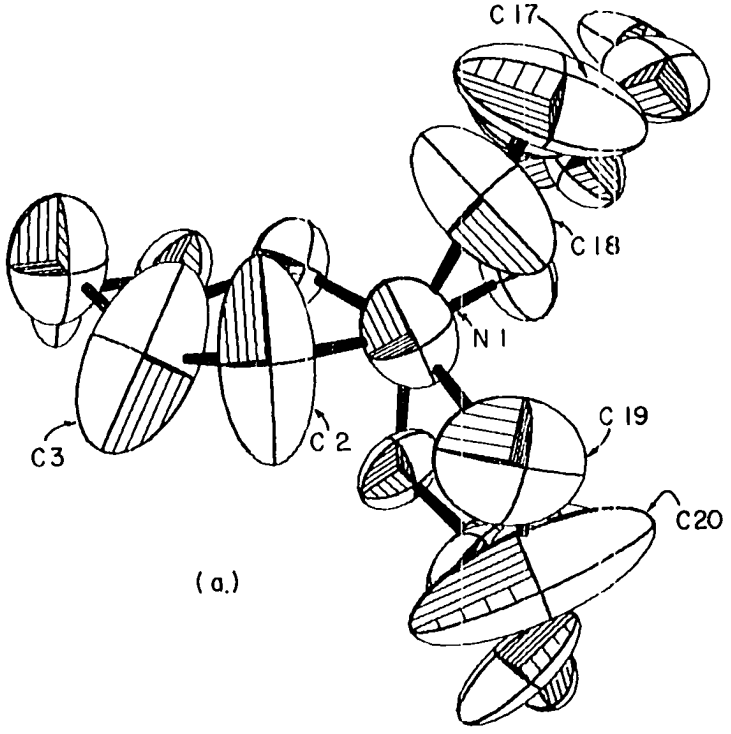

(a.)

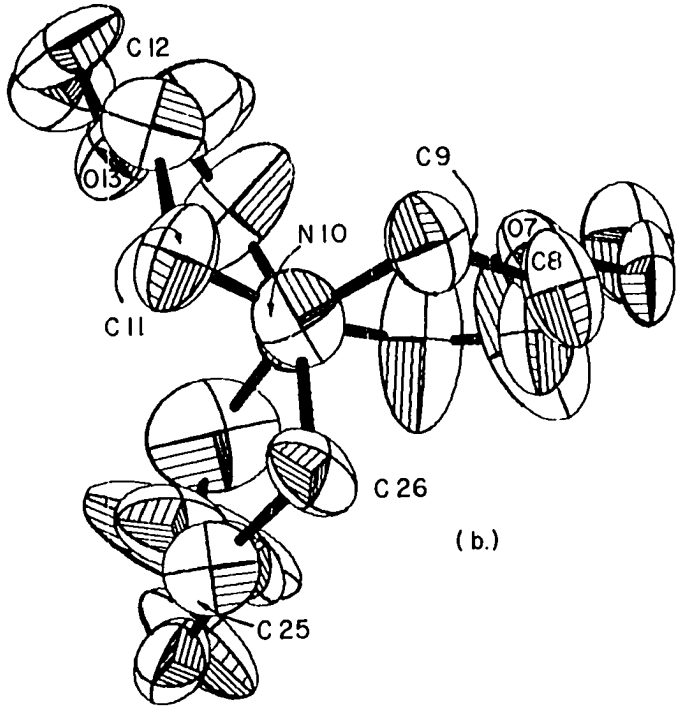

(b.)

been suspected in previous structures.[17,26] These four atoms were replaced by eight atoms at the locations indicated by the difference map, each with an occupancy of 0.50 and an isotropic temperature factor. Another map was calculated with C5 omitted since its temperature factor was similar to C2 and C3, but separate atoms at this location were unresolved. Refinement of all parameters converged at R = 0.122 (R_w = 0.148). Variation of the occupancies of the fractional atoms demonstrated that the occupancies and temperature factors were strongly coupled, even when they were varied in alternate cycles of refinement, and that the occupancies did not refine more than 1σ from 0.50, so these were fixed at that value. It did not seem appropriate to attempt anisotropic refinement of fractional carbon atoms in close proximity to each other and the bismuth atoms. Because of a small dependence of $||F_o| - |F_c||$ on F_o, and because the standard deviation for an observation of unit weight was 4.01, the data were reweighted in 20 overlapping groups sorted on F_{obs}, after which the refinement converged at R = 0.121 (R_w = 0.147) for 260 independent variables. The largest change as a result of this reweighting was a small ($\leq$ 8%) drop in positional standard deviations. The largest shifts during the last cycle of refinement were 0.12σ for light atom and 0.009σ for bismuth atom parameters. A difference Fourier map indicated a residual of 2.4 $e^-/A^{\circ 3}$ (at 0.240, 0.995, 0.693) which could not be connected with any feature of the structure, while the rest of the map was flat to $<\pm 1$ $e^-/A^{\circ 3}$ except near the bismuth atoms where variations were as great as ± 2 $e^-/A^{\circ 3}$. The final standard deviations in individual positional

parameters ranged from 0.0014 to 0.0017Å for bismuth, 0.02 to 0.03Å for oxygen and nitrogen, and 0.03 to 0.06Å for the carbon atoms, with the upper limit in the last being reached only for the disordered carbon atoms.

Although a final R value of 12.1% may seem somewhat large, it is not in this case indicative of a defective structure when the more pertinent positional errors are considered. Standard deviations of these are all acceptable, those for the light atoms being in fact equal to or better than those in other low symmetry structures involving crypt cations with lighter anion components (Ge, Sn, and Sb from other reports[17,26,27] and Te elsewhere in this dissertation) which also refined to comparable residuals. The larger but relatively random errors in the data set are believed to arise from the need to collect data from two crystals with the consequent need for two major decay and absorption corrections.

Structure determination of Zr_6Cl_{12}

The complex powder pattern of an unknown and previously unobserved zirconium chloride was indexed by comparison of the observed pattern with a calculated pattern obtained using the atom positions for Zr_6I_{12}, the lattice parameters for Sc_7Cl_{12},[70] and the scattering factors for zirconium and chlorine. The 30 sharpest lines from the indexed pattern were used to obtain lattice parameters of a = 12.973(1)Å, and c = 8.782(1)Å.

With the improved lattice parameters, a better match of observed

and calculated intensities was obtained by using the atom positions for Sc_7Cl_{12}, but omitting the isolated metal atom at the origin. It was clear from the differences in the calculated intensities that the correct formula for this compound is Zr_6Cl_{12} and not Zr_7Cl_{12}.

The correct space group for this compound is $R\bar{3}$, (C_{3i}^2, No. 148) with 3 M_6 clusters in each unit cell, the same as Zr_6I_{12} and Sc_7Cl_{12}. Although over 50 lines were indexed, this powder data was insufficient to carry out a least squares refinement due to the fact that in the $\bar{3}$ Laue symmetry numerous sets of reflections which have the same diffraction angle, such as 520 and 250, are not equivalent, and there is no way to apportion the observed intensity between them. A further improvement in the agreement between the observed and calculated intensities (to $R_I = (\Sigma|I_o-I_c|)/\Sigma I_o = 0.27$) was obtained by adjusting the atom positions so as to approximate the bond lengths observed in the compound Zr_6Cl_{15}, which is also based on a Zr_6Cl_{12} structure unit.

Data collection for $3R\text{-}ZrCl_2$

Initial orientation for a crystal grown by R. L. Daake in a 750° to 650° gradient and believed to have a composition of $ZrCl_{1.75}$[30] indicated that the crystal had a c-centered monoclinic unit cell with $a = 5.91\text{Å}$, $b = 3.36\text{Å}$, $c = 7.53\text{Å}$, and $\beta = 121.3°$. Examination of 259 reflections for a primitive cell showed no violation of the c-centering condition, $h + k = 2n$ for an observed reflection, so the remainder of the 570 reflections examined were only those allowed for c-centering. All 447 allowed reflections were observed in a complete hemisphere to

a maximum 2Θ value of 60° using MoK_α radiation. The parameters listed in the first column of Table II were obtained by a least squares fit[58]

Table II. Lattice parameters for $3R\text{-}ZrCl_{2.0}$

Parameter	Monoclinic	Hexagonal	Rhombohedral
a	5.860(1)Å	3.3819(3)Å	6.748(1)Å
b	3.3816(6)Å	-	-
c	7.553(2)Å	19.378(3)Å	-
α	-	-	29.025(3)°
β	121.20(2)°	-	-
Volume	128.04(4)Å^3	191.94(4)Å^3	63.98(3)Å^3

to the 2Θ values of 20 reflections (40° < 2Θ < 50°), each of which was tuned on both Friedel-related peaks.

All of the statistical tests indicated that the structure was acentric, and this, coupled with c-centering, limited the choice of space groups to three, C2 (C_2^3, No. 5), Cm (C_S^3, No. 8), and Cc (C_S^4, No. 9). The last of these can be eliminated since the volume limits Z to 2, and Cc has only four-fold positions.

Structure determination and refinement for $3R\text{-}ZrCl_2$

C-centering, which is a translation of (1/2, 1/2, 0) for all atoms, together with the condition $a = \sqrt{3}b$, generates, within experi-

mental error, a hexagonal close packed layer parallel to the a-b plane. The two-fold special positions in both space groups generate one such layer per unit cell.

Since in both space groups it is necessary to fix the origin by fixing the position of at least one atom, a location which was common to the special positions in both space groups, (0,0,0), was selected and used as the fixed location of the zirconium atom in an effort to phase the structure. The resulting monoclinic electron density map had 8 peaks which could be interpreted in two ways. The peaks could either represent one chlorine on a general (four-fold) position in C2, and a false set of inversion related peaks resulting from the centric phasing produced with only the metal atom present, or they could represent two chlorines on special (two-fold) positions in Cm, with their inversion related shadows. After testing both possibilities, the latter was shown to be correct by the fact that it refined better.

Refinement of the structure using the 199 unique reflections (when the data were averaged for monoclinic symmetry) produced an R of 0.102 with isotropic temperature factors and offered no evidence of an additional, fractionally occupied zirconium position. Further refinement with anisotropic temperature factors produced an R of 0.088, but still no sign of the fractional zirconium required if the composition were $ZrCl_{1.75}$. Some difficulties encountered at this point were a tendency for one of the zirconium temperature factors to go negative and large standard deviations (about 0.01Å) for chlorine atoms.

These difficulties, together with the previously mentioned nearly

hexagonal arrangement within the sheets of atoms, led to a careful reexamination of the results. From this reexamination it was apparent that the data could be reindexed onto a rhombohedral unit cell which in its hexagonal setting has nearly the same dimensions as the cell deduced by Daake for this compound from powder data.[30] This reindexing was accomplished by multiplying the reflection indices, taken as column matrices, by:

$$\begin{vmatrix} -1/2 & -1/2 & 0 \\ 1/2 & -1/2 & 0 \\ 2 & 0 & 3 \end{vmatrix}$$

With the data reindexed, the second and third unit cells in Table II were obtained. Because the primitive rhombohedral cell and the reduced cell for the c-centered monoclinic cell are the same in terms of axes (but not in terms of symmetry) all of the reflections for the rhombohedral cell had been examined. After reindexing, averaging for trigonal symmetry produced 98 unique reflections with no rejections and $R_{ave} = 0.040$.

Daake had suggested that the structure of $ZrCl_{1.75}$ was very similar to that of 3R-NbS_2, but not identical, as he had observed extra lines not allowed for rhombohedral symmetry. Although this suggestion had been deliberately ignored at first to see where the loss of symmetry indicated by the extra lines led, at this point it seemed clear that this crystal had full rhombohedral symmetry. The correct space group for 3R-NbS_2 is R3m (C_{3v}^5, No. 160), with all of the atoms located on the

3a (0,0,z) position.[71] The orientation of this cell with respect to the monoclinic one is such that the z axis of the hexagonal cell, which is a three-fold rotation axis, lies in the mirror plane, and all three atoms lie within one standard deviation of the axis.

When the atomic coordinates were converted from monoclinic to hexagonal they were found to be roughly the same as those reported for 3R-NbS_2, or 3R-MoS_2[71] which is isoelectronic with $ZrCl_2$. Refinement with isotropic temperature factors produced an R of 0.103, and gave no evidence of any other metal atoms, even at the octahedral site between slabs where one is believed to occur in 3R-$Nb_{1+x}S_2$[71]. At attempt to put a fractional atom at this site resulted in a large increase in R_w and a large temperature factor (nearly 100 times that of the other zirconium), indicative of the refinement's attempt to get rid of the atom by spreading it extremely thin. When the occupancy was allowed to vary with the temperature factor fixed at slightly larger than the first zirconium it dropped to 0.013 with a standard deviation of 0.012.

Conversion to anisotropic temperature factors allowed refinement to an R factor of 0.082 (R_w = 0.116) and still showed no evidence of any other atoms. Allowing the occupancy of the three atoms definitely present to vary did not result in a change from unity of even one standard deviation, and was taken as a final indication that the composition of the crystal examined was actually $ZrCl_{2.00(1)}$. Reweighting the dataset allowed the final refinement to go to an R of 0.094, with an R_w of 0.074. No absorption correction was carried out, as the

absorption coefficient for this compound was not large ($\mu = 58.6 cm^{-1}$)[64] and the shapes of the final refined thermal ellipsoids did not suggest any need for such a correction.

Further data collection and refinements on other $ZrCl_2$ crystals

Four other crystals were oriented and data collected as described above; their lattice parameters and other pertinent data appear in Table III.

The first of these crystals had a three slab repeat, based on the length of the c axis, but a primitive unit cell.

Examination of the data from crystal I indicated that almost all of the intensity arose from reflections allowed for either the obverse or reverse orientations of 3R-$ZrCl_2$. These two orientations actually are the same structure, with a 60° rotation (about c) in the choice of the hexagonal a and b axes used to define the coordinate system.[72] Because the hexagonal cell has three times the volume of the rhombohedral cell only a third of the possible reflections for a primitive hexagonal cell of the same dimensions are allowed for the R-centered hexagonal cell. These are those reflections with indices such that $-h + k + \ell = 3n$ if the obverse setting is chosen and $h - k + \ell = 3n$ if the reverse setting is chosen. As a result of this all reflections with $h \neq k$ are only allowed for one or the other, or neither, which creates two nearly unique sets of reflections. The coexistence of both sets of reflections indicates twinning with the components of the twin related by this 60° rotation. (For more details see the discussion of the slab-type compounds appearing later in the discussion section.)

Table III. Lattice parameters and number of observed reflections for four other dichloride crystals

Crystal	I	II	III	IV	
	3-slab	6-slab	6-slab	6-slab	
				3R-component	6T-component
a(Å)	3.3797(4)	3.3800(3)	3.3789(8)	3.3793(2)	3.3791(4)
c(Å)	19.386(2)	38.772(9)	38.721(21)	19.374(1)	38.713(7)
V(Å^3)	191.77(4)	383.60(12)	382.84(21)	191.60(2)	382.82(11)
Number of Reflections used in Lattice Calculation	21	26	9	6	6
Number of Reflections Observed	1149	1082	803	1452	
Fraction of Reflections Observed[a]	0.78	0.71	0.33	0.75	

[a] Based on a primitive lattice.

Also supporting this twinning hypothesis was the Patterson map calculated with these data which had all of the peaks expected for both rhombohedral orientations. The few observed reflections which were not allowed for either orientation and indicated a primitive cell were substantially weaker than the rest.

In an effort to learn something from this specimen a sorted dataset was prepared containing the reflections allowed only for the rhombohedral obverse setting at full intensity. Those either allowed for both rhombohedral settings, or forbidden for both, were included with their intensities reduced by a fraction equal to;

$$\frac{\Sigma I_{obv(h0\ell,0k\ell)}}{\Sigma I_{obv(h0\ell,0k\ell)} + \Sigma I_{rev(h0\ell,0k\ell)}}.$$

In this expression I_{obv} stands for the intensity of the obverse-allowed reflections, and I_{rev} the reverse-allowed reflections.

Using the atom positions obtained in the previous section, refinements led to an R of 0.136 (R_w of 0.284, with $w = \sigma_F^{-2}$) for P3 symmetry and an R of 0.154 (R_w of 0.519) for R3m symmetry. In neither case was there any evidence for the extra metal atom (or atoms) necessary to give a more reduced composition or to explain the observed loss of symmetry. Attempts to put extra atoms into the available holes in the structure led in the P3 case to R values of 0.33 to 0.35 (and R_w values of 0.49 to 0.55) even at very low fractional occupancies.

Another even less successful attempt to resolve this problem involved producing a dataset for the reverse orientation with

$$I_{rev} = I_{obs} - I_{calc(obv)}.$$

Refinement with this dataset led to an R of 0.41. This large R was directly attributable to very low values of I_{rev} as calculated above for the common reflections. It was quite apparent that these common reflections were not as intense as expected from the relative intensities of those unique to one set. A possible explanation for this lies in the differences in the makeup of the planes having indices allowing them to be observed for both orientations. These differences could lead to a lower diffracting efficiency for these reflections owing to destructive interference.

Crystal II had weak spots between those expected for a 3 slab repeat, indicating a doubled period in c, or 6 slabs to the stacking repeat. Because the superposition of the image of a 3 slab structure on top of a 2 slab can give the impression of a 6 slab structure, a careful examination of the data was in order. For such a superposition the only reflections observed for the 6 slab lattice will be those where ℓ is a multiple of 2 or 3 or both. The fact that a significant number of reflections were observed with ℓ being a prime number greater than 3 dismisses this possibility.

Like crystal I, most of the intensity was found in those reflections allowed for the 3R-$ZrCl_2$ structure in both orientations. For a 6-slab structure there are four ways this could come about; (1) a 6-slab structure based on 3-slabs in each orientation of the 3R form, (2) a twin of a 6-slab superstructure based on two repeats of the 3R structure in

either form, but both the same, (3) the same as above, but intergrown with segments of pure 3R-$ZrCl_2$, and (4) a 6-slab structure of some form (any other possible 6-slab stacking sequence) intergrown with both orientations of 3R-$ZrCl_2$ and with the 3R predominating.

A Patterson map was calculated and the first possibility immediately eliminated because of a peak at (0,0,1/2) which was ~90% the height of the origin peak. This requires most of the atoms in the unit cell to repeat after a z translation of c/2. The other three possibilities all allow this.

The second possibility could also be eliminated. If only the 6-slab was present, more intense peaks would be expected in the map for the extra atoms than were observed. Neither of the other possibilities could be eliminated and the structure could not be solved for this crystal which, while single, was not single phase to x-ray diffraction.

The most promising of these crystals, based on the relative spot intensities in Weissenberg photographs, was III, which appeared to be predominantly 6-slab material. Unfortunately once this crystal was mounted on the diffractometer so that it was possible to oscillate the crystal on all three axes it became apparent that the crystal was disordered in terms of random rotations about the c axis. This resulted in very broad peaks (width at half-height 0.6° in Ω, compared with 0.06° for a good crystal) and few observed reflections with ℓ greater than 10. The stacking order could not be determined although all 18 unique variations in the positions of the zirconium atoms, 12 acentric and 6 centric, were tried. In all cases the R factors, both

weighted and unweighted, were greater than 0.85 owing to the poor quality of the crystal.

The final crystal examined, IV, was of very good quality, giving sharp spots in all oscillations. This crystal once again was an example of intergrowth between the 3R and the 6 slab variations, however in this case it was possible to obtain separate lattice constants for the two variations by separating the 16 tuned reflections into those allowed for 3R and those not allowed. The difference between c for the 6 slab and twice c for the 3R components is 0.034(7)Å.

Using a dataset containing only the reflections allowed for a 3 slab cell with the obverse rhombohedral orientation it was possible to obtain an R of 0.121 (R_w = 0.174) for the 3R-$ZrCl_2$ component, with all atoms within 1σ of the values obtained previously. At attempt to use this component of the crystal to phase the rest failed to provide a coherent picture, showing only the obvious, that all of the atoms were on the 3-fold axes and spaced along c to agree with the slab type structure.

For the 6-slab component a structure was obtained using only the reflections with odd values of ℓ by assuming that the only strong vector observed in the Patterson map calculated with the data from crystal III represented a Zr-Zr vector for the 6 slab component. In retrospect this choice appears more fortuitous than prudent. The two atoms thus located revealed the presence of either one more, for a centric structure, or four more for an acentric structure. Assuming nothing about the symmetry, the four acentric atoms were put in and twelve chlorines located. Refinement of these atoms for both the

centric and acentric possibilities proceeded in parallel until the refinement of temperature factors for the acentric case showed coupling between temperature factors for inversion related atoms which was taken to indicate that the centric choice was correct.

The slab stacking in this structure is ABABAB, equivalent to three unit cells of 2H-MoS_2, and alone does not explain the observed 6-slab repeat. Examination of an electron density map at this point indicated the presence of a fractional zirconium atom in the octahedral hole centered on (0,0,0). With an atom at 0.5 occupancy on this site refinement proceeded to an R of 0.261 (R_w = 0.400) and after reweighting to R = 0.256 (R_w = 0.304).

Although this structure (henceforth called 6T) is based on a very high symmetry subcell (2H-MoS_2, space group $P6_3/mmc, D_{6h}^4$, No. 194) it has quite low symmetry, only that of space group $P\bar{3}m1$ (D_{3d}^3, No. 164).

Distances and drawings

All of the drawings of the structures appearing in this dissertation were produced using the program ORTEP2 by C. K. Johnson.[73] Unless otherwise noted in the individual figure, all thermal ellipsoids are of 50% probability size. Distances, angles, and their differences were calculated with the program ORFFE using the variance-covariance matrix calculated by ORFLS and include corrections for the uncertainties in the lattice parameters.[74]

Photoelectron spectroscopy data

All photoelectron spectroscopy data, both x-ray (XPS) and ultraviolet (UPS) were obtained on an AEI Model ES200B instrument coupled to a Nicolet 1180 minicomputer for data averaging and curve smoothing. Spectra were accumulated in either 128 channels or 256 channels and from 10 to nearly 500 scans were averaged to reduce noise, with the exact number varying with the specimen. Smoothing involved a nine point fit centered on each point of the spectrum. The instrument was operated by J. W. Anderegg.

Data were obtained using either an Al K_α (1486.6 eV) x-ray source or helium (HeI, 21.21eV) ultraviolet source. XPS spectra for materials without an apparent Fermi edge were referenced to silver metal on the back of the sample holder.

Samples were prepared by pressing the powdered material onto a strip of indium and attaching this to the sample holder with all manipulations carried out in a helium atmosphere drybox (H_2O and O_2 less than 1 ppm each) directly connected to the sample port of the instrument. All spectra are from unetched samples due to the fact that argon ion etching reduces $ZrCl_2$ instead of cleaning the surface. On the one occasion when etching was attempted, the entire surface of the specimen was converted from dichloride to monochloride.

SALTS OF THE CLUSTER ANIONS Te_3^{2-} AND Bi_4^{2-}

The tritelluride ion in $(crypt\ K^+)_2\ Te_3^{2-}\cdot en$

The final positional and isotropic thermal parameters are listed in Table IV with the anisotropic thermal parameters for tellurium and potassium in Table V. Bond lengths, angles, and significant non-bonded distances for the Te_3^{2-} anion, together with bond lengths and angles for the hydrogen-bonded ethylenediamine molecule and oxygen, nitrogen, and potassium atoms of the cryptated cations appear in Table VI. The remaining ligand distances and angles as well as the observed and calculated structure factors appear in reference 28.

The [110] view of the contents of one unit cell is shown in Figure 4. The most interesting feature of this compound is the hitherto unknown tritelluride ion, illustrated in Figure 5 in two views. The deviation of the ion from C_{2v} symmetry by 0.028Å (4σ) is probably significant and contrasts with the rigorous C_{2v} symmetry required by crystal symmetry for the congeneric S_3^{2-} and Se_3^{2-} anions.[10,11] This difference in bond lengths is probably the result of hydrogen bonding between Te(3) and N(1) of the ethylenediamine molecule which is 3.46(6)Å away. Hamilton and Ibers[75] suggest that evidence of a hydrogen bond in a crystalline salt is the observation of a distance between two non-hydrogen atoms, one of which is capable of donating electrons (tellurium in this case) and one of which is electronegative and bonded to hydrogen, which is less than the sum of the van der Waals radii. This sum is

Table IV. Final positional and thermal parameters for (crypt $K^+)_2Te_3^{2-}\cdot en$

Atom	Fractional Coordinates x	y	z	Atomic Temperature Factors (B)
Te(1)	0.1671(3)	0.1585(3)	0.0	a
Te(2)	0.0232(3)	0.2221(4)	0.0499(1)	a
Te(3)	0.0622(2)	0.2017(2)	0.1349(1)	a
K(1)	0.7250(7)	0.5365(7)	0.1244(2)	a
K(2)	0.3974(7)	0.8688(7)	0.1646(3)	a
N(101)[b]	0.723(3)	0.520(3)	0.028(1)	6.3(7)
C(102)	0.848(4)	0.609(4)	0.012(1)	7(1)
C(103)	0.900(4)	0.733(4)	0.030(1)	7(1)
O(104)	0.935(2)	0.731(2)	0.0779(8)	6.0(5)
C(105)	0.976(4)	0.853(4)	0.097(1)	7(1)

[a] See Table V.

[b] The first digit keys the crypt molecule, the others the atom number as in ref. 17.

Table IV. Continued

Atom	Fractional Coordinates x	y	z	Atomic Temperature Factors (B)
C(106)	0.017(3)	0.846(3)	0.142(1)	6.2(9)
O(107)	0.896(2)	0.759(2)	0.1642(7)	5.7(5)
C(108)	0.931(4)	0.772(4)	0.209(1)	6(1)
C(109)	0.787(3)	0.691(3)	0.232(1)	6.2(9)
N(110)	0.727(2)	0.558(2)	0.218(1)	5.5(6)
C(111)	0.592(4)	0.482(4)	0.236(1)	7(1)
C(112)	0.518(4)	0.528(4)	0.211(1)	6.5(9)
O(113)	0.509(2)	0.491(2)	0.1684(7)	5.4(5)
C(114)	0.415(3)	0.511(3)	0.145(1)	5.6(8)
C(115)	0.406(3)	0.468(3)	0.102(1)	4.9(7)
O(116)	0.517(2)	0.531(2)	0.0781(8)	5.8(5)
C(117)	0.511(5)	0.491(4)	0.035(1)	8(1)
C(118)	0.631(3)	0.553(3)	0.010(1)	5.6(8)
C(119)	0.682(4)	0.389(4)	0.018(1)	8(1)

Table IV. Continued

Atom	Fractional Coordinates x	y	z	Atomic Temperature Factors (B)
C(120)	0.745(4)	0.328(5)	0.041(1)	8(1)
O(121)	0.712(2)	0.318(2)	0.0864(8)	5.9(5)
C(122)	0.783(3)	0.268(3)	0.111(1)	5.3(8)
C(123)	0.741(3)	0.252(3)	0.154(1)	5.2(8)
O(124)	0.773(2)	0.375(2)	0.1734(8)	6.2(6)
C(125)	0.758(4)	0.362(4)	0.219(1)	8(1)
C(126)	0.803(4)	0.497(4)	0.237(1)	7(1)
N(201)	0.400(3)	0.863(3)	0.071(1)	7.4(8)
C(202)	0.336(4)	0.733(4)	0.057(1)	7(1)
C(203)	0.210(5)	0.651(5)	0.080(1)	9(1)
O(204)	0.226(2)	0.646(2)	0.1227(9)	6.7(6)
C(205)	0.108(4)	0.567(4)	0.144(1)	7(1)
C(206)	0.143(4)	0.549(4)	0.190(1)	7(1)
O(207)	0.192(2)	0.670(2)	0.2119(7)	5.9(5)

Table IV. Continued

Atom	Fractional Coordinates x	y	z	Atomic Temperature Factors (B)
C(208)	0.228(4)	0.655(4)	0.255(1)	6.7(9)
C(209)	0.265(5)	0.788(5)	0.277(1)	9(1)
N(210)	0.398(3)	0.877(3)	0.261(1)	8.0(9)
C(211)	0.439(4)	0.008(5)	0.275(1)	8(1)
C(212)	0.373(6)	0.070(6)	0.252(2)	11(1)
O(213)	0.396(2)	0.074(2)	0.2068(9)	6.8(6)
C(214)	0.332(3)	0.126(3)	0.185(1)	6.1(9)
C(215)	0.367(4)	0.143(4)	0.143(1)	7(1)
O(216)	0.343(2)	0.035(2)	0.1208(8)	6.5(6)
C(117)	0.361(5)	0.045(5)	0.074(1)	9(1)
C(218)	0.326(5)	0.919(5)	0.054(1)	8(1)
C(219)	0.521(5)	0.927(4)	0.055(1)	9(1)
C(220)	0.610(4)	0.893(4)	0.075(1)	7(1)
O(221)	0.614(2)	0.911(2)	0.1205(8)	5.9(5)

Table IV. Continued

Atom	Fractional Coordinates x	y	z	Atomic Temperature Factors (B)
C(222)	0.701(3)	0.888(3)	0.140(1)	4.9(7)
C(223)	0.718(3)	0.942(3)	0.187(1)	6.1(9)
O(224)	0.605(2)	0.872(2)	0.2107(7)	5.4(5)
C(225)	0.615(4)	0.903(4)	0.256(1)	8(1)
C(226)	0.497(4)	0.839(4)	0.276(1)	6(1)
N1(EN)	0.008(5)	0.226(5)	0.242(1)	11(1)
C2(EN)	0.99(1)	0.15(1)	0.263(5)	22(5)
C3(EN)	0.16(1)	0.27(1)	0.264(5)	25(5)
N4(EN)	0.174(4)	0.218(4)	0.301(1)	9(1)

Table V. Anisotropic temperature factors

Atom	β_{11}[a]	β_{22}	β_{33}	β_{12}	β_{13}	β_{23}
Te(1)	23.2(5)	22.2(5)	1.56(3)	14.6(4)	0.9(1)	0.6(1)
Te(2)	23.2(5)	30.0(6)	1.59(4)	20.4(5)	-0.3(1)	-0.1(1)
Te(3)	10.9(3)	11.6(3)	1.75(4)	5.3(2)	0.45(9)	0.20(9)
K(1)	10.6(9)	11.5(9)	1.22(9)	5.5(8)	0.2(2)	0.2(2)
K(2)	10.2(9)	9.8(9)	1.6(1)	5.6(8)	-0.2(2)	-0.4(2)

[a] $\beta_{ij} \times 10^3$.

Table VI. Distances and angles

Atom 1	Atom 2	Distance (Å)	Atom 1	Atom 2	Distance (Å)
Te(1)	Te(2)	2.692(5)	K(2)	N(201)	2.91(4)
Te(2)	Te(3)	2.720(4)	K(2)	O(204)	2.79(3)
Te(3)	N(1) (en)	3.46(6)	K(2)	O(207)	2.88(3)
			K(2)	N(210)	3.02(4)
Te(1)	Te(3)	4.516(4)	K(2)	O(213)	2.85(3)
Te(3)	Te(1)	7.456(5)	K(2)	O(216)	2.80(3)
K(1)	N(101)	2.99(4)	K(2)	O(221)	2.80(3)
K(1)	O(104)	2.88(3)	K(2)	O(224)	2.91(3)
K(1)	O(107)	2.76(3)			
K(1)	N(110)	2.95(3)	N(1) (en)	C(2) (en)	1.04(16)
K(1)	O(113)	2.77(3)	C(2) (en)	C(3) (en)	1.85(20)
K(1)	O(116)	2.89(3)	C(3) (en)	N(4) (en)	1.40(17)
K(1)	O(121)	2.85(3)			
K(1)	O(124)	2.78(3)			

Table VI. Continued

Atom 1	Vertex Atom 2	Atom 3	(°)	Atom 1	Vertex Atom 2	Atom 3	(°)
Te(1)	Te(2)	Te(3)	113.1(2)	N(201)	K(2)	N(210)	179.1(10)
Te(3)	N(1) (en)	C(2) (en)	121(5)	N(201)	K(2)	O(204)	61.4(9)
N(101)	K(1)	N(110)	178.5(12)	N(201)	K(2)	O(216)	62.5(8)
N(101)	K(1)	O(104)	61.7(8)	N(201)	K(2)	O(221)	59.4(11)
N(101)	K(1)	O(116)	61.5(10)	N(210)	K(2)	O(207)	60.1(8)
N(101)	K(1)	O(121)	61.7(10)	N(210)	K(2)	O(213)	59.2(9)
N(110)	K(1)	O(107)	59.5(7)	N(210)	K(2)	O(224)	61.0(11)
N(110)	K(1)	O(113)	59.2(9)	O(204)	K(2)	O(216)	98.5(9)
N(110)	K(1)	O(124)	61.5(10)	O(216)	K(2)	O(221)	100.0(8)
O(104)	K(1)	O(116)	100.1(8)	O(221)	K(2)	O(204)	91.3(9)
O(116)	K(1)	O(121)	97.7(9)	O(207)	K(2)	O(213)	97.0(9)
O(121)	K(1)	O(104)	100.0(9)	O(213)	K(2)	O(224)	98.6(9)
O(107)	K(1)	O(113)	98.5(8)	O(224)	K(2)	O(207)	98.3(8)

Table VI. Continued

Atom 1	Vertex Atom 2	Atom 3	(°)	Atom 1	Vertex Atom 2	Atom 3	(°)
O(113)	K(1)	O(124)	96.1(9)				
O(124)	K(1)	O(107)	97.3(9)				

Figure 4. The [110] view of the unit cell of (crypt K^+)$_2Te_3^{2-}$·en. Tellurium and potassium atoms are darkened.

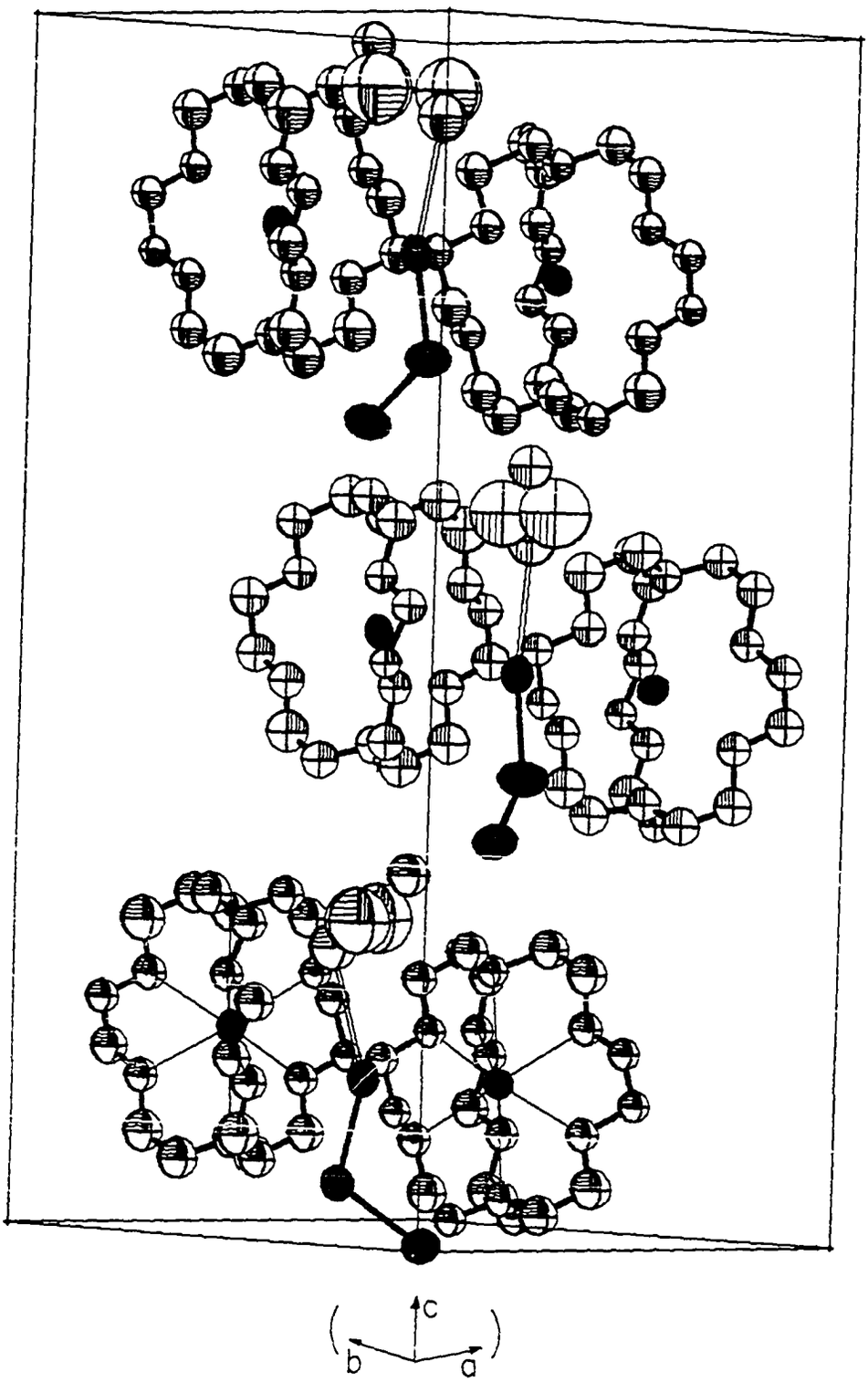
c
b
a

Figure 5. Details of the Te_3^{2-} ion in (crypt K^+)$_2Te_3^{2-}$. In (a) the ion is viewed normal to its plane. In (b) the view is nearly coplanar and the hydrogen bonded ethylenediamine is included. The less anisotropic thermal ellipsoid of Te3 is very clear in this view.

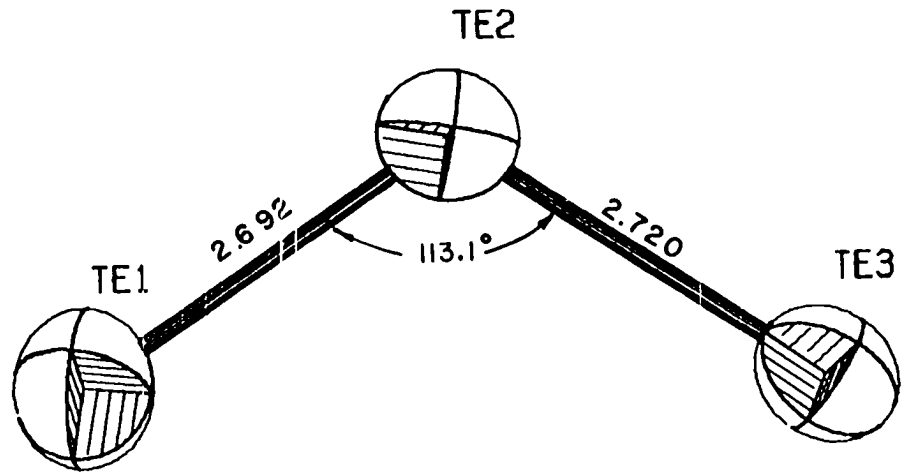

(a)

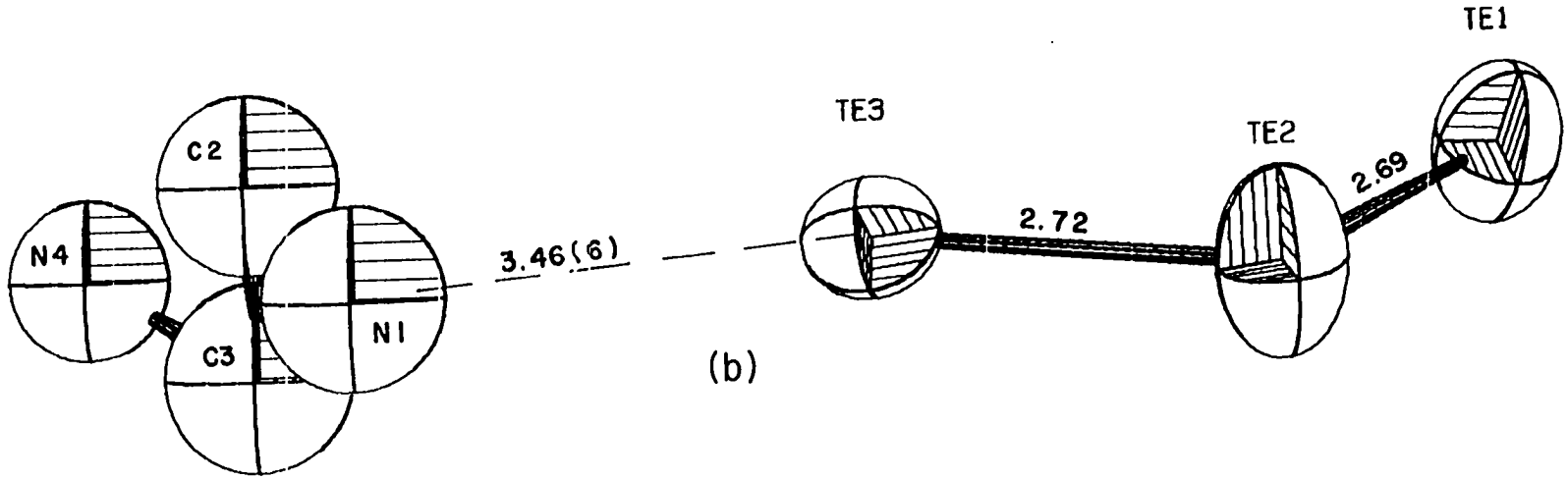

(b)

3.70Å according to Pauling,[76] or 0.24Å greater than the observed distance. Because of this rather large reduction from the expected distance and because the 2.20Å value for the tellurium(2-) radii may be inappropriately large for present purposes,[18] another estimate of the radii by Bondi[77] was also used. These values (2.06Å and 1.55Å) still sum to a distance 0.19Å greater than that measured, giving definite evidence of a hydrogen bond. Such a basicity for Te_3^{2-} was unexpected, however. The substantial differences in thermal parameters of the two end tellurium atoms also indicate the presence of the hydrogen bond. Those for Te(3) which participates in this bond are only about half the size found for the other two atoms and more nearly approximate a sphere, as seen in Figure 5(b). Thus the motion of Te(3) does appear more restricted, as would be expected with the additional bonding. The presence of only this hydrogen bond from the en molecule is in turn presumably responsible for the relatively large positional uncertainties and thermal parameters found, especially for the carbon atoms. There is no evidence for more than one conformation in the crystal, but random disorder and true thermal motion may both contribute.

Table VII lists bond lengths and angles for a number of species which may be compared with the tritelluride ion in this compound. The first of these is the nominally Te_3^{2-} ion found in In_2Te_5[15]. Although this ion is formally the same as the one in this report, a close examination shows substantial differences. The two Te-Te bond lengths are essentially identical in In_2Te_5 (the actual difference is 0.012(8)Å) but are 0.131(8)Å greater than the average of those in the crypt salt.

Table VII. Bond lengths and bond angles in some catenated compounds of group VI elements

Species	Te_3^{2-}	Te_3^{2-}	Se_3^{2-}	S_3^{2-}	I_3^{+}
Bond Length(s) (Å)	2.69(5) 2.720(4)	2.831(6) 2.843(6)	2.40(5)	2.076(5)	—[a]
Bond Angle(°)	113.1(2)	100.1(2)	110(3)	114.9(4)	97[c]
Compound	$(crypt\ K^+)_2$ $Te_3 \cdot en$	In_2Te_5	$BaSe_3$	BaS_3	I_3AlCl_4
Reference	This work	15	12	11	13

[a] Not known.

[b] Average of 4 values.

[c] Based on nqr spectrum analysis.

[d] Not comparable as ion is square planar.

Te	Se	S	Te_2^{2-}	Te_4^{2+}	Se_4^{2+}
2.835(2)	2.373(5)	2.047(3)[b]	2.70(1)	2.674(2) 2.663(2)	2.286(4) 2.280(4)
103.2(1)	103.1(2)	108.1(1)[b]	-	_d	_d

Te	trigonal-Se	S_8	$MgTe_2$	$Te_4(AlCl_4)_2$	$Se_4(HS_2O_7)_2$
78	79	80	81	18	82

This comes about because in the indium compound the tritelluride unit has indium neighbors 0.1Å closer to each end than the Te-Te bond length (2.837Å). In fact the length of the bonds in the indium compound, as well as the Te-Te-Te angle, are virtually the same as in the element, where the bond order is less than single.[78] When these two factors are considered together with the fact that $r_{In} \cong r_{Te}$ it appears that the bonding between the Te_3 unit and the indium is stronger than that within the Te_3 unit. This is in sharp contrast to the Te_3^{2-} ion in the crypt salt which has single bonds within the ion and, besides the previously mentioned hydrogen bond to an en molecule, only electrostatic bonding to the other ions.

Another isoelectronic species is the I_3^+ ion. This species has not been structurally well-characterized but the 97° bond angle estimated on the basis of its ^{127}I nqr spectrum[13] is distinctly smaller. Although some doubts could be raised regarding the simple bonding model used in analysis of the latter the trend may be real as ICl_2^+ shows a comparable angle. Some opening of the angle would be expected for the higher charged Te_3^{2-}.

Both angles and distances in Te_3^{2-}, Se_3^{2-} and S_3^{2-} are reasonable when account is taken of the lower precision of the Se_3^{2-} (powder) data. In the stable elemental forms selenium and tellurium are isostructural, consisting of infinite helixes of atoms parallel to the trigonal c axis. The M_3^{2-} ions may be considered as three-atom pieces of that chain, with the bonds at both ends reduced to complete the lone pair and furnish the charge. In the same way, S_3^{2-} could be formed from part of a S_8 ring.

A comparison of bond angles between the ions and the elements indicates considerable consistency. The ion S_3^{2-} has an angle 7° greater than S_8, Se_3^{2-}, about 7 ± 3° greater than in elemental selenium, and Te_3^{2-}, 10° greater than in the element. The bond lengths present a different story however; the bond length in S_3^{2-} is only 0.03Å greater than S_8, for selenium, the difference is less than the standard deviation of 0.05Å in the bond length in Se_3^{2-}, but with tellurium the average of the bond lengths in Te_3^{2-} is 0.129(5)Å less than in the element. This contraction is not really surprising when the structure of elemental tellurium is considered in more detail. Each atom therein has in addition to its two nearest "bonded" neighbors at 2.835(2)Å, four other atoms 3.495(3)Å away in other chains, close enough to suggest some form of bonding interaction which completes a distorted octahedron around each atom.[83] This secondary bonding, present in tellurium but virtually absent in the isostructural selenium, is not surprising considering the more metallic character of tellurium and appears to lower the bond order within the helical chain with a resulting increase in bond length.

Two other bonds to which Te_3^{2-} can be compared are those in Te_2^{2-} and Te_4^{2+}. The former (isoelectronic with I_2) is quite comparable in distance to that in $MgTe_2$ (2.70(1)Å) and not greatly different in $MnTe_2$ at 2.74(3)Å.[84] The tetratellurium(2+) cation has a bond order of 1.25, and appropriately contains bonds 0.038Å shorter than the presumed single bonds in Te_3^{2-}. For selenium, Se_3^{2-} has bonds 0.12Å longer than Se_4^{2+}, but the large standard deviation for the anion makes it impossible to tell if the magnitude of this difference is significant.

The tetrabismuthide ion in $(crypt\ K^+)_2\ Bi_4^{2-}$

The final atomic positional and thermal parameters appear in Tables VIII and IX, while important distances and angles in the Bi_4^{2-} anion and $(crypt\ K^+)$ cation are given in Table X. Additional cation distances appear in Table XI while the remaining angles as well as the observed and calculated structure factors appear in reference 29.

The most significant feature of this structure is the Bi_4^{2-} ion, shown in Figure 6, which is the first discrete anionic cluster of bismuth isolated, although cationic clusters Bi_9^{5+}, Bi_8^{2+} and Bi_5^{3+} are known.[1] As noted earlier, Zintl's original assignment for this ion, Bi_7^{3-}, was based on a substantial rounding of analytical results and on analogies with other Group V elements while the analysis appeared to indicate the correct Na_2Bi_4 stoichiometry. Although the only point symmetry required for the ion is C_i, which with two unique atoms produces a rigorously planar configuration, the anion does not vary significantly from D_{4h} symmetry. This is as expected considering the isoelectronic (in valence electrons) ions Te_4^{2+} and Se_4^{2+}, both of which are also only required to have C_i symmetry in their structures but come within experimental error of possessing D_{4h} symmetry.[18,82]

The remarkable red-green dichroic effect observed for the solutions from which these crystals grow and earlier noted by Zintl[9] et al. for other NH_3 solutions may arise from an uneven response of the human eye to colors at opposite ends of the visible spectrum. The characteristic intense green color of thin layers presumably arises from transmission in both the red and the blue end of the visible spectrum, whereas thicker

Table VIII. Final positional and thermal parameters for the non-disordered atoms of $(\text{crypt } K^+)_2\ Bi_4^{2-}$

	Fractional Coordinates			Atomic Temperature Factors					
Atom	x	y	z	β_{11}[a]	β_{22}	β_{33}	β_{12}	β_{13}	β_{23}
B11	0.1952(1)	0.8575(1)	0.0011(1)	14.6(1)	17.5(2)	14.3(1)	- 4.6(1)	0.9(1)	3.5(1)
B12	0.0216(1)	0.0671(1)	0.8454(1)	17.1(2)	17.0(1)	12.5(1)	- 6.6(1)	1.0(1)	3.6(1)
K	0.3215(6)	0.3243(6)	0.4100(6)	14.6(8)	11.9(6)	9.2(5)	- 5.7(5)	1.8(5)	0.1(5)
N1	0.302(3)	0.305(3)	0.145(2)	22(4)	18(3)	12(3)	-11(3)	5(3)	- 3(2)
O4	0.328(3)	0.518(2)	0.291(1)	36(5)	14(2)	7(1)	-13(3)	2(2)	2(1)
C5	0.245(5)	0.639(4)	0.342(4)	33(8)	18(5)	17(5)	-12(5)	8(5)	- 2(4)
C6	0.284(3)	0.644(3)	0.472(3)	24(5)	11(3)	12(3)	- 9(3)	- 0(3)	4(2)
O7	0.269(2)	0.563(1)	0.535(1)	18(2)	10(1)	10(2)	- 2(1)	4(1)	- 0(1)
C8	0.313(4)	0.573(3)	0.663(3)	27(6)	10(3)	10(3)	- 8(3)	3(3)	- 1(2)
C9	0.275(3)	0.486(2)	0.726(2)	15(3)	12(3)	9(3)	- 4(2)	0(2)	- 3(2)
N10	0.337(2)	0.347(2)	0.683(2)	15(3)	14(3)	10(2)	- 6(2)	- 0(2)	0(2)

[a] $\beta_{ij} \times 10^3$.

Table VIII. Continued

Atom	Fractional Coordinates			Atomic Temperature Factors[a]					
	x	y	z	β_{11}	β_{22}	β_{33}	β_{12}	β_{13}	β_{23}
C11	0.282(4)	0.278(3)	0.722(3)	23(5)	15(4)	12(3)	-11(3)	5(3)	0(3)
C12	0.146(3)	0.310(3)	0.657(3)	13(3)	17(4)	11(3)	- 1(3)	- 2(2)	2(3)
O13	0.167(2)	0.259(2)	0.526(1)	15(2)	16(2)	9(1)	-11(2)	- 1(1)	3(1)
C14	0.055(3)	0.264(4)	0.457(4)	9(3)	28(6)	24(6)	-12(3)	- 5(3)	13(5)
C15	0.088(3)	0.225(4)	0.320(4)	12(4)	19(5)	16(5)	- 4(3)	- 4(3)	- 5(4)
O16	0.100(2)	0.321(3)	0.283(2)	22(4)	28(4)	11(2)	-17(3)	- 3(2)	0(2)
C18	0.176(7)	0.298(8)	0.099(4)	4(1)	5(1)	13(5)	- 3(1)	- 4(6)	7(7)
C19	0.411(6)	0.176(5)	0.099(4)	32(9)	27(7)	14(5)	-13(7)	4(5)	- 7(5)
C21	0.517(2)	0.106(2)	0.289(2)	17(3)	18(3)	15(3)	- 3(2)	4(2)	- 1(2)
C22	0.640(6)	0.083(3)	0.343(4)	33(9)	14(4)	17(5)	12(5)	9(6)	- 4(4)
C23	0.654(3)	0.065(3)	0.470(4)	13(4)	11(3)	20(5)	- 7(2)	2(3)	- 2(3)
C24	0.561(2)	0.177(1)	0.538(2)	14(2)	6(1)	17(2)	- 0(1)	0(2)	- 0(1)
C25	0.568(3)	0.162(3)	0.665(2)	17(4)	16(3)	8(2)	- 7(3)	0(2)	2(2)
C26	0.484(3)	0.291(2)	0.727(2)	14(3)	9(2)	11(3)	- 3(2)	2(2)	- 2(2)

Table IX. Final positional and thermal parameters for the disordered carbon atoms

Atom	x	y	z	B
C2a	0.371(6)	0.378(6)	0.113(6)	5(1)$A^{\circ 2}$
C2b	0.282(5)	0.430(5)	0.096(5)	4(1)
C3a	0.294(8)	0.505(6)	0.158(7)	6(1)
C3b	0.37(1)	0.491(9)	0.149(9)	9(2)
C17a	0.112(7)	0.248(7)	0.162(7)	6(1)
C17b	0.070(8)	0.333(8)	0.143(7)	6(1)
C20a	0.559(9)	0.117(8)	0.171(8)	8(1)
C20b	0.496(7)	0.077(7)	0.163(7)	6(1)

[a] All atoms at 0.5 occupancy; see text.

Table X. Important distances and angles in Bi_4^{2-} and (crypt K^+)

Anion

Distances		
Atom 1	Atom 2	Å
Bi1	Bi2	2.936(2)
Bi1	Bi2'[a]	2.941(2)
Bi1	Bi1'	4.150(3)
Bi2	Bi2'	4.151(3)

Angles			
Atom 1	Atom 2	Atom 3	°
Bi1	Bi2	Bi1'[a]	89.85(6)
Bi2	Bi1	Bi2'	90.15(6)

Difference Between Distances		
Distance 1	Distance 2	Å
Bi1 - Bi2	Bi1 - Bi2'	0.005(3)
Bi1 - Bi1'	Bi2 - Bi2'	0.011(4)

Difference Between Angles		
Angle 1	Angle 2	°
Bi1 - Bi2 - Bi1'	Bi2 - Bi1 - Bi2'	0.29(12)

[a] Primed atoms are related to unprimed atoms by inversion through the origin.

Table X. Continued

Cation

Distances			Angles			
Atom 1	Atom 2	Å	Atom 1	Atom 2	Atom 3	°
K	N1	2.90(3)	N1	K	N10	179.3(8)
K	O4	2.83(2)	O4	O21	O16	60.0(7)
K	O7	2.78(2)	O4	O16	O21	60.2(7)
K	N10	2.99(3)	O16	O4	O21	59.7(7)
K	O13	2.78(2)	O7	O13	O24	59.1(5)
K	O16	2.76(3)	O13	O24	O7	61.5(5)
K	O21	2.80(3)	O24	O7	O13	59.4(5)
K	O24	2.78(2)				

Angle Between Planes		
Plane 1	Plane 2	°
O24-O16-O21	O7-O13-O24	0.7(7)

Table XI. Additional cation distances

Atom 1	Atom 2	d(Å)	Atom 1	Atom 2	d(Å)
N1	C2b	1.54(6)	O21	C22	1.38(8)
N1	C2a	1.52(8)	C22	C23	1.43(6)
C2b	C3b	1.56(13)	C23	O24	1.44(4)
C2a	C3a	1.39(9)	O24	C25	1.42(4)
C3b	O4	1.66(10)	C25	C26	1.49(4)
C3a	O4	1.47(8)	C26	N10	1.54(4)
O4	C5	1.37(5)	C2b	C2a	0.92(7)
C5	C6	1.46(6)	C3b	C3a	0.88(11)
C6	O7	1.34(4)	C17b	C17a	0.93(8)
O7	C8	1.45(4)	C20b	C20a	1.03(11)
C8	C9	1.56(5)	C2b	C3a	1.09(8)
C9	N10	1.48(4)	C2a	C3b	1.36(11)
N10	C11	1.39(4)	O4	O7	2.80(3)
C11	C12	1.52(5)	O13	O16	2.80(3)
C12	O13	1.49(4)	O21	O24	2.83(4)
O13	C14	1.39(4)	O4	O16	4.26(4)
C14	C15	1.57(7)	O4	O21	4.27(3)
C15	C16	1.35(6)	O16	O21	4.24(4)
O16	C17b	1.56(8)	O7	O13	4.28(3)
O16	C17a	1.47(8)	O13	O24	4.19(3)
C17b	C18	1.24(10)	O7	O24	4.17(2)

Table XI. Continued

Atom 1	Atom 2	d(Å)	Atom 1	Atom 2	d(Å)
C17a	C18	1.45(9)	N1	N10	5.90(4)
C18	N1	1.52(7)			
N1	C19	1.51(6)			
C19	C20b	1.34(9)			
C19	C20a	1.65(11)			
C20b	O21	1.41(8)			
C20a	O21	1.50(9)			

Figure 6. View down the effective 4-fold axis of the D_{4h} Bi_4^{2-} ion in (crypt K^+)$_2Bi_4^{2-}$.

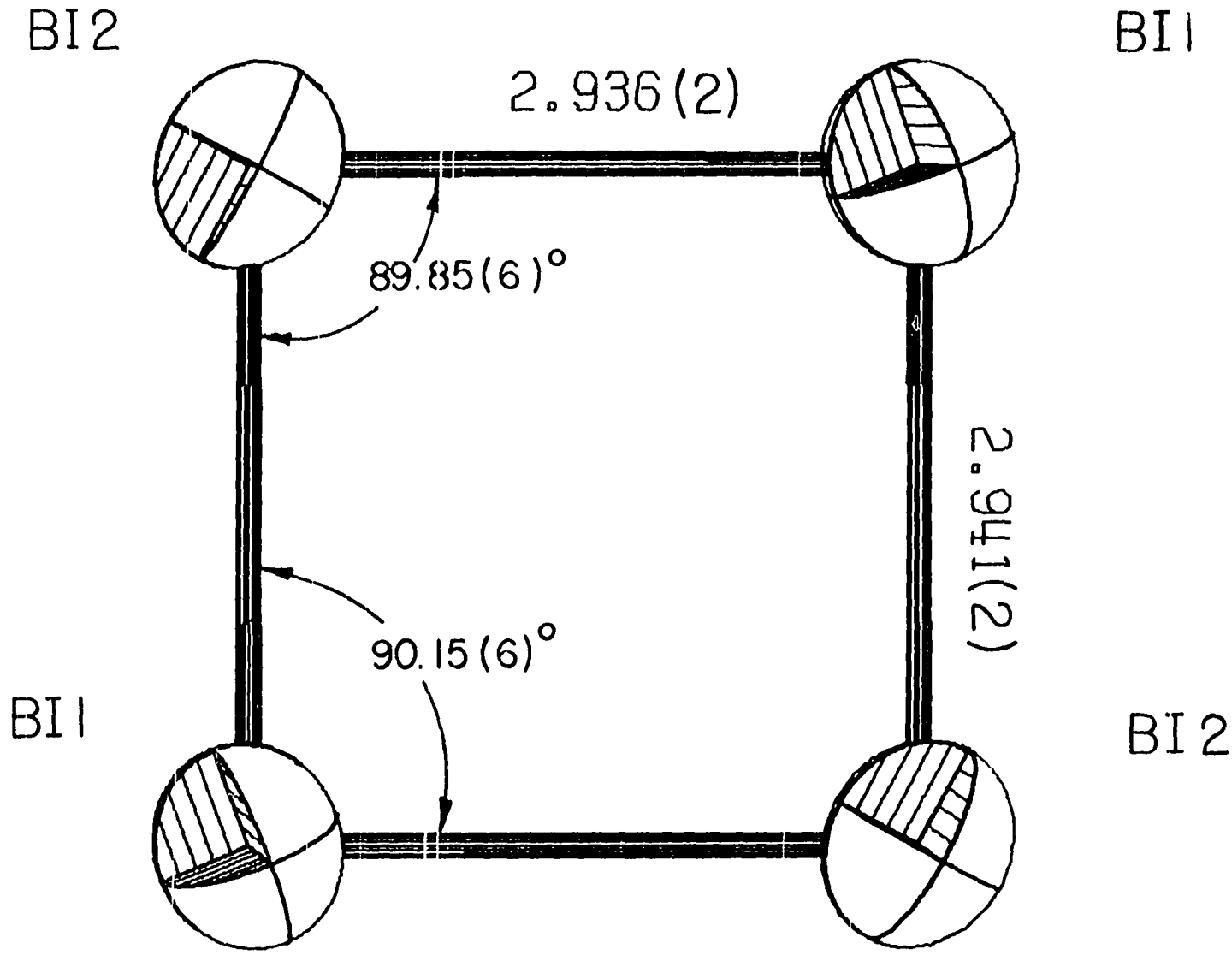
BI2
BI1
2.936(2)
89.85(6)°
2.941(2)
90.15(6)°
BI1
BI2

layers could appear red because of the lower sensitivity of the eye to blue.[85]

The bonding in Te_4^{2+} as well as Hg_4^{6-} has already been examined.[86] It is clear that the bond order based on molecular orbital treatment is 1.25, with five filled bonding (a_{1g}, b_{2g}, e_u, a_{2u}) and two filled and substantially non-bonding molecular orbitals (e_g) for the four edges. This high bonding order gives the ion shorter Bi-Bi bonds (2.939Å av.) than in Bi_9^{5+} where the bonds range from 3.078(6)Å to 3.286(12)Å[87,88] or the polymeric BiI, where the range is 3.038(4)Å to 3.058(4)Å.[89]

Recently the phase $Ca_{11}Bi_{10}$ was discovered to contain more or less isolated Bi_2 and Bi_4 groups,[90] and the latter appear to bear a definite relationship to Bi_4^{2-}. The unit cell contains four units of $Ca_{11}Bi_{10}$, with 16 isolated Bi atoms, eight Bi_2 groups (3.15Å bond length), and two Bi_4 rings (with D_{4h} site symmetry). The Bi_4 groups exhibit 3.20Å Bi-Bi bonds compared with 2.94Å in Bi_4^{2-} and 3.07(x3) plus 3.53(x3)Å in Bi metal.[91] All 8 of the Bi_2 groups are distributed 3.34Å away from the Bi_4 unit so as to maintain D_{4h} symmetry, as is shown in the diagonal section through one Bi_4 group shown in Figure 7.

As a zeroth approximation the 88 electrons from the calcium might be distributed by considering the isolated Bi atoms to be Bi^{3-}, the Bi_2 groups to be Bi_2^{4-} anions, isoelectronic with I_2, and the Bi_4 rings to be Bi_4^{4-} anions, the least reduced of the lot. In this scheme, the two additional electrons in the Bi_4^{4-} group would go into the lowest anti-bonding pi orbital (b_{2u}[86]), which effect would reduce the bond order from 1.25 to 1.0 and lengthen the bonds to about 3.05Å. This distance

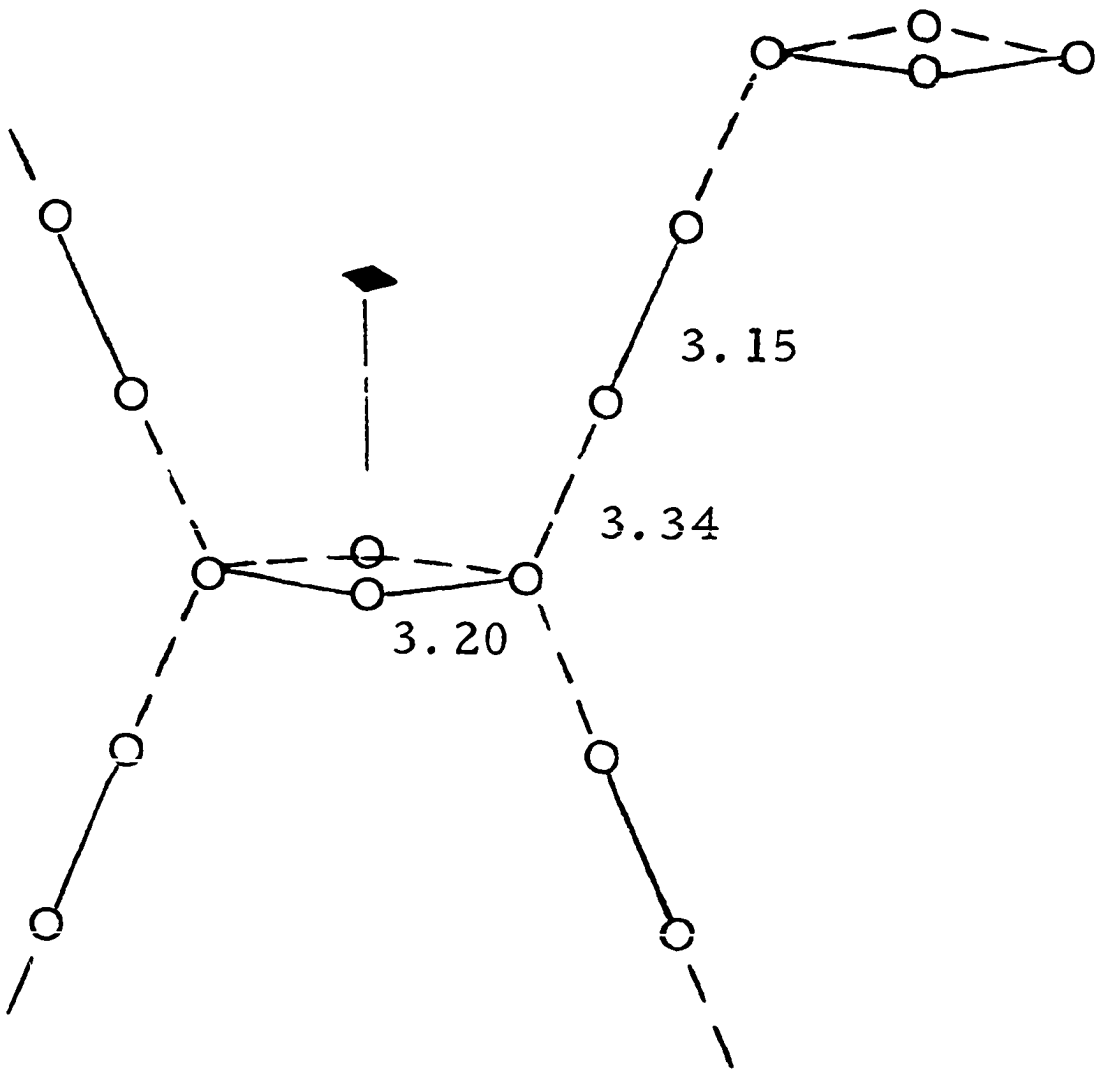

Figure 7. A [110] view of part of the bismuth substructure in $Ca_{11}Bi_{10}$. The rest of the substructure, excluding isolated bismuth atoms, can be generated by rotation about the tetragonal cell's indicated 4-fold axis. All distances are in Angstroms.

might also serve as a suitable approximation for singly bonded Bi_2^{4-} groups. The higher field of the calcium ions probably also serves to lengthen the bonds.

Such an assignment of all the valence electrons from calcium of course represents an unlikely extreme even for a polar intermetallic phase, and there are several likely routes for delocalizing charge back onto these cations, a process which should also lengthen bonds in what in the limit were termed Bi_4^{4-} and Bi_2^{4-} ions. Each of the so-called Bi_2^{4-} ions is surrounded symmetrically in a pi-like manner (D_{2h}) by four calcium ions at 3.25Å in a plane which comes within 0.08Å of including the two atoms in Bi_2, and these calcium atoms are in turn all 3.26Å from two isolated Bi plus more Ca atoms. The first four calcium atoms have the same symmetry as and would be expected to withdraw some charge from both the π and π^* orbitals of the Bi_2^{4-} ion, in the same manner as postulated for charge reduction of the square "anion" in Na_6Hg_4.[86]

For the Bi_4^{4-} group, the π orbitals (a_{2u}, e_g (non-bonding), and b_{2u}) are all in a position to lose charge to a pair of calcium ions immediately above and below the ring on the 4-fold axis (d_{Ca-Bi}= 3.6Å) or, perhaps even more likely in view of the remarkable geometry, into the σ^* orbitals of the formal Bi_2^{4-} ion. The 3.34Å separation between the Bi_4 groups and 8 symmetrically disposed Bi_2 units certainly must reflect a significant interaction. The fact that no atoms approach close to the Bi_4 square in or near its plane is consistent with the earlier observation[18] that this geometry provides a likely route for donation of charge from basic anions into the Te_4^{2+} and Se_4^{2+} ions.

The above description offers at least an heuristic approximation of the bismuth-bismuth bonding in $Ca_{11}Bi_{10}$, recognizing the principal fact that sufficient localization is present to define some direct covalent bonding even in a presumably conducting intermetallic compound such as this. While this model built up from a localized MO origin is only a crude description of the bonding in this compound, on going from bismuth to the less metallic antimony in the isostructural $Ca_{11}Sb_{10}$[90] and $Yb_{11}Sb_{10}$[92] and germanium in $Ho_{11}Ge_{10}$[93] the bonds within the M_4^{4-} and M_2^{4-} units are found to shorten in comparison with the distance between the units as the localized ionic model appears to be more closely approached.

The packing in $(crypt\ K^+)_2\ Bi_4^{2-}$

All of the other compounds studied to date which contain dinegative cluster anions, Sn_5^{2-}, Pb_5^{2-} and Te_3^{2-}, adopt a hexagonal Bravais lattice.[14] In the Bi_4^{2-} structure as well, the trigonal habit of the crypt in the presence of the relatively small anion so dominates the packing that the triclinic unit cell, two of which are shown in Figure 8, still comes out with nearly hexagonal proportions and packing (a differing from b by 1.6%, $\alpha \simeq \beta \simeq 98°$, and γ is only 1.4° from 60°). Likewise, the x and y coordinates of both nitrogen atoms and the potassium atom are all approximately 1/3, closely corresponding to a location on the three fold axis of a proper hexagonal cell. The gross packing of the cell is quite similar to that illustrated earlier[14] for $(crypt\ Na^+)_2\ Pb_5^{2-}$ save for the obvious addition of a three fold axis

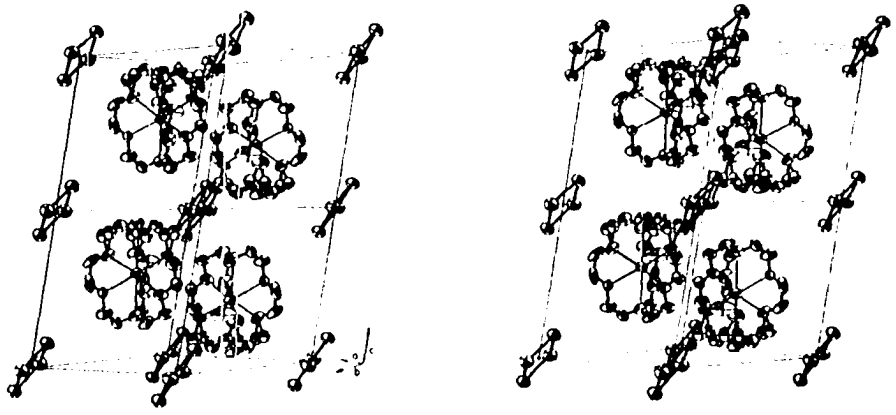

Figure 8. Stereoscopic [1$\bar{1}$0] view of two unit cells of (crypt K^+)$_2Bi_4^{2-}$. The Bi_4^{2-} anions at all corners of both cells are included. The packing is essentially the same as in (crypt Na^+)$_2Pb_5^{2-}$ and (crypt Na^+)$_2Sn_5^{2-}$.[14]

to that anion (D_{3h}) and a doubling of the c-axis, a second set of ions arising by a translation of c/2 and a 60° rotation.

The cryptate cations in these compounds

The two cryptated potassium cations in (crypt K^+)$_2$ Te_3^{2-} are essentially the same as dealt with in some detail elsewhere[94] and will not be discussed at length here. Two variations are observed however; first, a slight, but definite trend to generally longer bonds,[28] and second, a slight (0.04Å ≃ 1σ) shift of the potassium atom towards one end of the ligand in the present symmetry-unconstrained crypt cations relative to those reported earlier with a two-fold symmetry axis normal to the N-K-N axis.

This displacement is also observed in the crypt cation in (crypt K^+)$_2$ Bi_4^{2-}, only in this case the displacement is greater, 0.09Å, or 3σ, and the direction is towards the anion. Although no point symmetry is required for the cation, the potassium, nitrogen, and oxygen atoms have nearly three-fold symmetry, the two oxygen planes are parallel, and the N1-K-N10 angle is within 1σ of 180° (see Table X).

Although there is no difference in the final residual, the cation model involving the disordered carbons with more reasonable distances and thermal parameters (Tables IX and XI) is preferred to the one involving greatly anisotropic atoms (Figure 3). The ordered but anisotropic model requires a carbon-carbon bond length of 1.29Å (between C2 and C3) while corresponding distances in the disordered model are 1.39(9)Å and 1.56(13)Å. In the disordered model the two fractional

carbon chains (C2a-C3a and C2b-C3b) appear in an X configuration, perhaps to avoid what would be a short distance between these carbon atoms and the anion if the atoms adopted the normal arrangement. All of the disordered atoms except one (C2) are β to the nitrogen, a position where larger isotropic thermal parameters have been found previously and with the other compound in this work and were suspected to originate from disorder.[17,26] This disorder was resolved now because of its occurrence in a small cell of low symmetry which thereby yielded a larger ratio of observables per parameter. The disordered atoms are in the end of the ion which is significantly (0.2Å on the average) closer to the anion and has the closest contacts to the anion, 3.79(10)Å for C20a - Bi1 and 3.99(5)Å for C5-Bi2.

THE ZIRCONIUM DICHLORIDES

Prior to the work described in this dissertation all of the authentic powder patterns of zirconium dichloride could be explained either by a compound isostructural with 3R-MoS_2 or one having a very similar structure and the same size of unit cell, but only primitive symmetry.[30,48] In this dissertation two additional variations of the slab type structure are described and evidence for a third discussed.

The first of these variations has the same a axis length as 3R-$ZrCl_2$, but the repeat period for the stacking of the slabs is six slabs instead of three so that the c axis is doubled. This variation has only been observed in single crystals and then only intergrown with the 3R variation. An even longer repeat in the stacking period, eighteen slabs, has been observed in both single crystals and powder specimens. Like the previous example, the a axis remains the same as in the 3R variation.

Two low angle lines frequently appear which cannot be explained by any of the other stacking variations. These lines do fit a hexagonal unit cell with an a axis three times that of 3R-$ZrCl_2$ and a 6-slab repeat sequence.

Besides these, an entirely different zirconium dichloride is reported. This compound is a cluster compound of the M_6X_{12}-type, as is Zr_6Cl_{15}, and is isostructural with Zr_6I_{12} and (with one difference discussed below) Sc_7Cl_{12}.[30,70]

The cluster compound Zr_6Cl_{12}

This red compound has only been found in powdered products equilibrated at 650° and higher with the best material produced in isothermal equilibrations at 700° and initial compositions of $ZrCl_{2.00}$ and $ZrCl_{1.95}$. Because only powder data were available and because of the properties of $\bar{3}$ Laue symmetry the structure of this compound could not be refined once it was determined. The values for the positional parameters which appear in Table XII and the bond lengths derived from them which appear in Table XIII are only estimates arrived at by modifying the positions from Sc_7Cl_{12} to obtain bond lengths similar to those observed in Zr_6Cl_{15}.[70] Likewise the temperature factors are based on the best chlorine isotropic temperature factors from Sc_7Cl_{12} and the best zirconium values from Zr_6I_{12}.

The observed powder pattern, as well as the one calculated using the parameters given in Table XII, appear in Table XIV. As can be seen, there are some problems with the intensity match and with several unexplained lines. The two most intense lines are observed at about half of their calculated intensity, due to reciprocity failure. These lines are so much more intense than any of the others (101, the second most intense, is twice the intensity of 520, the third most intense) that any exposure long enough to bring out the weaker lines clearly overexposes the stronger. This was tested by comparison of the relative intensities of these two reflections and the reflections near them as measured by densitometer on films taken of the same sample with exposures of two and four hours. Although the intensities of the weaker reflec-

Table XII. Estimated positional and thermal parameters for Zr_6Cl_{12}

Atom	Fractional Coordinates x	y	z	Atomic temp factors (B) $\AA^2$
Zr	0.1160	0.1592	0.3511	0.77
Cl 1	0.1742	0.0473	0.1677	1.50
Cl 2	0.4145	0.9762	0.1667	1.50

Space Group $R\bar{3}$ (No. 148)

$a = 12.973(1)\AA$, $c = 8.782(1)\AA$

Table XIII. Estimated bond lengths for Zr_6Cl_{12}

Bond	Distance (Å) Zr_6Cl_{12}	Zr_6Cl_{15}[a]
Zr-Zr	3.20	3.207(4)
Zr-Cl 1	2.52	2.506(7)
Zr-Cl 2 (endo)	2.56	
Zr-Cl 2 (exo)	2.79	2.588(5)

[a] From reference 30.

Table XIV. Powder pattern of Zr_6Cl_{12}

hkl	d_o(Å)	d_c(Å)	I_o[a]	I_c
101	6.953	6.919	34[b]	68
110	6.505	6.487	23	31
012	4.097	4.090	9	13
211	3.826	3.823	10	12
300	3.751	3.745	11	14
202	3.486	3.460	2	0.2
220	3.254	3.243	11	13
122	3.0547	3.0525	11	14
131	2.9390	2.9366	5	7
	2.8680		3	
113	2.6691	2.6682	7	12
13-2	2.5431	2.5412	46[b]	100
321	2.4726	2.4732	10	9
140	2.4521	2.4517	8	10
	2.4266		2	
042	2.3667	2.3661	9	9
303	2.3067	2.3063	3	4
	2.2668		2	

[a] Observed intensities are scaled so that $\Sigma I_o = \Sigma I_c$.

[b] These reflections were overexposed beyong the linear range of the films: see text.

Table XIV. Continued

hkl	d_o (Å)	d_c (Å)	I_o [a]	I_c
232	2.2239	2.2228	12	14
051	2.1755	2.1769	16	12
22-3		2.1731		
104	2.1556	2.1547	14	11
	2.0917		2	
241	2.0642	2.0638	13	9
502	2.0002	2.0003	4	4
511	1.9661	1.9666	4	2
214	1.9502	1.9503	2	1
24-2	1.9115	1.9115	5	6
143	1.8796	1.8796	7	6
152	1.8349	1.8335	5	3
520	1.7991	1.7990	30	33
134	1.7944	1.7948	29	32
161	1.6797	1.6816	3	2
125	1.6221	1.6230	6	3
612	1.5983	1.5961	2	2
351	1.5785	1.5788	3	2
054	1.5706	1.5703	2	1
523	1.5330	1.5327	7	2
244	1.5258	1.5262	4	4

Table XIV. Continued

hkl	d_o(Å)	d_c(Å)	I_o[a]	I_c
35-2	1.5059	1.5074	10	2
710	1.4889	1.4881	9	4
262	1.4683	1.4683	15	16
006	1.4638	1.4637	4	5
235	1.4510	1.4514	4	5
44-3	1.4184	1.4185	5	2
630	1.4151	1.4155	5	5
	1.3767		29	
173	1.3262	1.3265	6	5
27-2	1.3104	1.3101	3	3
811	1.3004	1.3005	2	2
53-4	1.2961	1.2957	3	4
633	1.2738	1.2743	11	8
624	1.2705	1.2706	13	14
37-1	1.2514	1.2511	5	4
372	1.2155	1.2147	4	3
912	1.1374	1.1375	12	16
526	1.1352	1.1354	10	17

tions varied, as expected, the two intense reflections were saturated and overexposed in both. This is a clear indication of reciprocity failure.

There are also five lines in the powder pattern which do not correspond to any lines expected for this, or any other known zirconium chloride. Four of these lines are relatively weak (I_o from 2 to 3), but one is fairly intense (I_o = 29) and its presence is an unresolved problem. An unidentified phase is presumably responsible. Besides these, the original powder pattern also had several other unexplained lines, but these lost intensity much more rapidly than the cluster lines when the sample was exposed to air and were thus proven to be impurity derived.

As mentioned before, this compound is isostructural with Zr_6I_{12} and, if the isolated Sc^{3+} ion is ignored, Sc_7Cl_{12}. This structure is unique among the known M_6X_{12} clusters in having all of the halide ions bridging the edges of the M_6 octahedron. Half of the halide ions are triply bridging as they also occupy exo sites at the corners of other metal octahedra.[70] In many other cluster compounds, such as Zr_6Cl_{15}, these exo positions are occupied by halides which only bridge between clusters.

Like Zr_6I_{12}, this compound has twelve bonding electrons in the metal octahedron. According to the bonding scheme developed by Cotton and Haas[95] this should result in two unpaired electrons in a cluster T_{2g} orbital, and produce a paramagnetic compound. Zr_6I_{12} has proven to be diamagnetic however,[96] and Zr_6Cl_{12} probably behaves likewise.

The molecular orbital scheme proposed by Cotton and Haas was arrived at with tantalum as the metal in the M_6X_{12} cluster and may not be completely valid for zirconium, although the diagram indicates no important ordering changes occur over a wide range of bond lengths. If this ordering is accepted for O_h symmetry, there are two distortions observed which lower the symmetry and could serve to alter the molecular orbitals so that twelve electrons produce a filled highest occupied molecular orbital.

The first of these is a slight, although in Zr_6I_{12}, not crystallographically significant, distortion of the M_6 cluster from perfect octahedral symmetry. The second, and greater, distortion is brought about by the non-equivalence of the twelve bridging chlorines which give the cluster a $\bar{3}$ environment, for a larger effective symmetry loss.

The structure of 3R-$ZrCl_{2.0}$

The atomic positional and thermal parameters for 3R-$ZrCl_{2.0}$ appear in Table XV. The bond lengths, angles, and other important distances appear in Table XVI with the observed and calculated structure factors in Table XVII.

In this structure, as in the similar dichalcides,[50] all of the atoms occur on the three-fold axes located at (0,0,z), (2/3, 1/3, z) and (1/3, 2/3, z).

Because all of these lines lie in a common plane (110), that plane shows the contents of the unit cell. A (110) section of 3R-$ZrCl_2$ appears in Figure 9. This method will be used in all of the representations of slab-type compounds in this dissertation.

Table XV. Atomic parameters for 3R-$ZrCl_2$

Atom	z[a]	B_{11}[b]	B_{22}[c]	B_{33}	B_{12}[c]	B_{13}[d]	B_{23}[d]
Zr	0.0	0.41(7)	0.41	1.02(9)	0.20	0.0	0.0
Cl1	0.2449(3)	0.72(14)	0.72	1.1(2)	0.36	0.0	0.0
Cl2	0.4220(3)	0.75(14)	0.75	1.2(2)	0.38	0.0	0.0

[a] All atoms are on the 3a position and have x = y = o.

[b] Anisotropic temperature factors are in units of $Å^2$ and of the form exp [- 1/4 (B_{11} h^2a^{*2} + B_{22} k^2b^{*2} + $B_{33}\ell^2$ c^{*2} + $2B_{12}$ hk a^* b^* + $2B_{13}$ hℓ a^* c^* + $2B_{23}$ kℓ b^* c^*)].

[c] For this special position B_{22} and B_{12} are not independent, $B_{22} = 2B_{12} = B_{11}$.

[d] For this special position $B_{13} = B_{23} = 0$.

Table XVI. Interatomic distances and angles for 3R-$ZrCl_{2.0}$

Atom 1	Atom 2	d(Å)	Notes
Zr	Zr	3.3819(3)	Closest Zr approach
Zr	Zr	6.7479(3)	Nearest Zr in next slab
Zr	Zr	7.5480(4)	Second nearest Zr in next slab
Zr	Cl 1	2.598(4)	Bonding to coordinating Cl
Zr	Cl 2	2.601(4)	Bonding to coordinating Cl
Zr	Cl 1	4.746(6)	Nearest Cl in next slab
Cl 1	Cl 1	3.3819(3)	Translation
Cl 2	Cl 2	3.3819(3)	Translation
Cl 1	Cl 2	3.431(7)	Within slab
Cl 1	Cl 2	3.603(6)	Between slabs

Angles

Atom 1	Vertex Atom 2	Atom 3	(°)
Cl 1	Zr	Cl 2	82.6(1)
Cl 1	Zr	Cl 1	81.2(1)
Cl 2	Zr	Cl 2	81.1(1)
Cl 1	Zr	Cl 2	135.88(4)

Table XVII. Observed and calculated structure factors (x 10) for 3R-$ZrCl_2$

H = 0

K	L	FO	FC
0	3	521	946
0	6	115	119
0	9	807	966
0	12	979	1141
0	15	383	348
0	18	190	159
0	21	653	578
0	24	513	497
0	27	106	98
1	2	662	767
1	5	917	1276
1	8	652	823
1	11	579	578
1	14	546	528
1	17	722	716
1	20	418	376
1	23	295	293
1	26	315	302
2	1	557	580
2	4	765	822
2	7	815	809
2	10	525	468
2	13	447	418
2	16	551	610
2	19	421	426
2	22	273	272
3	3	506	440
3	6	125	114
3	9	586	522
3	12	682	668
3	15	216	223
3	18	107	110
4	2	292	309
4	5	463	510

H = 1

K	L	FO	FC
0	1	661	808
0	4	795	1129
0	7	809	1066
0	10	566	583
0	13	516	502
0	16	698	715
0	19	497	490
0	22	328	309
0	25	266	269
1	0	1067	1277
1	3	675	644
1	6	176	154
1	9	705	729
1	12	847	906
1	15	310	291
1	18	126	137
1	21	479	504
1	24	446	438
2	2	509	466
2	5	822	769
2	8	568	538
2	11	393	398
2	14	367	384
2	17	477	539
2	20	291	291
3	1	364	356
3	4	485	506
3	7	514	510
3	10	287	306
3	13	279	281

H = 2

K	L	FO	FC
0	2	551	570
0	5	798	933
0	8	636	642
0	11	531	467
0	14	477	443
0	17	586	616
0	20	324	329
0	23	264	258
1	1	515	474
1	4	694	675
1	7	662	674
1	10	414	398
1	13	372	361
1	16	514	532
1	19	354	375
2	0	802	736
2	3	426	383
2	6	103	102
2	9	478	458
2	12	567	587
2	15	162	199

H = 3

K	L	FO	FC
0	0	893	849
0	3	495	440
0	6	118	114
0	9	586	522
0	12	702	668
0	15	232	223
0	18	94	110
1	2	363	350
1	5	590	579
1	8	412	410
1	11	304	306

H = 4

K	L	FO	FC
0	1	298	314
0	4	423	447

Figure 9. A (110) section through several unit cells of 3R-$ZrCl_2$. One unit cell is outlined with c vertical and $[1\bar{1}0]$ horizontal. The thermal ellipsoids are drawn at the 90% probability level.

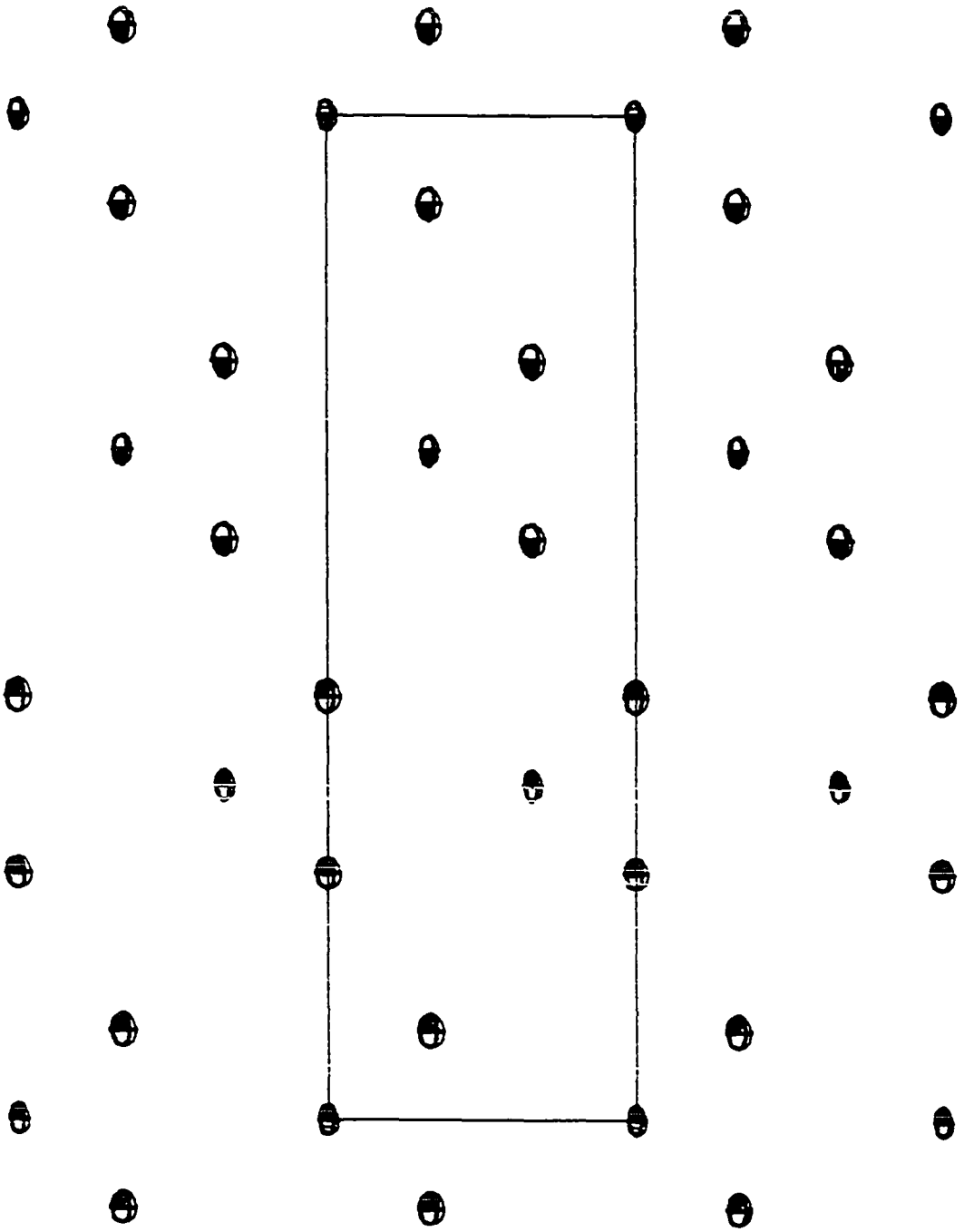

Figure 10 shows (110) sections of several structures with open circles replacing the actual thermal ellipsoids of the anions and dots the cations. All atoms are in idealized positions. The sections in 10a and 10b show the difference in appearance of the (110) sections for the obverse and reverse hexagonal settings of the same rhombohedral structure. (The obverse is normally chosen, by convention.[72]) Although these two views appear to be different, mirror image, structures, in reality they only represent a difference of 60° in the choice of the hexagonal axes used to represent the rhombohedral cell. All of the metal atoms in both 10a and 10b have trigonal prismatic coordination. This can be recognized in a (110) section by the fact that the non-metal atoms are stacked directly above each other with the metal atom off to one side. The only other coordination possible in this type of structure is octahedral, which is demonstrated for the x in 10c. This arrangement can be recognized by the fact that the metal atom is located on the diagonal which joins the two non-metal atoms. In both cases the remainder of the coordination sphere is formed by translations of these atoms.

The row of letters immediately below Figure 10a points out another feature of these slab-type structures. Because there are only three pairs of x and y coordinates allowed for this type of structure (barring distortion which reduces the symmetry to less than C_3), each type of position may be labeled; 0,0 as a, 1/3, 2/3 as b, and 2/3, 1/3 as c. If the non-metal atoms are represented by capital letters and the metal atoms by lower case letters, the entire structure can be reduced to a

Figure 10. A set of schematic (110) sections illustrating various features of the slab-type $ZrCl_2$. A) A section through a cell of 3R-$ZrCl_2$ using the conventional obverse orientation, for the hexagonal axes. The letters beneath the figure (a, b, and c) represent the three allowed sets of (x,y) coordinates. B) A section through a cell of 3R-$ZrCl_2$ with the hexagonal axes in the reverse orientation illustrating how different the same primitive cell appears when described with an equivalent axial system which is rotated by 60°. C) A section showing the proposed twinning mechanism in slightly substoichiometric 3R-$ZrCl_2$. The presence of an atom in the octahedral hole indicated with the x causes the zirconium atom in the next slab to locate in the b location instead of the c location. This shift is equivalent to a 60° rotation about c and, if the stacking continues in the same manner, the next slabs are in the reverse orientation relative to the coordinate system of the earlier slabs. D) A section through one unit cell of 6T-$Zr_{1+X}Cl_2$. The fractional atom in the octahedral hole is indicated by an x.

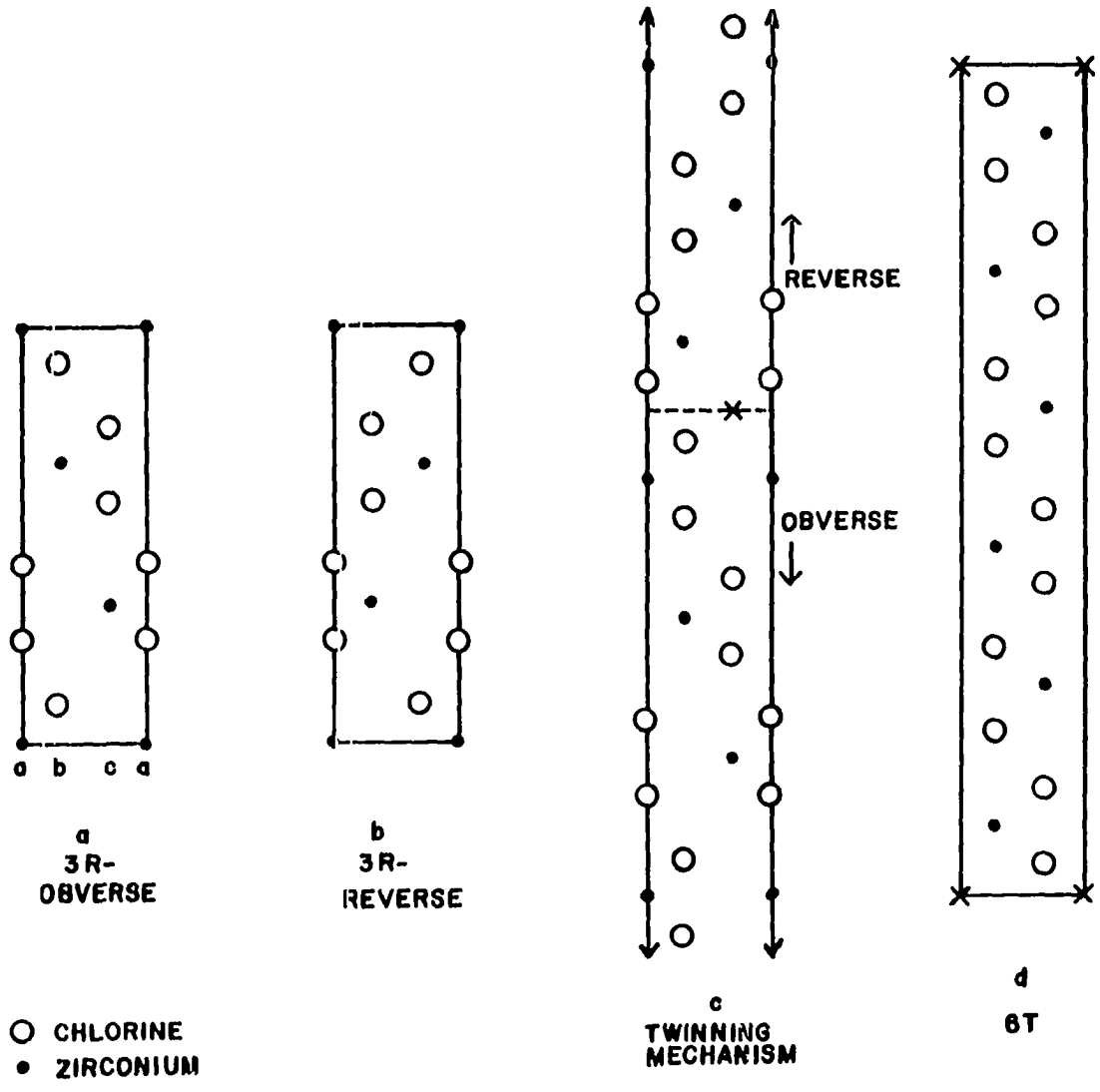

a
3R-
OBVERSE

b
3R-
REVERSE

c
TWINNING
MECHANISM

d
6T

short string of letters. For the obverse setting of 3R-$ZrCl_2$ the structure can be described as AcACbCBaB and the reverse setting as AbABcBCaC. It is immediately apparent that these can be shortened even further, the obverse to ACB and the reverse to ABC by only representing the outer atoms in each slab.

The atom positions found in this study differ from those reported by Troyanov and Tsirel'nikov[48] by 4σ, however this is not really a valid comparison. They report one less significant figure, and all of the values in this structure, if rounded to the same precision, differ by only one digit in the last place. The interatomic distances found here are likewise similar to theirs, but with smaller standard deviations. (The only exception to this is the interslab Cl-Cl distance which is reported as 3.06Å, but was found here to be 3.603(6)Å. This short distance is probably a misprint however, not a real difference in the structure.)

The trigonal prismatic coordination found in this compound, while relatively common among chalcides, is rare among halides. Only for ThI_2 has a refined crystal structure shown trigonal prismatic coordination of a metal by halides, and in that structure half of the cations have the more common octahedral coordination.[97] While this coordination is rare for halides, it is clear that $ZrCl_2$ conforms to the same criteria as the dichalcides with trigonal prismatic coordination. Like Mo^{4+} it is a d^2 ion, and since the d-orbital degeneracy is split by a trigonal prismatic field into three sets of orbitals (in order of increasing energy) a_1' (d_{z2}), e' ($d_{x^2-y^2}$,d_{xy}), and e'' (d_{xz},d_{yz}), this usually leads

to a filled orbital $(a_1')^2$ in a localized bonding model.[98]

An empirical rule which has been devised by Gamble for dichalcides states that if r+/r- exceeds 0.49 for an MCh_2 compound with a d^0, d^1, or d^2 metal ion that compound will have trigonal prismatic coordination.[99] For the purpose of this evaluation, r- = a/2 (the anions are assumed to be in contact) and r+ = d_{M-Ch} - r-. Although this is a rather circular approach, it does serve to draw a sharp distinction between the dichalcides having trigonal prismatic coordination and those having octahedral coordination. When $ZrCl_2$ is analyzed this way, the ratio found is 0.538, well above the minimum value required and even slightly above the hard sphere value of 0.527.

Daake has reported $ZrBr_2$ can be indexed on a hexagonal cell with a = 3.5257(2)Å and c = 13.726(2)Å.[30] These dimensions are what would be expected for a 2-slab structure and the reflections observed agree with the extinctions expected for space group $P6_3/mmc$, the correct space group for both $2H_a$-NbS_2 and $2H_b$-MoS_2. Unfortunately the $ZrBr_2$ was part of a mixture and the quality of the intensity measurements made was such that no further conclusions as to the structure ($2H_a$ or $2H_b$) could be made. If Gamble's rule is applied to this compound the ratio obtained is 0.516 if the radius of Zr^{2+} in $ZrBr_2$ is assumed to stay constant at its value in $ZrCl_2$ and 0.551 if the radius of Zr^{2+} is assumed to have the same apparent fractional increase as does Zr^{4+} between ZrS_2 and $ZrSe_2$. This clearly indicates that the compound probably has trigonal prismatic coordination. This result is only partially in agreement with another report which gives $ZrBr_2$ the 3R structure based on a nine line powder

pattern (eight lines of which can be explained by the $2H_b$ structure) plus a partial examination of a single crystal,[100] however $ZrBr_2$ could well be polymorphic.

Although the only point symmetry required for the trigonal prism surrounding the zirconium is C_{3v}, the observed symmetry in $ZrCl_2$ is D_{3h}. The two independent Zr-Cl distances differ by 0.003(6)Å, and the angles between the central metal atom and each pair of end atoms are identical.

The ideal reduced axial ratio (c/3a) for the 3R structure is 1.8165 which is nearly achieved for the metallic 3R-NbS_2 (which as a d^1 ion [$(a_1')^1$] lacks one electron of $ZrCl_2$). The isoelectronic [to $ZrCl_2$ $(a_1')^2$] 3R-MoS_2 is semiconducting and has a large c/3a ratio, 1.938. 3R-$ZrCl_2$, with c/3a = 1.9100, differs significantly from the ideal, but only 3/4 as much as does MoS_2. Along with the axial ratios, the axis lengths themselves offer an interesting comparison. Although the crystal radius of sulfur is slightly larger than that of chlorine (1.70Å compared with 1.67Å),[101] the a axis in $ZrCl_2$ is longer than the same parameter in either MoS_2 (3.166Å) and NbS_2 (3.3303Å).[50] The c axis shows a slightly different pattern, with $ZrCl_2$ still the largest, but with MoS_2 being larger than NbS_2 (18.41Å and 17.918Å respectively).

The behavior of the two disulfides can be explained by the extra d electron in MoS_2 which presumably increases the bonding between the metals reducing a, and at the same time producing a taller prism in an effort to keep the M-S bond length constant. While this hypothesis concurs with the observed similarity in the c/3a ratios for the isoelectron-

ic $ZrCl_2$ and MoS_2, it does not explain the overall lattice expansion. This latter may be a result of the greater ionicity of the halide compound.

The structure of $6T\text{-}Zr_{1+x}Cl_2$

The atomic positional parameters for $6T\text{-}Zr_{1+x}Cl_2$ appear in Table XVIII. The values in the column marked z (ideal) are based on a unit cell having three unit cells of the $2H_b$ type,[50] full $P6_3/mmc$ symmetry, and the same Cl-Cl separation (slab thickness) as observed in $3R\text{-}ZrCl_2$. The actual symmetry is $P\bar{3}m1$, with all of the atoms except Zr4 on the 2d special position which restricts (x,y) to (1/3, 2/3) or (2/3, 1/3). Atom Zr4 is on the 1a position (0,0,0).

Table XIX contains the observed and calculated structure factors for the partial set of reflections used in this determination. With a final R of 0.256, this structure cannot be considered fully refined but, given the limitations imposed on the data, is satisfactory. First among these limitations was the use of a partial data set obtained from the minority component of an intergrown crystal. This minority nature is quite apparent on comparing Figures 11 and 12. Figure 11 is a print of a Weissenberg photograph of a twinned crystal of $3R\text{-}ZrCl_2$ showing the two out of three pattern of spots resulting from the superposition of the obverse and reverse reflection sets. Figure 12 is a Weissenberg photograph taken for a crystal similar to crystal IV. Here the extra spots generated by the six slab structure are clearly apparent with the most prominent being between the pairs of reflections seen in the previous figure. That these are of lesser intensity is readily apparent.

Table XVIII. Atomic positions for 6T-$Zr_{1+x}Cl_2$

Atom	x	y	z(obs)	z(ideal)	B($\AA^2$)
Zr1	1/3	2/3	0.0815(2)	0.0833	0.3(2)
Zr2	2/3	1/3	0.2490(2)	0.2500	0.4(2)
Zr3	1/3	2/3	0.4181(2)	0.4167	0.5(2)
Zr4[a]	0.0	0.0	0.0	0.0	2.0
Cl1	2/3	1/3	0.0355(6)	0.0390	2.3(4)
Cl2	2/3	1/2	0.1226(7)	0.1277	2.6(4)
Cl3	1/3	2/3	0.1985(12)	0.2057	4.5(7)
Cl4	1/3	2/3	0.2927(6)	0.2943	1.7(4)
Cl5	2/3	1/3	0.3755(5)	0.3724	1.3(3)
Cl6	2/3	1/3	0.4592(10)	0.4610	3.8(6)

[a] At 50% occupancy giving a composition of $Zr_{1.08}Cl_2$ (or $ZrCl_{1.85}$).

Table XIX. Observed and calculated structure factors (x 10) for the reflections used in the solution of the structure of $6T\text{-}Zr_{1+x}Cl_2$

K = 0			2 17	164	189	2 1	157	36	0 45	399	462	-1 37	666	800
H	L	FO	FC	2 19	213	171	2 3	765	570	1 3	710	627	-1 39	350	198
0	3	20	171	2 21	778	627	2 5	165	31	1 5	89	97	-1 39	506	755
0	5	100	246	2 23	175	191	2 7	255	40	1 7	143	145	-1 41	94	88
0	7	107	243	2 25	173	95	2 9	1234	1347	1 9	1271	1168	0 1	57	60
0	9	28	136	2 27	723	690	2 11	273	165	1 11	280	85	0 19	94	92
0	11	91	329	2 29	167	155	2 13	260	125	1 13	269	28	0 25	125	90
0	13	83	57	2 31	244	289	2 15	990	972	1 15	1316	1202	0 29	51	77
0	15	38	30	2 33	1152	958	2 17	150	57	1 17	168	130	0 31	48	40
0	17	411	195	2 35	248	248	2 19	158	113	1 21	652	505	1 1	141	58
0	19	528	150	2 37	210	220	2 21	580	529	1 23	184	123	1 3	576	510
0	21	255	222	2 39	676	969	2 23	136	118	1 25	173	56	1 5	80	2
0	23	708	259	2 41	103	103	2 25	127	117	1 27	600	600	1 7	86	35
0	25	766	325	2 43	106	202	2 27	545	600	1 29	134	140	1 9	982	942
0	27	240	192	2 45	417	452	2 29	139	102	1 31	182	251	1 11	156	111
0	29	395	120	2 47	105	42	2 31	150	196	1 33	842	800	1 15	753	710
0	31	402	197	3 1	59	60	2 33	995	873	1 35	174	158	1 19	85	58
0	33	100	79	3 5	81	47	2 35	205	244	1 37	126	200	1 21	489	453
0	35	131	155	3 7	55	65	2 37	153	144	1 39	452	755	1 25	86	98
0	37	238	210	3 19	43	83	2 39	575	565	1 41	97	89			
0	39	166	144	3 23	109	78	2 41	90	120	2 1	93	46	K = 4		
0	41	636	206	3 25	80	90	3 1	132	8	2 5	61	32	H	L	FC	FC
0	43	694	172	3 29	68	77	3 3	550	511	2 17	103	58	-3	1	102	8
0	45	320	93	3 31	91	39	3 5	118	76	2 25	82	72	-3	3	535	511
0	47	619	175	4 1	75	48	3 7	145	104				-3	5	83	78
0	49	601	40	4 7	132	31	3 9	952	817	K = 3			-3	7	127	104
0	51	301	92	4 9	677	807	3 11	231	65	H	L	FO	FC	-3	9	927	817
0	53	149	94	4 11	133	91	3 13	186	39	-2	1	225	86	-3	13	113	39
1	1	187	143	4 13	162	53	3 15	750	873	-2	3	730	570	-3	17	86	71
1	5	209	126				3 17	95	72	-2	5	166	30	-3	19	63	100
1	9	1720	2477	K = 1			3 19	101	100	-2	7	294	40	-3	21	437	456
1	11	389	274	H	L	FO	FC	3 21	442	456	-2	9	1264	1347	-3	23	67	53
1	13	374	285	0	3	1018	825	3 23	79	53	-2	11	296	164	-2	19	56	70
1	15	1469	1619	0	9	1741	2181	3 25	83	76	-2	13	233	126	-1	3	498	510
1	17	263	145	0	13	351	3				-2	15	941	972	-1	9	926	941
1	19	246	250	0	15	1563	1958	K = 2			-2	19	90	113	-1	15	770	709
1	21	955	851	0	17	269	303	H	L	FO	FC	-2	21	599	525	-1	17	74	30
1	23	312	138	0	19	298	220	-1	5	60	119	-2	23	114	118	-1	21	499	453
1	25	238	163	0	21	957	540	-1	23	58	150	-2	25	79	117	-1	23	105	87
1	27	859	767	0	23	269	284	-1	37	172	179	-2	27	525	600	-1	25	74	88
1	29	243	64	0	25	276	112	-1	47	60	143	-2	29	102	102	0	1	61	3
1	31	206	303	0	27	368	824	-1	49	71	42	-2	31	131	196	0	9	679	703
1	33	1354	1246	0	29	231	171	0	1	79	108	-2	33	1123	873	0	11	158	57
1	35	297	363	0	31	277	341	0	3	876	597	-2	35	163	244	0	13	120	42
1	37	237	206	0	33	1012	1125	0	9	1465	1714	-2	37	122	144				
1	39	866	724	0	35	386	320	0	15	1178	1196	-2	39	635	565				
1	41	214	174	0	37	272	243	0	17	187	87	-2	41	76	120				
1	45	628	515	0	39	807	1011	0	19	173	161	-1	3	699	627				
1	47	192	191	0	41	242	123	0	21	747	576	-1	7	112	145				
1	49	276	194	0	43	220	236	0	23	239	144	-1	9	1264	1167				
1	51	605	487	0	45	650	489	0	25	177	138	-1	11	152	85				
1	53	171	202	0	47	275	77	0	27	676	670	-1	13	218	28				
2	1	127	60	0	49	142	140	0	29	207	90	-1	15	986	1201				
2	5	143	105	0	51	632	483	0	31	228	240	-1	17	85	130				
2	7	198	185	0	53	307	186	0	33	1100	1030	-1	19	93	139				
2	9	1257	1491	1	1	128	118	0	35	242	294	-1	21	616	505				
2	11	263	103	1	21	34	167	0	37	190	172	-1	23	124	122				
2	13	257	17	1	41	56	156	0	39	520	637	-1	25	96	86				
2	15	1150	1470	1	47	100	143	0	41	110	142	-1	27	598	600				

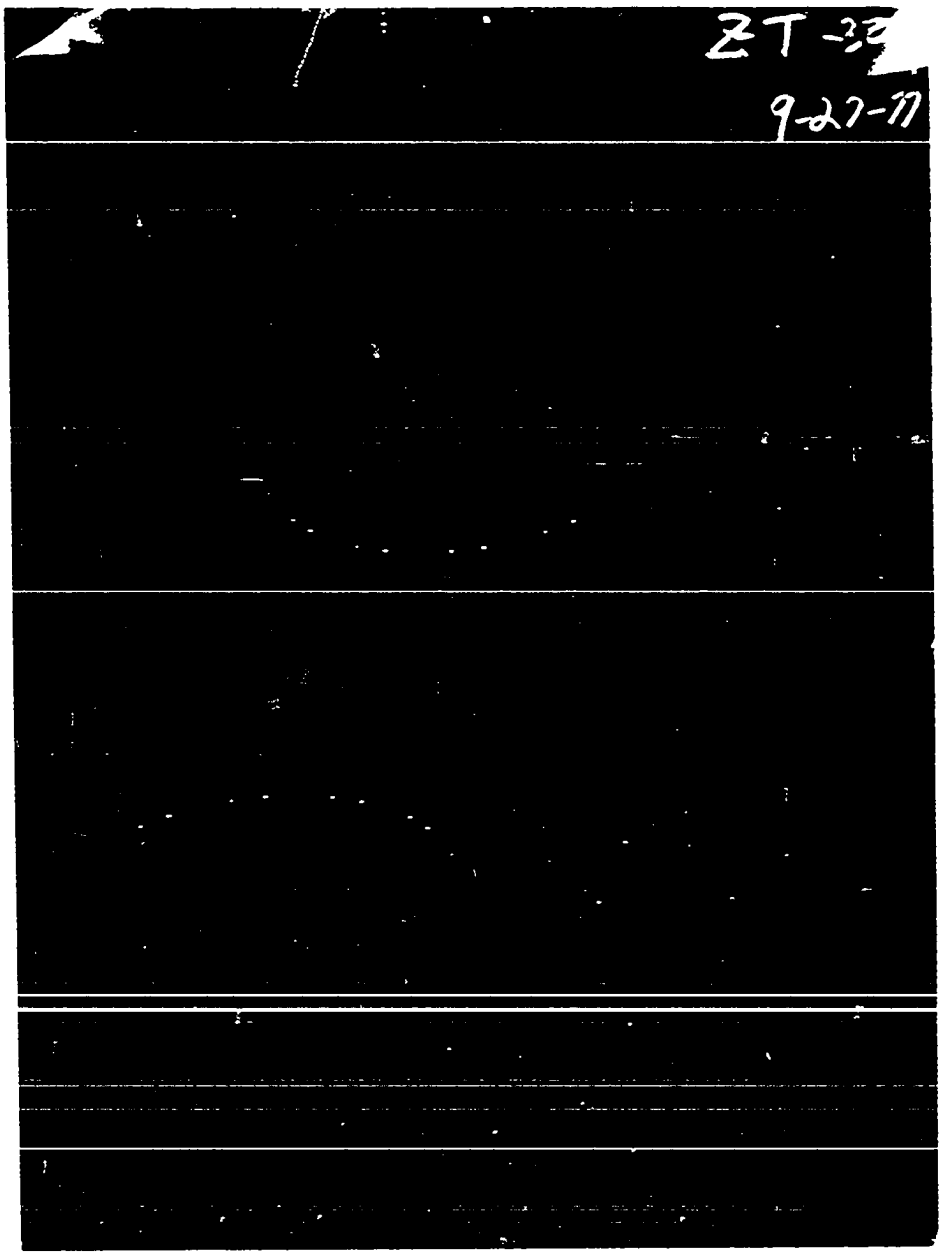

Figure 11. A Weissenberg photograph (rotated about b) of a twinned crystal of 3R-$ZrCl_2$. The spot pairs are h,0,ℓ and h,0,ℓ + 1 generated by superimposing the obverse (-h+k+ℓ = 3n) and reverse (h-k+ℓ = 3n) rhombohedral reflection sets.

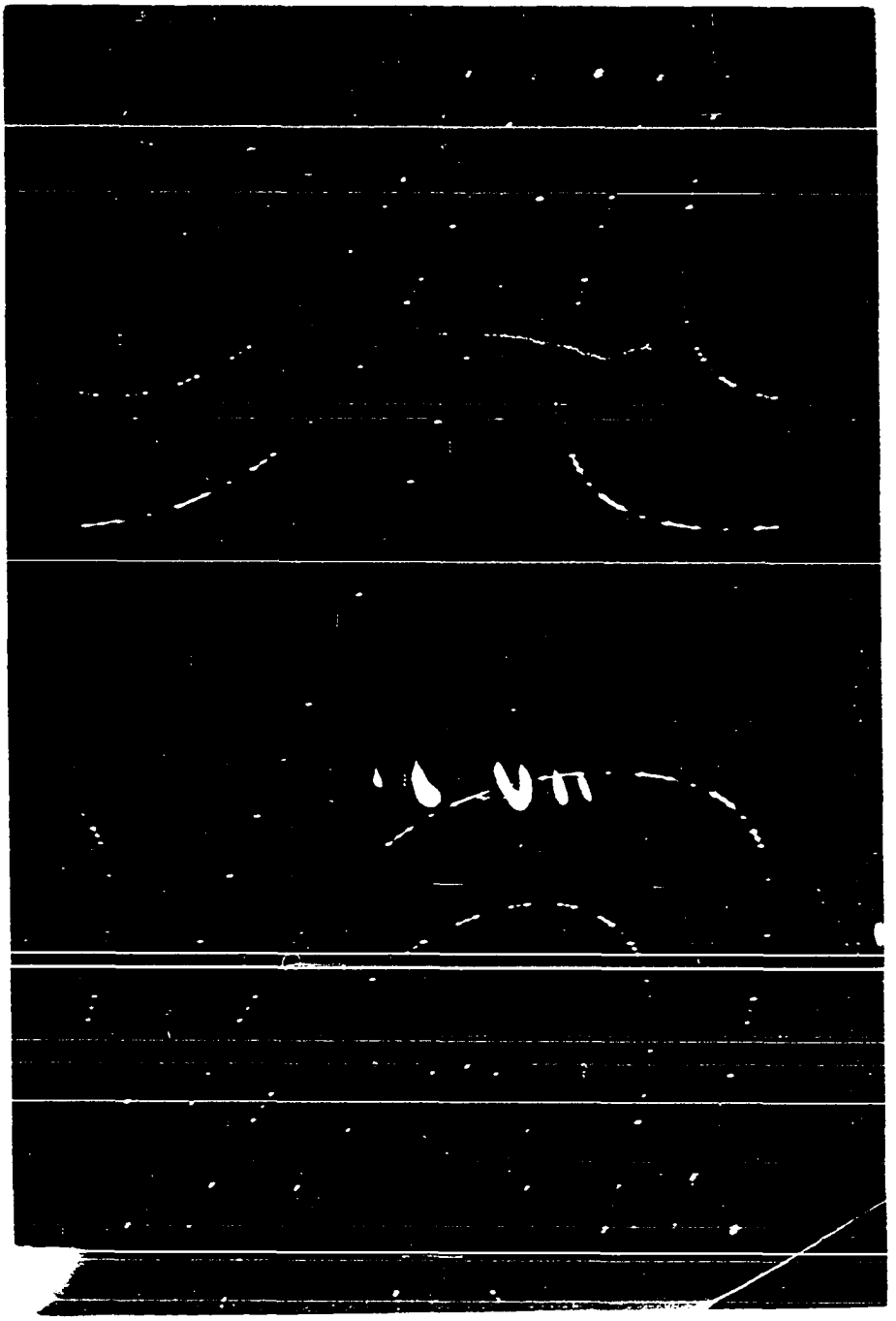

Figure 12. A Weissenberg photograph (rotated about b) of a crystal consisting of 3R-$ZrCl_2$ intergrown with 6T-$Zr_{1+x}Cl_2$.

Also visible in this figure is the streaking along the festoon between pairs of 3R-spots. All of the 6T-containing crystals examined exhibited this streaking, with this streak intensity being typical. In fact, in crystal II the streak was nearly as intense as the spot. The best explanation of this streaking is the presence of a nearly continuous set of different stackings with different periods each occurring only enough to diffract a trace of radiation and all completely in register in the a and b directions. This observation is in close agreement with the powder data where continuous bands but not lines are found between the lines attributed to these reflections.

A further limitation is imposed by the superposition of non-equivalent reflections. If the crystal were single this would not occur, but it is very likely that the 6T component is twinned with such severe twinning occurring in the other (3R) component. In space group $P\bar{3}m1$ there are two equivalent possibilities for the selection of the a and b axes, with these possibilities differing by a rotation of 60° about the c axis. Depending on which choice is made, the same plane can have different indices (121 and $3\bar{1}1$ for example), but in either orientation these indices do not interconvert, for they are not equivalent by symmetry. The result of this is that in a crystal which is twinned by this 60° rotation each hkℓ reflection is the average of the two non-equivalent contributors.

For the 6T-$Zr_{1+x}Cl_2$ the structure could be solved only because the $2H_b$ subcell has higher symmetry for which these reflections are equivalent. Because of this, all of the observed differences between this

structure and three cells of the $2H_b$ type represent the average of the two orientations, although the basic structure is correct.

A (110) section for the 6T-$Zr_{1+x}Cl_2$ structure appears in Figure 10d. As mentioned above, this structure is approximately equivalent to three unit cells of the $2H_b$-MoS_2 type (for a total of six slabs) with an extra metal atom in an octahedral hole every six slabs. The $2H_b$-MoS_2 structure is unique in several respects, not the least of which is that it is the only slab-type structure which occurs exclusively for d^2 compounds. Besides this, it is the only structure having only trigonal prismatic coordination of the cations where every cation has two anion second nearest neighbors directly above and below it through the triangular ends of the prism (ThI_2 also has this, but half the cations have octahedral coordination). It is also the only structure where an extra metal atom in an octahedral hole between slabs does not share at least one face of its coordination sphere with another metal atom. This latter is no doubt quite important in the structures occurring for the substoichiometric halide.

Because of the degree of refinement in this structure nothing can be gained by comparing the individual interatomic distances within the structure. The average Zr-Cl bond length in this structure is 2.57(2)Å slightly, but not significantly, less than that observed in 3R-$ZrCl_2$. At 3.33(3)Å the slab height also fits that description, and the interslab distance at 3.59(4)Å is essentially the same as the 3R form. The reduced axial ratio at 1.9094 is virtually unchanged.

The search for an alternative to the 3R structure for the substoi-

chiometric zirconium dichloride originally began because of the presence of extra lines in the powder pattern of reduced samples. With the identification of Zr_6Cl_{12} and the two variations described in the next section almost all of these lines could be accounted for. There was no evidence for any of the lines from the 6T structure which do not overlap those of 3R.

The implication of this is that the 6T structure is present in larger single crystals, always intergrown with the 3R variation, never alone, but not in the microcrystalline powder samples, at least not enough to be visible to x-rays. This indicates that the conditions in which the transport grown single crystals containing 6T-$Zr_{1+x}Cl_2$ form are distinctly different from those under which powders are produced in isothermal reactions.

18T-$Zr_{1+x}Cl_2$ and other variations

Before now the longest repeat sequence characterized for any trigonal prismatic slab type compound was six slabs in 6R-TaS_2, where half the cations have octahedral coordination.[50] The only cell reported which is longer than this is a 12-slab supercell observed but not further characterized and based on the 6R cell.[102] No increase in a has ever been observed.

Figure 13 is a print of a Weissenberg photograph showing many extra reflections along the h0ℓ festoons. An enlargement of part of it appears in Figure 14. A careful examination of this film indicated that between many pairs of reflections which could be explained with some variation of

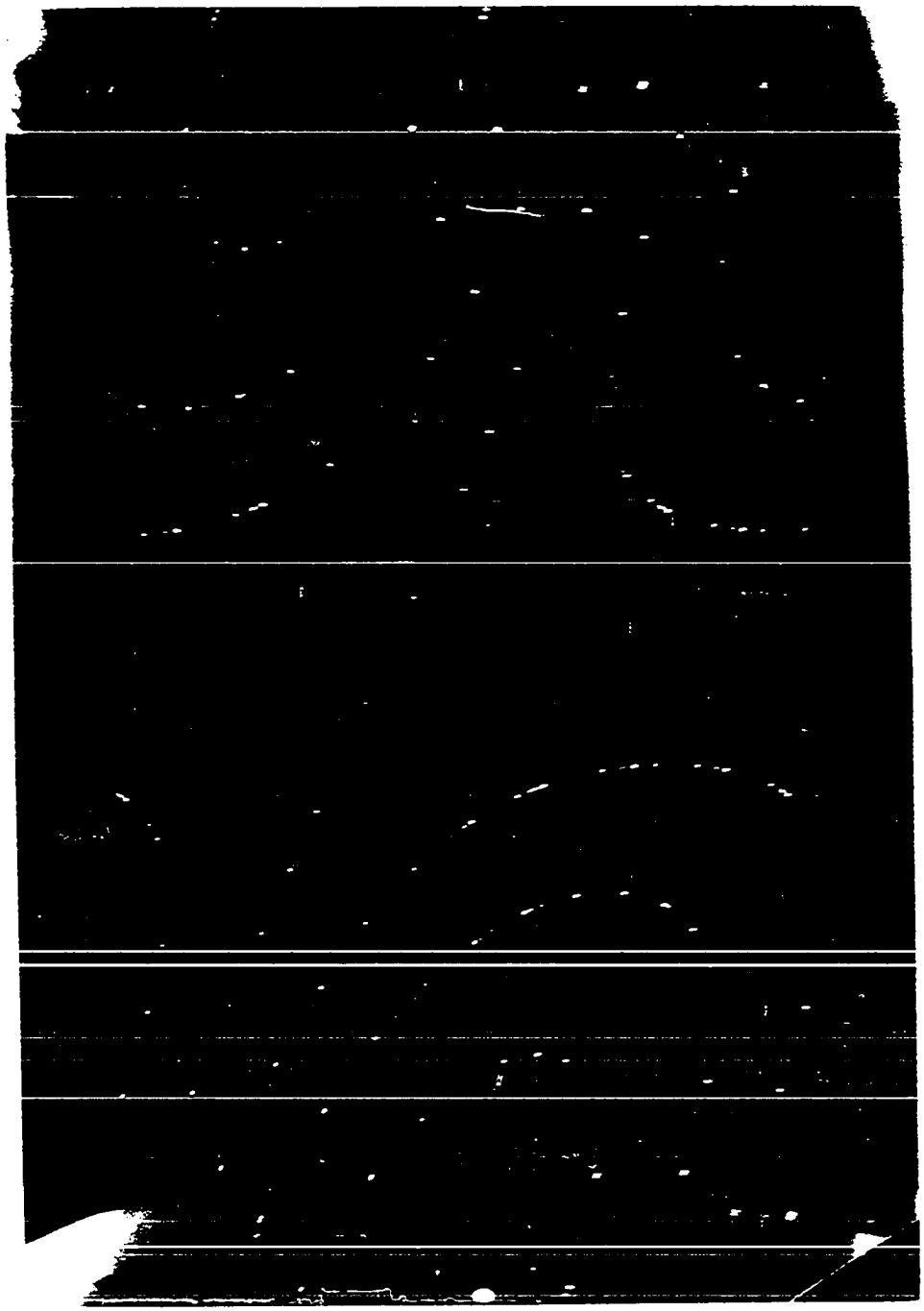

Figure 13. A Weissenberg photograph (rotated about b) of a crystal of 18T-$Zr_{1+x}Cl_2$.

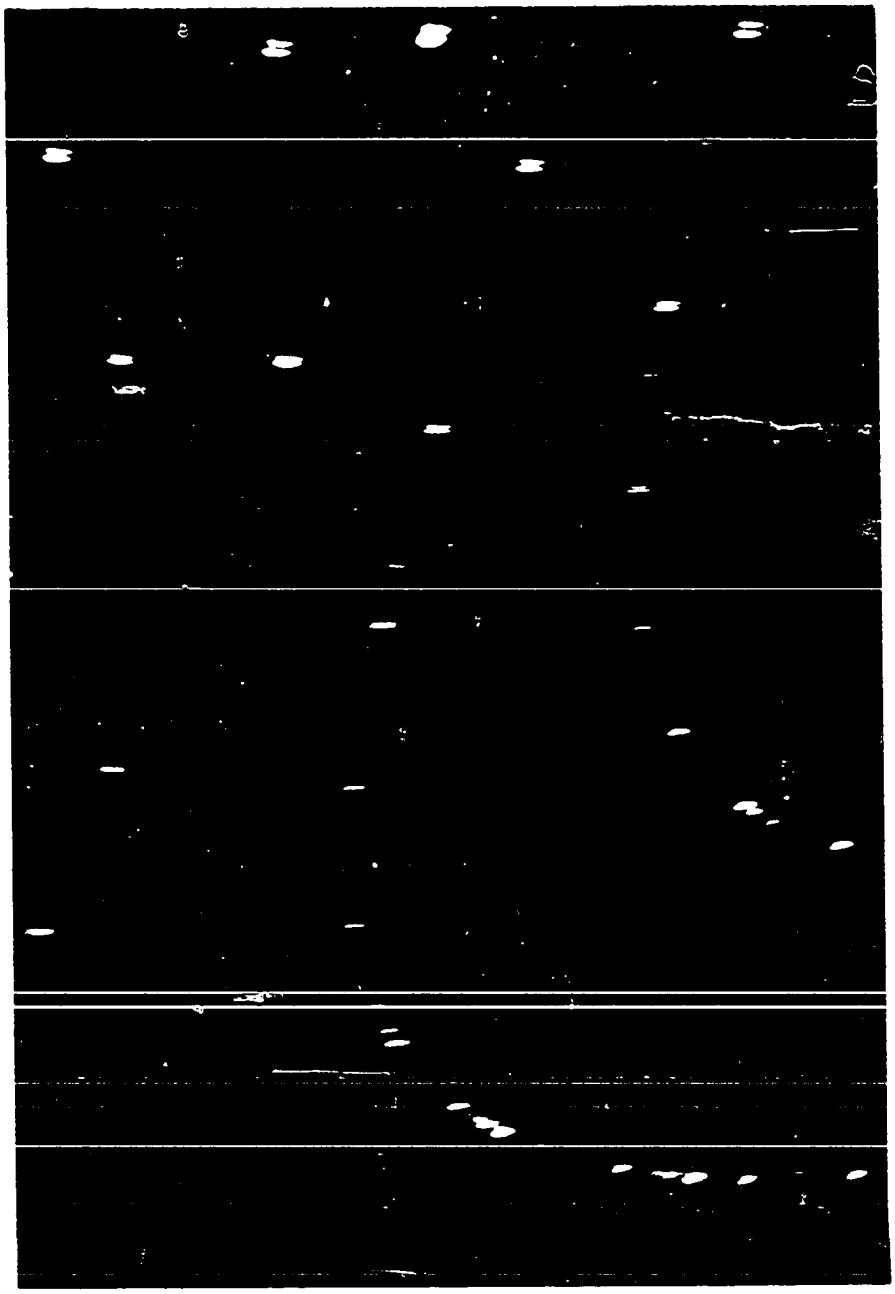

Figure 14. Enlargement of the upper right quarter of Figure 13 showing details of the festoon with the spots observed for 18T-$Zr_{1+x}Cl_2$.

the 3-slab unit cell there were three additional spots. The relative center to center distances for an entire series of five spots were 2:1:1:2. These proportions indicate that the three center spots were the center three from the series of five which would be expected in that interval for a unit cell with eighteen slabs in the repeating sequence.

With this evidence for the existence of a compound with an 18-slab unit cell, several previously unindexable lines in two powder patterns could be understood and lattice parameters obtained for this variation (which will be designated 18T in the absence of any symmetry information). These parameters are; a = 3.3820(2)Å, c = 116.312(15)Å, and c/18a = 1.9106. Although c is slightly greater (0.044(23)A) than six times the c axis in 3R-$ZrCl_2$, no conclusion can be drawn from this without knowledge of the phase purity of the specimen.

While an investigation of this structure might have proven interesting, it was unlikely to prove profitable enough to justify the effort it would entail. Because of the length of the c axis it would not be possible to resolve the individual reflections with an automated diffractometer, for even employing copper radiation the spot separation was less than the spot diameter. Data could be obtained using copper radiation with film techniques and the large investment of time this entails, but there is no guarantee that the crystal was single. Furthermore, absorption would be a severe problem for a crystal this anisotropic (width:thickness $\geq$ 10:1) and with $\mu_{Cu} = 533\ cm^{-1}$.

Four lines frequently appear together in powder patterns of $Zr_{1+x}Cl_2$

which cannot be fully explained by any of the varieties of $ZrCl_2$ described previously. One of these lines will index as 114 for a primitive cell with the same dimensions as 3R-$ZrCl_2$ and another is almost within experimental error of 111 for this type of cell. The other two have 2θ less than 003 (the lowest allowed reflection) from 3R-$ZrCl_2$ with one found very close to 003 from ZrCl. All three of these irregular lines can be indexed on a unit cell with $a = 3a_{3R}$ and six slabs to the repeating sequence. For this cell the lowest line is 100, the second 103, and the line near where 111_{3R} should be 333.

While this may be sufficient data to define the lattice size ($a \simeq 10.146\text{Å}$ and $c \simeq 38.77\text{Å}$) of this supercell, given the demonstrated trends to polymorphism and supercell formation of the slab-type $ZrCl_2$, there are so many possible arrangements for a cell of this size that speculation on its structure is pointless. This structure is definitely distinct from the 6T structure, for no evidence was ever observed for an extension of a in 6T and when these four reflections (100, 103, 333, and 338) were sought in a crystal of 6T they were not found.

The most significant feature of this superstructure is the ordering along a. This is the only evidence to date of ordering parallel to the slabs in any slab-type compound.

There is not sufficient evidence to define either any additional orderings of the slab type compound or a different type of halide, although there is some scanty evidence for the existence of other compounds. This evidence is the set of otherwise uninterpretable lines found in the original powder pattern of Zr_6Cl_{12} which faded away on

exposure to air and a pattern obtained from material scraped from the walls of a tantalum tube used in a 700° to 750° transport reaction.

In the six weeks this reaction ran, barely enough material was obtained for one powder pattern, and even this meager amount was obtained only after scraping the entire interior of the tube, most of which was covered by tiny particles of a reflective material. Because the material was collected over such a wide temperature range it is not clear that the sample was single phase, although the distribution seemed even. Furthermore, it is not even clear that the material was transported to the walls of the tube; it may have been formed from a reaction occurring with material sticking to the walls from the initial filling of the tube. What is quite clear is that this material does not contain a significant amount of any known zirconium chloride or oxide, zirconium, tantalum, or tantalum oxide.

Photoelectron spectroscopy of zirconium chlorides

Table XX lists the peak maxima from the x-ray photoelectron spectra (XPS) of most of the zirconium chlorides. Ultraviolet photoelectron spectra were also obtained for most of these compounds and served only to confirm the XPS results for the Zr4d and Cl3p bands. The slab-type dichloride spectra are not labeled as to polytype because of the difficulty in obtaining powder specimens which are purely one polytype. However it is unlikely that the difference between polytypes would be detectable by XPS, the spectrum being almost entirely dependent on the bonding within the slab. However the valence portion of the spectrum

Table XX. X-Ray photoelectron spectra of zirconium chlorides

Level	Zr[a]	ZrCl	$ZrCl_{\sim 2.0}$[b]	$ZrCl_{1.6}$[c]	Zr_6Cl_{12}	$ZrCl_3$	$ZrCl_4$[d]
Zr4d	0.8 eV	1.15	1.2	1.2	1.45		
Cl3p		6.4	6.55	6.5	6.50	6.55	5.0
Cl3s		17.3	17.65	17.9	17.3	16.95	e.
$Zr3d_{5/2}$	178.8	179.4	180.15	180.1	179.9	182.15	182.8
$Zr3d_{3/2}$	181.2	181.75	182.7	182.5	182.6	184.45	185.2
$Cl2p_{3/2}$		199.6	200.0	200.05	199.1 199.55	199.7	198.5
$Cl2p_{1/2}$		201.15	201.5	201.65	200.7 201.1	201.25	200.1

[a] From reference 103.

[b] Composite from two specimens. Because of difficulties in standardizing, the spectrum was referenced by minimizing the differences in the core levels with $ZrCl_{1.6}$.

[c] $Zr_{1.25}Cl_2$.

[d] From reference 30.

[e] Not reported.

labeled $ZrCl_{2.0}$ was obtained on a specimen of 3R-$ZrCl_2$. The values for ZrCl found here are within 0.1 eV of those obtained previously on another instrument[30] and so it can be assumed that the values for $ZrCl_4$ would agree as well.

The Cl2p (core) levels exhibit the expected trend to lower binding energy in $ZrCl_4$, where they are formally more ionic, as compared with the relatively covalent ZrCl. The total shift is not large ($\leq$ 1.5 eV) and the trend is not linear however, with most of the change coming between $ZrCl_3$ and $ZrCl_4$. A similar pattern is found in the Cl3p (valence) levels, with all of the reduced chlorides falling within experimental error of 6.5 eV and $ZrCl_4$ falling 1.5 eV lower. No pattern is present for the Cl3s data.

The Zr3d (core) levels show an interesting pattern, consisting of the expected monotonic increase in binding energy with oxidation state (a change of 4 eV between Zr° and Zr^{+4}). The rate of this change is not linear however, with just over half of the increase coming between $ZrCl_2$ and $ZrCl_3$. This is the same gap over which the Zr4d (valence) band disappears and thus may correlate with the changes in conduction which occur as the material becomes more oxidized.

These changes in conduction can be followed by examining the Zr4d band. In elemental zirconium (Zr°, $4d^4$) this band is centered at 0.8 eV below the Fermi edge with a sizable density of states at that level, as expected.[103] In ZrCl ($4d^3$) the band maximum is shifted to 1.15 eV below the Fermi level and the density of states at that level is lower, as expected.

The shift in position for Zr4d on going to the slab-type dichloride is negligible (in fact, the 0.05 eV shown is about 1/6 of the estimated accuracy). What is significant is that the band in $ZrCl_2$ is smaller, compared with Cl3p, and narrower. The change in size is entirely as expected, coming from a doubling of the number of chlorine atoms per zirconium atom and a loss of one electron (to $4d^2$) for each zirconium. The narrowing of the band appears to be a consequence of a fundamental change in the conductivity with the density of states at the Fermi level dropping to nearly zero (see Figure 15). This indicates that slab-type $ZrCl_2$ is either a very poor metallic conductor or, far more likely, a narrow gap semiconductor. The only way to determine this definitely would be to measure the single crystal conductivity as a function of temperature, and as yet all crystals obtained have been too small for such measurements. In either case, the electrons appear sufficiently delocalized at room temperature to give a metallic appearance to large single crystals.

For the cluster type dichloride, Zr_6Cl_{12}, the Zr4d band is shifted to slightly higher (0.2-0.3 eV) binding energy, which is reasonable in the light of the more localized metal-metal bonding in the clusters. Interestingly the Zr 3d levels have shifted by a slight, but not significant, amount to lower binding energy. If this shift is real it could represent an effect of improved local delocalization within the cluster in comparison with the slab structure. This is in line with the observed bond lengths of 3.20Å(x4) in Zr_6Cl_{12} compared with 3.382Å(x6) in 3R-$ZrCl_2$.

Figure 15. The valence region of the XPS spectrum of slab-type $ZrCl_2$ with an actual composition of $ZrCl_{1.6}$. This is a smoothed 440 scan spectrum obtained with monochromatized AlK_α radiation (1486.6 eV). Vertical scale is arbitrary.

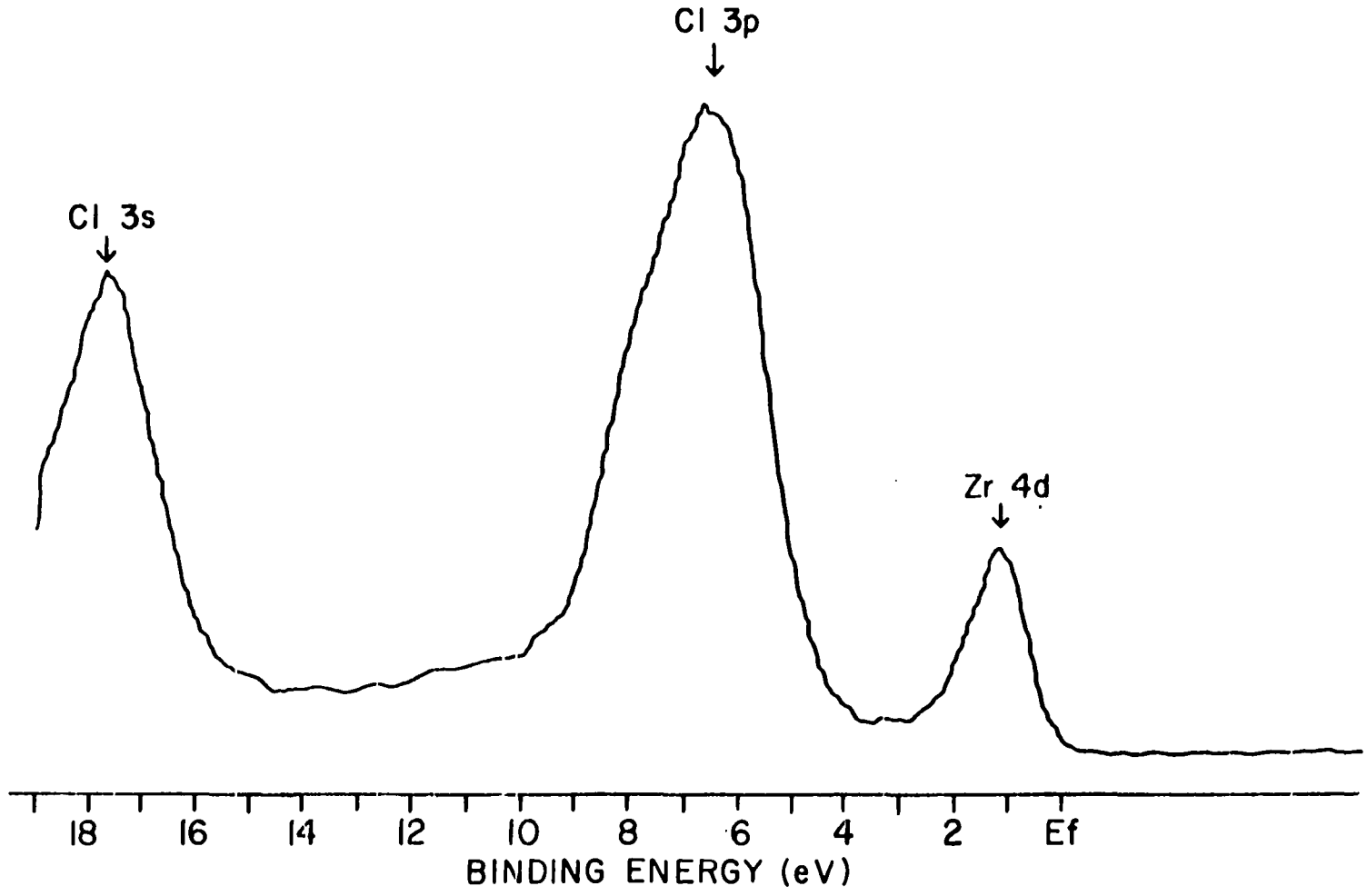
Cl 3p
Cl 3s
Zr 4d
18
16
14
12
10
8
6
4
2
Ef
BINDING ENERGY (eV)

In the trichloride, the Zr4d band is unobserved. This is somewhat surprising, for while it would be expected to be smaller (relative to Cl3p) than in $ZrCl_2$ by a factor of three, it should still be visible, unless it had also shifted to at least 3 eV higher binding energy. While the Cl3p band in $ZrCl_3$ is wider compared with $ZrCl_2$, (3.35 eV at $h_{1/2}$ versus 3.1 eV), a shift of 3 eV for Zr4d seems unlikely. Large crystals of this compound still show a luster and the compound is still a semiconductor, although there are definitely fewer electrons available for conduction in any unit volume of this compound.

The sudden increase in the Zr3d binding energy is probably a result of this increase in electron localization in $ZrCl_3$ relative to the more reduced chlorides. This would seem to be a very clear cut correlation from the XPS data alone; however, the fact that the closest Zr-Zr distance in $ZrCl_3$ is 0.315Å shorter than the closest distance in 3R-$ZrCl_2$ (3.067Å(x2) vs 3.382Å(x6) clouds this argument. It would be interesting to have XPS data from Zr_6Cl_{15}; unfortunately none of this compound was available. Based on the results here the Zr_6 cluster would be expected to dominate and with the delocalization within the cluster the Zr3d levels may be expected to occur around 180.5 eV ($3d_{5/2}$) and 182.9 eV ($3d_{3/2}$).

The tetrachloride shows the same shift in core levels relative to $ZrCl_3$ as $ZrCl_2$ does relative to ZrCl.

Figure 16 shows an interesting effect which is observed with the cluster dichloride Zr_6Cl_{12}, namely, the apparent splitting of the Cl2p levels for the two different types of chlorines present. With barely

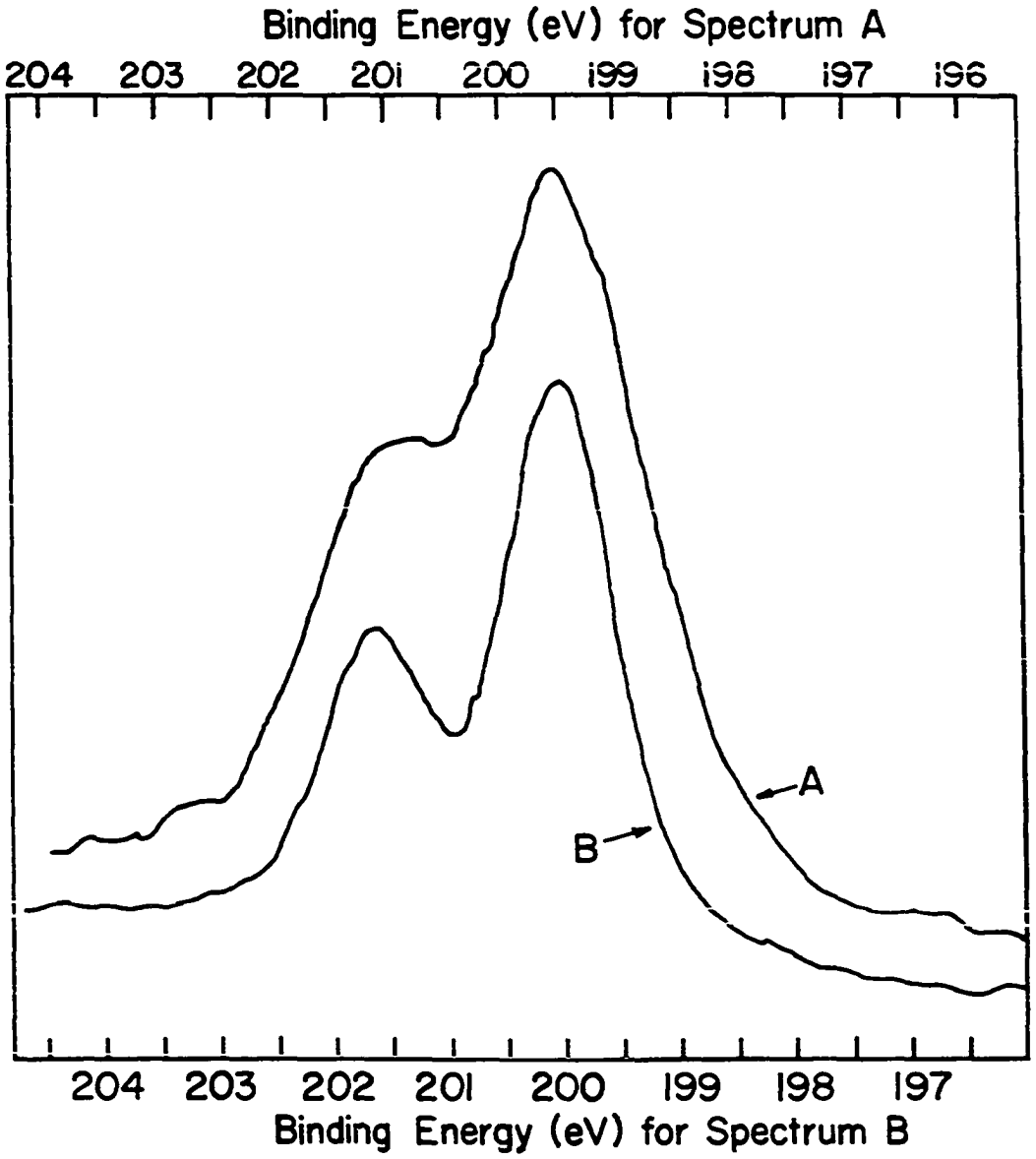

Figure 16. Cl2p bands from the XPS spectra of Zr_6Cl_{12}(A) and $ZrCl_2$(B). The shoulders in A at 199.1 eV and 201.1 eV are exactly what would be expected for the sum of two doublets, both the shape of B, offset by 0.4 eV.

1 eV shift between ZrCl and $ZrCl_4$ it is surprising to find this separation (~0.4 eV) and doubly and triply bridging chlorines in the same compound.

It is also interesting that there is no apparent shift on reduction of $ZrCl_2$ to near its reduced limit. A mixture of slab-type varieties with the same predominant component in each can be ruled out by the fact that in all cases the lines in the powder pattern were sharp and different stoichiometries were clearly indicated for the samples. Another possibility arises from the fact that XPS is essentially a surface technique with most of the electrons coming from the top few unit cells. With materials that can be etched with an argon ion gun, deeper material can be examined by successively burning away layers and examining new surfaces which were originally buried, but the zirconium chlorides reduce instead of etching. It is entirely possible that in a sample with a bulk composition of $ZrCl_{1.6}$ the surface layer could be stoichiometric $ZrCl_{2.0}$. This could come about by the oxidation of the surface layer by the $ZrCl_4$ gas phase as it condenses on cooling. In this situation the surface layer, as examined by XPS, would appear identical in both the stoichiometric and reduced samples. In the reduced material this surface would represent only an insignificant fraction of the whole, a fraction too small to observe by x-ray diffraction, and not be representative of the bulk.

The narrow gap semiconductor behavior observed in slab-type $ZrCl_2$ fits nicely into the previously observed progression in the conductivities of the zirconium chlorides from metallic ZrCl through the wide gap semiconductor $ZrCl_3$ to the insulating $ZrCl_4$. This same behavior also fits in

quite nicely with the isostructural chalcides, MoS_2 and NbS_2. As mentioned earlier, $ZrCl_2$ exhibits a reduced axial ratio deviating from the ideal in the same direction as the semiconducting MoS_2, although the difference is not as great. In this setting $ZrCl_2$, as a narrow gap semiconductor, fits nicely between the metallic NbS_2 and MoS_2.

Although the XPS spectra of 3R-MoS_2 and 3R-NbS_2 are not available, those of 2H-MoS_2 and 2H-$NbSe_2$ are.[104] Since the bonding within the slabs is so dominant, it is unlikely that the difference in packing has a measurable effect.[105] The spectrum of $NbSe_2$ shows the expected metallic behavior, in agreement with other measurements and calculations[105] done on this compound, and supporting the expectation of a similar spectrum for NbS_2. Both previous measurements and calculations classify MoS_2 as a semiconductor, and this is confirmed by the XPS results which show the highest occupied band Mo4d to be centered at 3 eV below the Fermi edge with at least a 2 eV gap between the top of the band and the edge.[104] The XPS results also show an overlap in binding energy between this band and the S3p band which is not predicted by the calculations.[105] This overlap, which is clearly not present in $ZrCl_2$ (see Figure 15), is most likely a manifestation of the greater covalence of the dichalcide.

Given the differences observed between the calculated and observed valence band structures for MoS_2, any extrapolation of the calculated band structure to the isoelectronic but less covalent $ZrCl_2$ can only be valid for the most general features. The splitting of the d orbitals such that the highest orbital is filled completely, resulting in non-

metallic properties, is just such a result.[105] This is the same result as is obtained in a localized ligand field model[98] but for different reasons.[105]

One interesting conclusion drawn from the comparison of the $ZrCl_2$ and MoS_2 valence band spectra is that the conduction in the two compounds is fundamentally different. In MoS_2 the observed overlap of metal and sulfur binding energies indicates a likely contribution to the conduction from the sulfur electrons. In $ZrCl_2$ the lower covalency results in a separation of the Zr4d and Cl3p bands. At the same time zirconium, as a result of having a lower nuclear charge, has a greater d orbital extension than molybdenum. This is further accentuated in the case of these compounds by a lower formal charge in $ZrCl_2$ compared with MoS_2. Therefore, the metal-metal overlap in $ZrCl_2$ is at least as good as the overlap in MoS_2, even though the atoms are more widely separated and the sulfide ligands would be expected to slightly extend the molybdenum d orbitals. The result of this is that the conduction in $ZrCl_2$ is due to a band which is nearly pure metal in origin.

Intercalation

Intercalation, the insertion of neutral molecules or ions into the van der Waals gap between slabs, is an important part of the chemistry of both the slab-type dihalides and the slab-type dichalcides. While the group V dichalcides (such as NbS_2 and $TaSe_2$) tend to substoichiometry and intercalate a wide variety of materials,[106] the group VI dichalcides (such as MoS_2) only occur on stoichiometry and only inter-

calate the alkali metals easily.[107] Because $ZrCl_2$ contains a d^2 core like MoS_2 but has a significant region of non-stoichiometry like NbS_2 it is not clear which, if either, furnishes a better model for possible intercalation. Several attempts were made to intercalate this compound, all of which were unsuccessful.

Direct reaction of $ZrCl_2$ with anhydrous ammonia for 20 hours, three at -20° and 17 at ~ -80°, produced NH_4Cl and a slight degradation in the powder pattern of the unreacted $ZrCl_2$. Pyridine condensed on $ZrCl_2$ at 0° reacted in minutes to produce a dark brown solution. Standing overnight had no effect on the appearance of either the solution or the solid at the bottom. Evaporation of the pyridine left a brown solid on the walls of the container. The only lines present in the powder pattern were those of $ZrCl_2$ with no evidence of intercalation.

The brown material formed lost pyridine rapidly if not in a pyridine-rich atmosphere and no powder pattern was obtained. Based on its occurrence, color, and solubility in pyridine the brown product was most likely $ZrCl_3 \cdot 2py$ which has been previously reported as the product formed by the reaction of $ZrCl_3$ with pyridine at room temperature.[108] Its presence here suggests a disproportionation of the dichloride with the formation of either metal or monochloride in a poorly crystalline form.

Attempts to intercalate both sodium and potassium from the liquid ammonia solutions were unsuccessful. In the former case much gas was evolved but no crystalline solid products were identified in the powder

pattern. In the case of potassium the only solid products found were NH_4Cl and KCl.

Relationships between the dichlorides: the cluster dichloride

The cluster dichloride, Zr_6Cl_{12}, is the most enigmatic of the dichloride variations. It is structurally related to the rarely observed Zr_6Cl_{15}, but thermodynamically it is difficult to relate to any of the other compounds in the Zr-Cl system.

Evidence for the presence of traces of the cluster dichloride has been found in numerous specimens in the form of the strongest lines from Zr_6Cl_{12} powder pattern showing through the pattern of the predominant slab-type material, but only twice has Zr_6Cl_{12} been the predominant product.

Several attempts were made to interconvert the slab and cluster dichlorides, with no clear results. Since both of the reactions in which the cluster compound had predominated had been carried out at 700° it seemed possible that this was the form of $ZrCl_2$ stable at high temperature. If this was the case, a specimen of the cluster compound would be expected to convert to the slab-type at a lower temperature. However, when a specimen of the cluster compound was equilibrated for a month at 625° the only change visible in the powder pattern was a slight sharpening of the lines.

When a mixture of the two, with a net composition of $ZrCl_{1.5}$, was equilibrated at 675° for six weeks no change was observed, but when this same material was combined with enough $ZrCl_4$ to give a solid with a

composition of $ZrCl_{2.0}$ plus six atmospheres of $ZrCl_4$ and was heated to 700° for two weeks the result was a mixture of 3R-$ZrCl_2$, $ZrCl_3$, and a trace of ZrCl with one extra line that might have been from Zr_6Cl_{15}.

Another experiment was tried which involved a quantity of Zr_6Cl_{12} in one tube and a quantity of slab-type material, with a composition about $ZrCl_{1.7}$, in an outer, concentric tube, with the two sharing a common gas phase. What actually happened was the formation of a pinhole in the tube and the partial disproportionation of the entire contents. Interestingly the powder patterns revealed both the inner and the outer sections of the tube contained a mixture of cluster dichloride and monochloride. This suggests that the cluster may have been formed in the outer section by the disproportionation of the slab-type compound and that the cluster compound is more stable to disproportionation than the slab-type compound. Whether this stability is thermodynamic, resulting from lower vapor pressure over the cluster, or kinetic, resulting from the lack of an efficient mechanism for disproportionation, is unknown.

Given just the data from these experiments it would appear that the cluster compound might be more reduced than the slab. However, the x-ray data for the cluster agrees too well with that calculated for Zr_6Cl_{12} for the compound to be very substoichiometric, and the ratio of the area of the Cl3p peak to the Zr4d peak in the XPS spectrum of the cluster is virtually the same as that ratio in the slab compound.

Another possibility is that one type of the dichloride is actually only metastable. It is nearly impossible that the slab-type compound is metastable considering the variety of conditions under which numerous

investigators have made this compound. It is possible that Zr_6Cl_{12} is only metastable, but no data indicate this directly.

The final possibility is that this is an impurity stabilized phase. This is unlikely however as the XPS spectrum showed only zirconium, chlorine, oxygen, and carbon to be present in significant amounts. Either of the latter two could be the stabilizing impurity, but given the knowledge that the specimen had been handled several times prior to taking the spectrum it is more likely that those represent surface impurities. Given the clear evidence that the zirconium is divalent it is also unlikely that any divalent anionic impurity is present in a significant amount.

Thus, the relationship between the slab and the cluster dichlorides must remain undefined at this time.

Relationships among the slab dichlorides

This investigation began as an attempt to explain the non-stoichiometry of the slab-type zirconium dichloride. With the results described and discussed in the previous sections this can largely be accomplished.

The results indicate that 3R-$ZrCl_2$ only exists in a rather narrow range near stoichiometry. Within this range truly single crystals only exist right on stoichiometry. If symmetry is to be maintained, there is only one site available for the insertion of extra metal atoms, the octahedral hole between the slabs located at (0,0,5/6) (and two other equivalent points). In all of the chalcide reports, including a recent single crystal study of $Nb_{1+x}S_2$,[109] substoichiometry is achieved by a fractional occupancy of this site.

In 3R-$ZrCl_2$ occupancy of this site would result in 3.23Å Zr-Zr distance, a distance which would have to be accompanied by some form of interaction. Since a bonding interaction would distort the slab it is likely that the interaction is at least partly repulsive, and since repulsive interactions are avoided whenever an alternative is available an alternative accommodation for the extra atoms would seem favored.

Figure 10c shows such a mechanism. In this figure it can be seen that the stacking starts out as the rhombohedral obverse form. At an octahedral hole between slabs an extra atom, indicated by the x, is inserted. In the next slab the trigonal prism which is expected to hold the metal atom is vacant and that atom instead occupies the adjacent trigonal prism, which is equivalent in all ways except for the lack of sharing of a face with the octahedron. From this point the stacking continues as before, only with this slight shift which is equivalent to a rotation of 60° in the orientation of the rhombohedral coordinate system relative to the hexagonal, and the stacking appears to have the reverse rhombohedral orientation.

This mechanism produces two effects. The first gives a minimum metal-metal distance of 3.77Å for an atom in an octahedral hole between the slabs where the stacking slip occurs. Two neighbors at this distance share opposing edges of the octahedron with it. The second effect is a twinned crystal. Actually in any given crystal there may be many such changes in the stacking, but regions of the crystal separated by two changes will be in the same relative orientation as they would with no changes so only two types of regions are generated and the crystal

appears twinned. It is the frequent observation of such twinned crystals, generally growing in the region just hotter (more reduced) than that where the untwinned 3R-$ZrCl_2$ crystals were found, that supports this mechanism for absorbing small amounts of extra metal.

Although this essentially random distribution model will allow the absorption of small amounts of extra metal, some concentration limit will be reached at which the extra metal atoms begin to interact with each other, and develop a periodicity. As described earlier, three larger unit cells are observed, and of these, 18T-$Zr_{1+x}Cl_2$ appears to be the best candidate for a simple interstitial ordering.

The fact that this compound has only been observed in samples equilibrated at over 700° and cooled rapidly (in comparison with the multi-week periods needed to approach equilibrium) suggests that it may be only metastable at temperatures below 700°. From the degree of tube bulging it is clear that at these temperatures 18T has a tetrachloride partial pressure of > 5 atm over it. Above 725° the dissociation pressure climbs rapidly, to over 30 atm at 800° based on the degree of tube bulging and the amount of gas generated by a sample which had completely dissociated to ZrCl and $ZrCl_4$ before it was quenched from 800°.

In the series of isothermal equilibrations in which powder pattern evidence of 18T was found the 18T was only observed in samples just slightly reduced from $ZrCl_{2.0}$ in composition. This gives its composition limits as approximately $ZrCl_{1.85}$ to $ZrCl_{1.95}$, with the upper limit presumably in equilibrium with twinned 3R-$ZrCl_2$ (t-3R).

The fact that 6T-$Zr_{1+x}Cl_2$ is found intergrown with t-3R is a strong indication that some variation, probably 18T, forms at high temperature and on cooling disproportionates by ionic diffusion and slab slippage to t-3R at its reduced limit and 6T at its oxidized limit. If this disproportionation temperature is high enough to ensure good ionic mobility, which it seems to be, numerous regions of the crystal will grow into separate microcrystals (with dimensions on the order of 100 to 1000Å from the observed peak sharpness) with all of their axes in register. That this diffusion mechanism is not perfect, and that all of the atoms do not always end up in their equilibrium positions, is clear from the streaks observed along the festoons in all of the crystals of this type examined.

As was noted earlier, the 6T variation is a superstructure of the $2H_b$ stacking scheme, not of the 3R scheme. Because of this the 6T phase would be very apparent if a significant amount were present in a powder specimen. The only evidence found for the existence of this compound has been in intergrown single crystals. This could indicate that the kinetics of growth for this variation are quite poor in the isothermal equilibrations and favored in the single crystal disproportionation reaction described above. Alternatively, but less likely, it could indicate that the 6T variation has a minimum temperature for stability and in the powder specimens has undergone a phase transition which is usually blocked in the single crystal. If the latter is the case, it may also be true that when the fraction of the crystal which is 6T exceeds a certain value the phase transition occurs, and in the process

the crystal becomes multiple and as such is rejected for extensive x-ray examination. This stabilization of the high temperature form by essentially dissolving it in t-3R is analogous to the stabilization of the cubic (high temperature) form of zirconia by stuffing it with calcium or magnesium. This would serve to explain why in every good crystal containing 6T it is the minority component. From the available data it is impossible to tell which is correct.

Exactly where the variation with the $a' = a_{3R} \times 3$ and $c' = 6$ slabs fits is difficult to say. It is present in many, if not most, substoichiometric powder specimens, but it is not clear in what quantity, and without this knowledge it will be difficult to determine more.

Most non-stoichiometric compounds are disordered and display a definite variation in lattice parameters with composition which, once determined, furnishes a quick method of determining an approximate composition. While the lattice parameters of $ZrCl_2$ vary with composition, the direction of the trend depends on the temperature of equilibration.

At 650° and below both a and c expand with increasing interstitial concentration (reduction), as would be expected from the increase in the Zr-Cl bond length arising from the reduction of the zirconium. At 700° both a and c increase with increasing interstitial occupancy for the composition region $ZrCl_{2.0}$ to $ZrCl_{1.9}$ and then contract for the region $ZrCl_{1.9}$ to $ZrCl_{1.5}$. At 725° no change is apparent. Although all changes mentioned are significant (5-6σ) they are also quite small (< 0.5%). If these results indicate anything, it is that the arrangement of the interstitial atoms varies as much with the temperature as with the composition.

Daake reported an apparent stoichiometry range for zirconium dichloride of $ZrCl_{1.5 \text{ or } 1.6}$ to $ZrCl_{\sim 1.75}$ based on equilibrations done at 600° and below.[30] Based on the results obtained for this dissertation the range is $ZrCl_{1.5}$ to $ZrCl_{1.75}$ at 600°. At 650° the oxidized limit is about $ZrCl_{1.9}$. At 700° and above the range is from somewhere between $ZrCl_{1.5}$ and $ZrCl_{1.6}$ and $ZrCl_{2.0}$, although the single crystal data indicates that there is a gap occupied by a two phase region somewhere in that range at temperatures just below 700°.

Initially it was postulated that there was one compound, $ZrCl_2$, which by continuous variation in the occupancy of one, or more, interstitial sites achieved a very large stoichiometry range with a fixed structure. This is the typical behavior of a true non-stoichiometric compound. Clearly, this is not the case.

What is actually found is a series of ordered compounds, at least four in number and probably many more. At this point it is not clear if any of them are nonstoichiometric, but if any are, it is only over a limited range. The observed properties could just as easily be explained by a series of structures, each consisting of a slab-type subcell with an extended ordered arrangement of interstitial atoms and each differing only slightly in composition and structure from its neighbors. While no exactly analogous system is known, both large degrees of polytypism in slab-type compounds[50] and compositionally closely spaced, structurally related phases[110] are known in other systems.

FUTURE WORK

Although there are still numerous polyanions of the post-transition elements left to be found, it is very unlikely that anymore polytellurides or polybismuthides will be produced with cryptated potassium cations in ethylenediamine. A better possibility for polytellurides is in liquid ammonia solution. Both reports of Te_4^{2-} described work done in liquid ammonia[7,9] and this dissertation describes the synthesis of a compound from K_2Te and excess tellurium in liquid ammonia with a powder pattern drastically different from that calculated for $(crypt\ K^+)_2Te_3^{2-}\cdot en$.

It may be possible to make other polybismuthides in ethylenediamine using sodium instead of potassium. An earlier report describes rose-colored crystals, which were too soft to handle, produced using sodium and 2,2,2-crypt.[19]. The use of 2,2,1-crypt, with its greater affinity for sodium[24] should lead to a more tractable product, and the identification of other polybismuthides.

The composition range between ZrCl and $ZrCl_2$ offers many possibilities for new compounds or polytypes. A wide variety of polytypes for one compound is a common feature of the slab-type dichalcides, and the results in this dissertation indicate that it is for the slab-type dihalides as well. There is still a good possibility of finding other polytypes for $ZrCl_2$, and it is not clear where the $a = 3 \times a_{3R}$, 6 slab variation fits in relation to the other types. Besides the dichlorides,

the dibromides represent a virtually untapped but potentially very interesting area for investigation.[30,100]

Although all attempts at intercalation have been unsuccessful, it is still possible that a method might be found, possibly in the form of an easily oxidized organic compound, to put something between the slabs.

With the results reported in this dissertation it was not possible to explain how the cluster compound Zr_6Cl_{12} relates to the other compounds in the Zr-Cl system. This is a feature which it shares with Zr_6Cl_{15}.[30] Fitting either, or both, of these compounds into their appropriate places in the Zr-Cl system and finding a method of producing these in quantity would open the door to a vast area of interesting chemistry. This area is the reactions of the cluster, in analogy to the wide variety of reactions known for the tantalum and niobium M_6X_{12} clusters.

BIBLIOGRAPHY

1. J. D. Corbett, Prog. Inorg. Chem., 21, 129 (1976).

2. H. Schäfer, B. Eisenmann, and W. Müller, Angew. Chem., Int. Ed., 12, 694 (1973).

3. A. Joannis, C. R. Acad. Sci., 113, 795 (1891).

4. F. H. Smyth, J. Amer. Chem. Soc., 39, 1299 (1917).

5. C. A. Tibbals, J. Amer. Chem. Soc., 31, 902 (1909).

6. "Gmelins Handbuch der Anorganischen Chemie - System Number 11." Verlag Chemie, Berlin, 1940, p 272.

7. C. A. Kraus and C. Y. Chiu, J. Amer. Chem. Soc., 44, 1999 (1922).

8. C. A. Kraus and E. H. Zeitfuchs, J. Amer. Chem. Soc., 44, 2714 (1922).

9. E. Zintl, J. Goubeau, and W. Dullenkopf, Z. Phys. Chem. Abt. A, 154, 1 (1931).

10. A. F. Wells, "Structural Inorganic Chemistry," 4th ed, Clarendon Press, Oxford, 1975, pp 613-615.

11. N. K. Goh, Doctoral Dissertation, Münster, 1974.

12. H. G. von Schnering and N. K. Goh, Naturwissenshaften, 61, 272 (1974).

13. D. J. Merryman, J. D. Corbett, and P. A. Edwards, Inorg. Chem., 14, 428 (1975).

14. P. A. Edwards and J. D. Corbett, Inorg. Chem., 16, 903 (1977).

15. H. H. Sutherland, J. H. C. Hogg, and P. D. Walton, Acta Crystallogr. Sect. B, 32, 2539 (1976).

16. E. Zintl and W. Dullenkopf, Z. Phys. Chem. Abt. B, 16, 183 (1932).

17. D. G. Adolphson, J. D. Corbett, and D. J. Merryman, J. Amer. Chem. Soc., 98, 7234 (1976).

18. T. W. Couch, D. A. Lokken and J. D. Corbett, Inorg. Chem., 11, 357 (1972).

19. J. D. Corbett, D. G. Adolphson, D. J. Merryman, P. A. Edwards and F. J. Armatis, J. Amer. Chem. Soc., 97, 6267 (1975).

20. L. Diehl, K. Khodadadeh, D. Kummer and J. Strähle, Chem. Ber., 109, 3404 (1976).

21. D. Kummer and L. Diehl, Angew. Chem., Int. Ed., 9, 895 (1970).

22. B. Dietrich, J. M. Lehn and J. P. Sauvage, Tetrahedron Lett., 34, 2885 (1969).

23. J. M. Lehn, Struct. and Bond., 16, 1 (1973).

24. J. M. Lehn and J. P. Sauvage, J. Amer. Chem. Soc., 97, 6700 (1975).

25. J. L. Dye, C. W. Andrews, and S. E. Mathews, J. Phys. Chem., 79, 3065 (1975).

26. J. D. Corbett and P. A. Edwards, J. Amer. Chem. Soc., 99, 3313 (1977).

27. C. H. E. Belin, J. D. Corbett, and A. Cisar, J. Amer. Chem. Soc., 99, 7163 (1977).

28. A. Cisar and J. D. Corbett, Inorg. Chem., 16, 632 (1977).

29. A. Cisar and J. D. Corbett, Inorg. Chem., 16, 2482 (1977).

30. R. L. Daake, Ph.D. Thesis, Iowa State University, Ames, Ia., 1976.

31. L. F. Dahl, T. Chiang, P. W. Seabaugh, and E. M. Larsen, Inorg. Chem., 3, 1236 (1964).

32. J. Kleppinger, J. C. Calabrese, and E. M. Larsen, Inorg. Chem., 14, 3128 (1975).

33. R. L. Daake and J. D. Corbett, Inorg. Chem., 17, in press (1978).

34. D. B. Copley and R. A. J. Shelton, J. Less-Common Metals, 20, 359 (1970).

35. R. S. Dean, U. S. Patent 2,941,931, June 21, 1960.

36. A. W. Struss and J. D. Corbett, Inorg. Chem., 9, 1373 (1970).

37. D. G. Adolphson and J. D. Corbett, Inorg. Chem., 15, 1820 (1976).

38. R. L. Daake and J. D. Corbett, Inorg. Chem., 16, 2029 (1977).

39. O. Ruff and R. Wallstein, Z. Anorg. Chem., 128, 96 (1923).

40. J. Lewis, D. J. Machin, I. E. Newnham, and R. S. Nyholm, J. Chem. Soc., 2036 (1962).

41. I. E. Newnham, J. Amer. Chem. Soc., 79, 5415 (1957).

42. A. G. Turnbull and J. A. Watts, Aust. J. Chem., 16, 947 (1963).

43. H. L. Schlaefer and H. W. Wille, Z. Anorg. Allg. Chem., 327, 253 (1964).

44. K. Uchimura and K. Funaki, Denki Kagaku, 33, 163 (1965).

45. O. G. Polyachenok, L. D. Polyachenok, and V. I. Sonin, Russ. J. Phys. Chem., 43, 1082 (1969).

46. S. I. Troyanov and V. I. Tsirel'nikov, Russ. J. Phys. Chem., 48, 1174 (1974).

47. B. Swaroop and S. N. Flengas, Can. J. Chem., 43, 2115 (1965).

48. S. I. Troyanov and V. I. Tsirel'nikov, Vestn. Mosk. Univ. Khim., 28, 67 (1973).

49. J. V. Smith, Ed., "Powder Diffraction File 1969," Am. Soc. Test. and Mat., Philadelphia, Pa., 1969, p 14534.

50. F. Hulliger, "Structural Chemistry of Layer-Type Phases," D. Reidel Pub. Co., Boston, Ma., 1976, pp 9-11, 234-242, and 270-273.

51. D. F. Shriver, "The Manipulation of Air-sensitive Compounds," McGraw-Hill Book Co., New York, N. Y., 1969.

52. M. Hansen and K. Anderko, "Constitution of Binary Alloys," 2nd ed, McGraw-Hill Book Co., New York, N. Y., 1958, p 882.

53. W. Klemm, H. Sodomann, and P. Langmesser, Z. Anorg. Allg. Chem., 241, 281 (1939).

54. A. Taylor and B. J. Kagle, "Crystallographic Data on Metal and Alloy Structures," Dover Publications, New York, N. Y., 1963, p 44.

55. R. P. Elliot, "Constitution of Binary Alloys, First Supplements," McGraw-Hill Book Co., New York, N. Y., 1965, p 185.

56. M. Okada, R. A. Guidotti, and J. D. Corbett, Inorg. Chem., 7, 2118 (1968).

57. H. Schäfer, "Chemical Transport Reactions," Academic Press, New York, N. Y., 1964, pp 11-14.

58. F. Takusagawa, Iowa State University, personal communication, 1976.

59. C. M. Clark, D. K. Smith, and G. G. Johnson, "A FORTRAN IV Program for Calculating X-Ray Powder Diffraction Patterns - Version 5," Penn. State Univ., Univ. Park, Pa., 1973.

60. G. H. Stout and L. H. Jensen, "X-Ray Structure Determination," Collier-Macmillan Ltd., London, 1968, pp 83-147 and 270-299.

61. D. R. Schroeder and R. A. Jacobson, Inorg. Chem., 12, 210 (1973).

62. R. A. Jacobson, J. Appl. Crystallogr., 9, 115 (1976).

63. D. E. Williams, USAEC Report IS-1052, Ames Laboratory, ISU, Ames, Ia., 1964.

64. "International Tables for X-Ray Crystallography," Vol. III, Kynoch Press, Birmingham, England, 1968.

65. W. R. Busing, K. O. Martin, and H. A. Levy, USAEC Report ORNL-TM-305, Oak Ridge National Laboratory, Oak Ridge, Tenn., 1962.

66. C. R. Hubbard, C. O. Quicksall and R. A. Jacobson, USAEC Report IS-2625, Ames Laboratory, ISU, Ames, Ia., 1971.

67. W. C. Hamilton, Acta Crystallogr., 18, 502 (1965).

68. R. L. Lapp, Iowa State University, personal communication, 1977.

69. H. P. Hanson, F. Herman, J. D. Lea, and S. Skilman, Acta Crystallogr., 17, 1040 (1964).

70. J. D. Corbett, R. L. Daake, K. R. Poeppelmeier, and D. H. Guthrie, J. Amer. Chem. Soc., 100, 652 (1978).

71. F. Jellinek, G. Brauer, and H. Müller, Nature, 185, 376 (1960).

72. "International Tables for X-Ray Crystallography," Vol. I, Knyoch Press, Birmingham, England, 1952.

73. C. K. Johnson, USAEC Report ORNL-3794 (2nd rev.), Oak Ridge National Laboratory, Oak Ridge, Tenn., 1970.

74. W. R. Busing, K. O. Martin, and H. A. Levy, USAEC Report ORNL-TM-306, Oak Ridge National Laboratory, Oak Ridge, Tenn., 1964.

75. W. C. Hamilton and J. A. Ibers, "Hydrogen Bonding in Solids," W. A. Benjamin, New York, N. Y., 1968, pp 14-18.

76. L. Pauling, "Nature of the Chemical Bond," 3rd ed, Cornell Univ. Press, Ithaca, N. Y., 1960, p 260.

77. A. Bondi, J. Phys. Chem., 68, 441 (1964).

78. P. Cherin and P. Unger, Acta Crystallogr., Sect. B, 23, 670 (1967).

79. P. Cherin and P. Unger, Inorg. Chem., 6, 1589 (1967).

80. A. Caron and J. Donohue, Acta Crystallogr., 18, 562 (1965).

81. S. Yanagisawa, M. Tashiro, and S. Anzai, J. Inorg. Nucl. Chem., 31, 943 (1969).

82. I. D. Brown, D. B. Crump, and R. J. Gillespie, Inorg. Chem., 10, 2319 (1971).

83. H. Krebs, "Fundamentals of Inorganic Crystal Chemistry," McGraw-Hill Book Co., London, 1968, p 137.

84. J. M. Hastings, N. Elliot, and L. M. Corliss, Phys. Rev., 115, 13 (1959).

85. D. S. Martin, Jr., Iowa State University, personal communication, 1976.

86. J. D. Corbett, Inorg. Nucl. Chem. Lett., 5, 81 (1969).

87. A. Hershaft and J. D. Corbett, Inorg. Chem., 2, 979 (1963).

88. R. M. Friedman and J. D. Corbett, Inorg. Chem., 12, 1134 (1973).

89. H. G. von Schnering, H. von Benda, and C. Kalveram, to be submitted for publication.

90. K. Deller and B. Eisenmann, Z. Naturforsch. B, 31, 29 (1976).

91. P. Cucka and C. S. Barett, Acta Crystallogr., 15, 865 (1962).

92. H. L. Clark, H. D. Simpson, and H. Steinfink, Inorg. Chem., 9, 1962 (1970).

93. G. S. Smith, Q. Johnson, and A. G. Tharp, Acta Crystallogr., Sect. B, 23, 640 (1967).

94. P. Moras, B. Metz, and R. Weiss, Acta Crystallogr., Sect. B, 29, 383 (1973).

95. F. A. Cotton and T. E. Haas, Inorg. Chem., 3, 10 (1964).

96. D. H. Guthrie, Iowa State University, personal communication, 1978.

97. L. J. Guggenberger and R. A. Jacobson, Inorg. Chem., 7, 2257 (1968).

98. C. Haas in "Crystal Structure and Bonding in Inorganic Chemistry," C. J. M. Rooymans and A. Rabenau, Eds., North Holland Pub. Co., Amsterdam, 1975 pp 103-125.

99. F. R. Gamble, J. Solid State Chem., 9, 358 (1974).

100. G. S. Marek, S. I. Troyanov, and V. I. Tsirel'nikov, Vestn. Mosk. Univ. Khim., 32, 64 (1977).

101. R. D. Shannon, Acta Crystallogr., Sect. A, 32, 751 (1976).

102. A. H. Thompson, Solid State Commun., 17, 1115 (1975).

103. T.-H. Nguyen, Iowa State University, personal communication, 1978.

104. G. K. Wertheim, F. J. DiSalvo, and D. N. E. Buchanan, Solid State Commun., 13, 1225 (1973).

105. L. F. Matheiss, Phys. Rev. B, 8, 3719 (1973).

106. F. R. Gamble and T. H. Beballe, in "Treatise on Solid State Chemistry," Vol. 3, N. B. Hannay, Ed., Planum Press, New York, N. Y., 1976, pp 89-203.

107. R. B. Somoane, V. Hadek, and A. Rembaum, J. Chem. Phys., 58, 697 (1973).

108. G. W. A. Fowles and G. R. Willey, J. Chem. Soc., Part A, 1435 (1968).

109. D. R. Powell and R. A. Jacobson, to be submitted to J. Solid State Chem..

110. N. N. Greenwood, "Ionic Crystals, Lattice Defects and Nonstoichiometry," Chemical Publishing Co., New York, N. Y., 1970, pp 121-146.

ACKNOWLEDGMENTS

The author wishes to express his appreciation to Professor John D. Corbett for his advice and patience during the course of this work. He also wishes to thank Dr. R. A. Jacobson and the members of his research group for the use of the automated diffractometer and access to the crystallographic programs, and James Anderegg for obtaining the XPS and UPS spectra. The author has enjoyed his association with Physical and Inorganic Chemistry Group IX of the Ames Laboratory and wishes to thank them for their helpful suggestions and interesting discussions throughout the course of this research. He would also like to thank his wife Marilyn for her support and presence throughout the last 2 1/2 years and her support at long distance for the 2 1/2 years before that.